Local Calibration of Material Characterization Models for Performance-based Flexible Pavement Design

by

Alexander Afuberoh

A Thesis Submitted to the Faculty of Graduate Studies of

The University of Manitoba

In Partial Fulfillment of the Requirements of the Degree of

MASTER OF SCIENCE

Department of Civil Engineering

University of Manitoba,

Winnipeg, Manitoba

Abstract

The Mechanistic Empirical Pavement Design Guide (MEPDG) method, currently known as Pavement ME, recommends using locally calibrated material characterization models developed from laboratory testing of local materials under specific environmental and traffic loading conditions. The Pavement ME design method offers a more realistic design procedure and reduces the uncertainty that arise from empirical design procedures.

This thesis developed a locally calibrated indirect tensile (IDT) strength material model for low temperature cracking predictions of hot mix asphalt (HMA) in Manitoba, Canada. In addition, the research investigated the integration of locally calibrated HMA, and unbound granular material characterization models into the Pavement ME framework to improve the design of flexible pavements.

Laboratory IDT testing was conducted on typical HMA mixtures containing extracted binders and varying percentages of reclaimed asphalt pavement (RAP). The laboratory measured IDT strengths were used to calibrate a local IDT strength predictive model for Manitoba. The predictions from the local Manitoba model were compared to the predictions from the global Pavement ME IDT model, and a Michigan calibrated IDT model, using a statistical analysis. It was found that the global Pavement ME IDT strength model, if used without local calibration, produced inaccurate predictions of the IDT strength for Manitoba mixtures. It was also found that binder characterization methods in Level 2 and Level 3 can significantly impact the accuracy of IDT strength predictions. A case study using developed local HMA, base, and subgrade material characterization models in Manitoba were compared to designs using default (Level 3) material input values in Pavement ME design software.

The results of integrating the locally calibrated models for HMA, base and subgrade layers demonstrated that the locally calibrated materials model inputs produce lower pavement structural thicknesses with higher reliability in the predicted distresses when compared to the default materials inputs. The effect of using calibrated material inputs was more pronounced for higher traffic loadings. The results of the study demonstrate that the use of calibrated models can potentially produce optimized pavement thicknesses due to improved pavement designs.

Acknowledgments

I wish to express my profound gratitude to my academic advisor, Dr. Ahmed Shalaby P.Eng, for his academic advice, guidance, financial support, and patience through the course of this thesis. Many thanks to members of the examining committee, Dr. Young-Jin Cha, and Dr. Mohammad Khoshdarregi for their valuable inputs and suggestions towards improving the quality of this research work.

Special thanks goes out to Dr. Leonnie Kavanagh, for her indefatigable guidance, suggestions, and encouragement towards making this research work a reality. I acknowledge the invaluable technical support provided by Materials Engineering department at Manitoba Infrastructure. I would also like to thank Mr. Scott Sparrow, for his kind assistance during the laboratory testing program. Many thanks to my peers in the Pavement Research Group for their encouragement and providing a healthy working environment that made learning a fun-filled experience.

I am sincerely grateful for financial support from the University of Manitoba (IGSES), NSERC Discovery grant, Kenneth Peaker Memorial Engineering Award and GETS funding.

Lastly, I will like to dedicate this thesis to my late father, Mr. Christopher Ikechukwu Afuberoh, who sacrificed everything within his reach to lay a solid foundation for my education. I am immensely grateful to my loving mother and amazing sisters, for their unwavering love, support and prayers through the course of this thesis.

Table of contents

List of Tables

List of Figures

Notations and Abbreviations

AASHTO	American Association of State Highway and Transportation Officials
AC	Asphalt Concrete
|E*|	Dynamic Modulus
DOT	Department of Transportation
EICM	Enhanced Integrated Climate Model
FHWA	Federal Highway Administration
G*	Complex shear modulus
HMA	Hot-Mix Asphalt
IDT	Indirect Tensile Test
MC	Moisture content
ME	Mechanistic-Empirical
MEPDG	Mechanistic-Empirical Pavement Design Guide
MI	Manitoba Infrastructure
M_R	Resilient Modulus
N	Sample size
NCHRP	National Cooperative Highway Research Program
LTPP	Long-Term Pavement Performance
RAP	Reclaimed Asphalt Pavements

RAS	Recycled Asphalt Shingles
TCMODEL	Thermal Cracking Model
UGM	Unbound Granular Material
δ	Binder phase angle
θ	Bulk stress
σ_d	Deviator stress
σ_1	Total vertical stress
σ_2, σ_3	Horizontal principal stresses

Chapter 1: Introduction

1.1 Background

For over several decades, the empirical based American Association of State Highway & Transportation Officials (AASHTO) design guides (from 1962 through 1993) has served as the primary design procedure employed for pavement structural design (AASTHO, 1993). According to Schwartz and Carvalho, (2007), a major drawback of the 1993 AASHTO flexible pavement design procedure is the identification of only a few input parameters (drainage coefficients, structural layer coefficients, and subgrade resilient modulus) as material properties. Additionally, these parameters do not adequately describe the complex time and temperature dependent response of asphalt concrete mixtures as well as stress-dependent stiffness of unbound granular and subgrade materials under local traffic and environmental loading conditions (Schwartz and Carvalho, 2007). Consequently, pavement structures could either be overdesigned or undersigned due to uncertainties associated with empirical design procedures (Soliman and Shalaby, 2014).

To address these perceived drawbacks, the Mechanistic-Empirical pavement design Guide (MEPDG) procedure, which incorporates improved material characterization and constitutive models to account for rate effects, nonlinearities and other realistic features of material behavior, was thereby developed under the National Cooperative Highway Research Program (NCHRP) Project 1-37A study (Carvalho, 2006; NCHRP, 2004). This method offers a more rational and realistic pavement design procedure and reduces the uncertainty that arises from empirical design procedures (NCHRP, 2004).

Characterization of pavement materials to effectively capture the mechanistic properties of pavement layers under local environmental and traffic loading conditions is essential in the

successful design of longer lasting and cost-effective pavements. For flexible pavements, the material mechanical properties utilized primarily as inputs for design are: the dynamic modulus |E*|, creep compliance and indirect tensile strength (IDT) for Hot-Mix Asphalt (HMA) layer. In addition, the resilient modulus (M_R) serves as the primary material input for unbound granular and subgrade layers. These mechanistic properties are utilized by calibrated mechanistic models to predict critical pavement responses (stresses, strains, and deflections) based on climatic and traffic loading. The predicted pavement responses then serve as inputs in the empirically correlated distress prediction models to simulate the cumulative pavement surface distresses (damage) over its service life (AASHTO, 2015). The flexible pavement performance indicators obtained from the MEPDG analysis includes (AASHTO, 2008): longitudinal cracking (AC top-down fatigue cracking), alligator cracking (bottom-up fatigue cracking), transverse cracking (thermal cracking), total permanent deformation (rutting) and pavement surface roughness.

Depending on the availability of resources and desired reliability of the project, highway agencies select material design input parameters used in the Mechanical–Empirical Pavement design software program (Pavement ME) based on a hierarchical approach. This approach comprises of three levels of user-defined material design inputs for predicting pavement deterioration over time (NCHRP, 2004; AASHTO, 2015). As described by AASHTO, (2015), Level 1 inputs represent project-or site-specific material data, which are measured directly by comprehensive laboratory or field-testing. These input data have the highest level of accuracy, lowest level of uncertainty and are said to provide the most reliable pavement designs and analysis outputs. Furthermore, Level 2 input data are generally obtained through mathematical correlation or regression equations based on other measured mixture properties and/or obtained through limited laboratory or field-testing.

These data have an intermediate level of reliability. Lastly, Level 3 input data are determined from typical regional or agency default values and have the lowest level of reliability.

Conducting laboratory testing to determine Level 1 material input properties for flexible pavement asphalt concrete (AC), unbound granular and subgrade layers can be very costly, requires research grade facilities and skilled labor. As such, predictive models are recommended to fill a gap between laboratory data and default values. It is imperative to note that these predictive models were globally calibrated and validated majorly based on the Long-Term Pavement Performance (LTPP) diverse test section database spread across the United States and only a few test sections in Canada. However, the diverse database does not necessarily represent all local materials, traffic, climatic and subgrade conditions in Manitoba. Therefore, the Guide for Local calibration of the MEPDG developed to facilitate regional local calibration emphasizes the need for transportation agencies to calibrate predictive models to local materials, traffic and environmental conditions (AASHTO, 2010). This is a vital step to establish confidence in the design procedure as well as improve the reliability of predicted pavement performance.

To facilitate the adoption and implementation of the Pavement ME design framework in Manitoba, The University of Manitoba's pavement research group in partnership with Manitoba Infrastructure have been conducting comprehensive material characterization laboratory testing on locally available materials used for construction in Manitoba. The test results, obtained from laboratory testing provides a comprehensive database of mechanical properties (dynamic modulus, creep compliance, and IDT test for asphalt concrete and the M_R for unbound granular and subgrade materials) which can be used to calibrate the global Pavement ME predictive models.

Soliman (2015) developed a comprehensive laboratory-testing program to evaluate the resilient modulus (material stiffness) and permanent deformation (material stability) of typical unbound granular materials and subgrade soils in Manitoba. The research culminated in the development of models for predicting the resilient modulus of subgrade and unbound granular materials to improve the reliability of Level 2 inputs in the Pavement ME design software (Soliman, 2015). Likewise, Esfandiarpour, (2017) carried out laboratory characterization and evaluation of asphalt mixes containing recycled asphalt shingles (RAS) and reclaimed asphalt pavements (RAP) in Manitoba. In addition, the research also culminated in the calibration of the global Pavement ME creep compliance and NCHRP 1-37A and NCHRP 1-40 D dynamic modulus predictive models to local materials and conditions (Esfandiarpour, 2017). This was necessary to optimize the accuracy of the prediction models used in the design and analysis of flexible pavements in Manitoba. These developed predictive models for HMA, unbound granular base, and subgrade layers are discussed in detail in chapter three of this thesis.

Since Manitoba Infrastructure is currently conducting parallel designs, and also in the evaluation stage of implementing the Pavement ME design method, it is necessary to apply and investigate the impact of integrating the developed material characterization prediction models into the Pavement ME framework to improve the designs of flexible pavements.

1.2 Research Objectives

The objectives of this research are to develop a locally calibrated IDT strength material characterization model for HMA in Manitoba, and integrate locally calibrated HMA, base and subgrade material characterization models into the Pavement ME design framework to improve the design and performance of flexible pavements.

The specific objectives of this research thesis are to:

1. Develop and update design input data based on locally calibrated material models (dynamic modulus, creep compliance, IDT strength) as a means of improving the reliability of flexible pavement designs.
2. Investigate the reliability of the Pavement ME IDT strength global model for predicting the IDT strength at -10°C.
3. Calibrate the Pavement ME IDT strength global model to local conditions and materials in order to improve the reliability of low-temperature HMA performance predictions.
4. Evaluate and compare structural design thickness and the predicted pavement distresses using default and locally calibrated material input parameters.
5. Evaluate the impact of the locally calibrated HMA, base, and subgrade input data on the long-term performance of typical pavement sections with varying design conditions (traffic levels and subgrade types) using the Pavement ME design software.

1.3 Scope of the Research

Adopting the Mechanistic-Empirical pavement design method requires adequate understanding of the required traffic, material, and climatic design inputs to effectively accomplish its implementation. The scope of the research is limited to the application of developed locally calibrated characterization models for typical HMA, base and subgrade materials in Manitoba. In addition, an important HMA layer prediction model, the IDT strength model is calibrated in this thesis. The calibration and validation of distress prediction models are not included in this research.

1.4 Significance of Research

Accurate prediction models for all pavement layers provide more reliable predictions of the long-term pavement performance. The purpose of this thesis is to improve flexible pavement performance predictions and to save agencies time, money and effort related to the laboratory testing of construction materials used in the design of pavements. Furthermore, highway agencies can potentially save cost related to initial pavement construction and long-term pavement maintenance. This research thesis provides adaptable guidelines for the application of developed locally calibrated models to improve the design of flexible pavements. The findings from the research can be used to develop and update locally calibrated material input parameters for flexible pavement design in Manitoba based on local conditions and materials when Level 1 laboratory test input data could not be obtained. This research demonstrates the significance of developing design inputs based on locally calibrated material models as a means of improving the performance of flexible pavements.

1.5 Thesis Organization

The research thesis is organized as follows:

Chapter 1 presents the background of the study, thesis objectives, scope of the research, significance of the study, and the general organization of the thesis.

Chapter 2 presents a summary of the current state of practice for flexible pavement design as well as material property models for flexible pavement layers. The need for local calibration of predictive models and different local calibration methods are also presented in this chapter.

Chapter 3 presents the progress on local calibration of material models with a focus in Manitoba.

Chapter 4 presents the research methodology used in achieving the objectives of the research. The laboratory test program and investigated HMA mixtures are also presented.

Chapter 5 discusses the results of the IDT strength test for the investigated laboratory mixtures, assessment of the global pavement ME IDT predictive model and the results of the local calibration of the global Pavement ME IDT predictive model.

Chapter 6 details the impact of integrating locally calibrated HMA, base, and subgrade models on design and performance of flexible pavements using a case study.

Chapter 7 presents the summary and conclusions based on the findings of the research. In addition, recommended future work is also presented in this chapter.

Chapter 2: Literature Review

2.1 Introduction

This chapter presents the literature review on the state of current practice for flexible pavement design, material layer property models for flexible pavements, and the need for local calibration with a summary of local calibration efforts across North America.

2.2 Current State of Practice for Pavement Design Methods

A number of pavement design methods have been developed over the years. According to Haas and TAC, (1997), the different pavement design methods may be categorized as follows:

- Experienced-based design, using standard sections
- Empirical pavement design methods
- Mechanistic-empirical design method

Standard section design methods involve the selection of standard layer thicknesses for different design conditions (class of highway, traffic level, subgrade type etc) based on successful past designs (Haas and TAC, 1997). The major limitation of this design methods is that they are unsuitable and unreliable for design conditions other than which they were developed. As such, this method may only be used where the probability for large variations in traffic volume over the pavement design life is low and the risk associated to early pavement failure is low (Boone, 2013).

Empirical pavement design methods basically utilize experience and/or experimentations to develop correlations between pavement design inputs (traffic loadings, environment, pavement layer materials) and measured pavement responses. The limitation of the standard section design method also applies to the empirical approach in that the empirical correlations developed are

limited for the range of design conditions for which they were developed (Boone, 2013; Haas and TAC, 1997). The AASHTO 1993 guide for design of pavement structures is one of the most commonly used empirical methods for the design of new and retaliated flexible pavements across North America (AASHTO, 1993).

Mechanistic-Empirical methods offer dramatic improvements in pavement design when compared to empirical methods. The mechanistic-empirical method consists of the mechanical, and the empirical component. The mechanical component utilizes mechanistic models to compute critical pavement responses (stresses, strains, and deflections) based on climatic, material, and traffic loading. The empirical component utilizes the predicted pavement responses as inputs into the empirically correlated distress prediction models to simulate the cumulative pavement surface distresses (damage) over its service life (AASHTO, 2015). The Pavement ME method is becoming the most commonly used mechanistic-empirical design method by highway and transportation agencies for both flexible and rigid pavements.

2.2.1 Pavement Design Methods Across North America

A survey was conducted by Pierce and McGovern (2014), under the NCHRP Project 20-05 to determine the implementation efforts of the Pavement ME design method by different state highway agencies and provincial transportation agencies across North America. Results of the survey showed that pavement design methods differ amongst agencies ranging from empirical, MEPDG mechanistic-empirical to other mechanistic-empirical methods. Figure 2.1 shows a summary of the pavement design methods utilized across North America according to the survey results. Pierce and McGovern (2014) reported that about 14% of respondents use empirical pavement design method together with other ME methods. 56% of respondents use the empirical

pavement design method, while 22% of the respondents use a combination of empirical & MEPDG design method. 6% of the respondent indicated using other ME design methods such as (Pierce and McGovern, 2014):

- CalME for flexible pavement design — California Department of Transportation (DOT)
- MnPAVE for new flexible and overlay design — Minnesota DOT
- Shell ME pavement design modified for Saskatchewan — Saskatchewan Highways and Infrastructure.
- Dynatest ELMOD program for asphalt overlay of flexible pavements and semi-rigid pavements — Mississippi DOT.

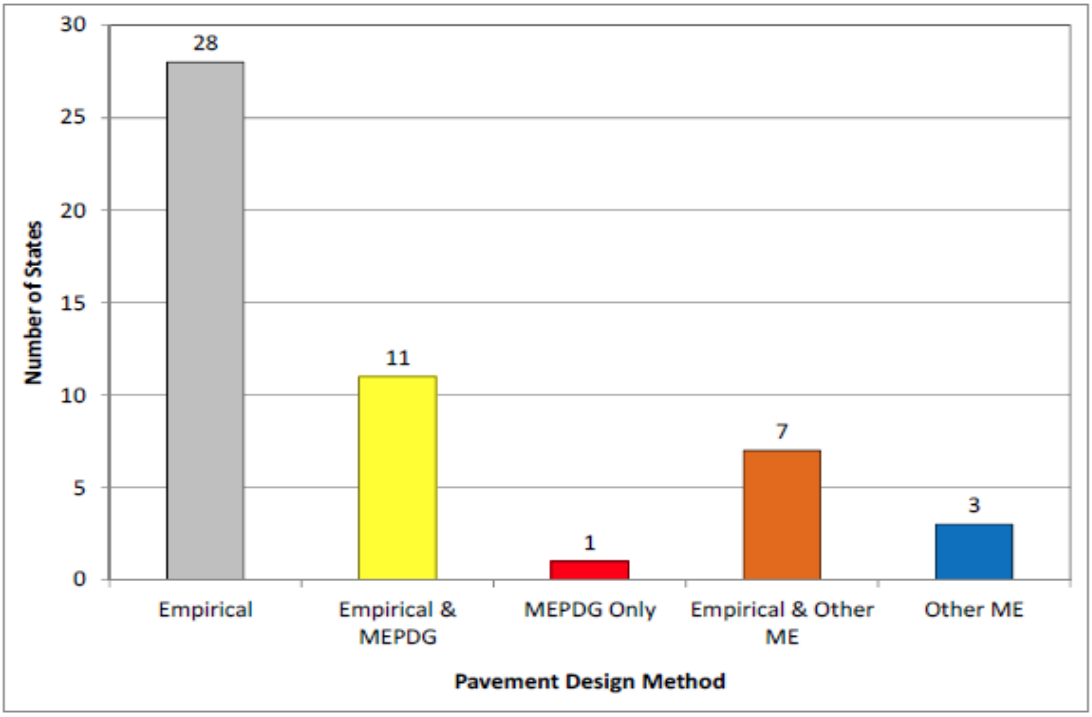

Figure 2.1: Summary of pavement design methods. (Pierce and McGovern, 2014; Timm et al. 2014)

2.2.2 Mechanistic-Empirical Pavement Design Guide Method

2.2.2.1 Major Components of the Mechanistic-Empirical Pavement Design Guide

Generally, the Mechanistic-Empirical design framework comprises five (5) modules, which make up the design and analysis system. These modules are the input system (traffic module, climatic module, pavement structural response module, material characterization module) and the output system (the distress-performance prediction module). However, Von Quintus et al. (2016) reported that, to some extent, the material characterization module relates to all other components of the design framework and as such is generally considered the most important to predicting the performance of pavements (Von Quintus et al. 2016). This is further illustrated in Figure 2.2.

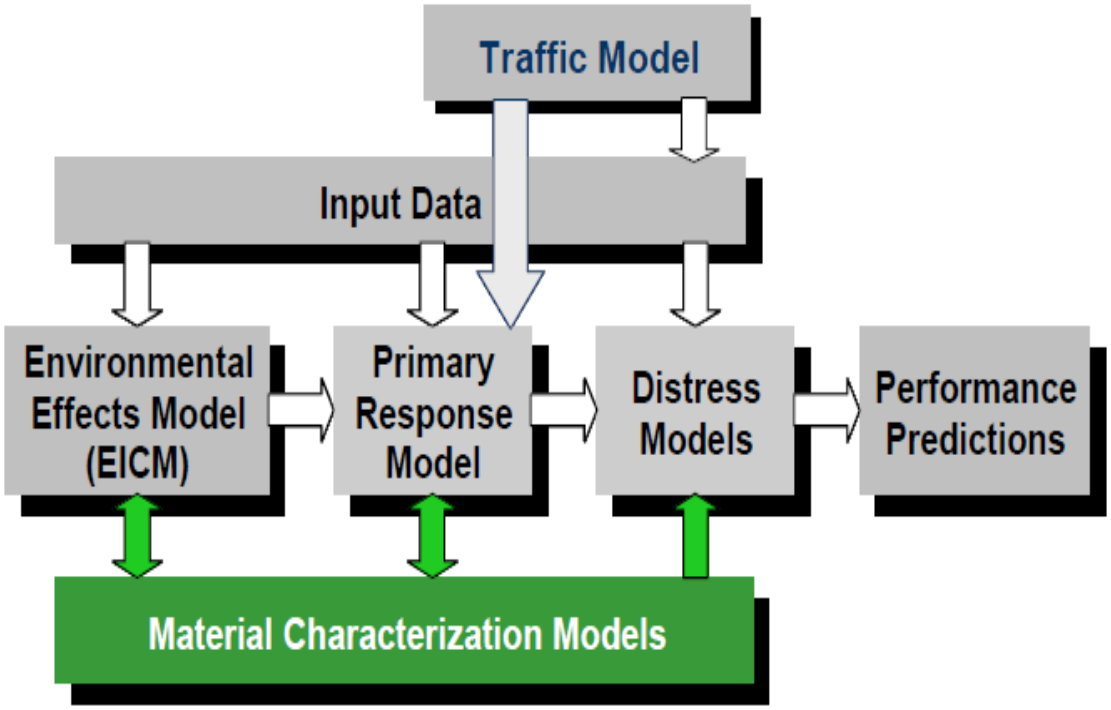

Figure 2.2: Interaction between the materials module with other components of the M-E design framework. (NCHRP, 2004).

2.2.2.2 Pavement Structural Response Models

Structural response models for flexible pavements are used to evaluate stresses, strains and, deflections as a response to environmental factors, and traffic loadings (NCHRP 2004). The MEPDG incorporates a linear elastic analysis (LEA) and a Finite element analysis (FEA) method for structural response computations of flexible pavements. For pavement structural materials which are realistically considered as linear elastic, the JULEA program, based on the multilayer elastic theory (MLET) is used to calculate the pavement response. When considering the non-linear behavior of unbound materials (base and subgrades), a 2 dimensional finite element analysis (FEA) program, DSC2D (only recommended for research purposes) is utilized for structural response computations (NCHRP, 2004; Kavanagh, 2013).

The critical stresses and strains are usually calculated at specific locations of interest within the pavement structure. These locations are outlined as follows (NCHRP, 2004):

- Bottom/top of HMA layer due to tensile horizontal strains (used for fatigue cracking)
- Within the HMA layer due to compressive vertical strains (used for HMA rutting)
- Bottom of subbase/base layer due to compressive vertical strains (for unbound layer rutting)
- Top of subgrade due compressive vertical strains (for subgrade rutting).

2.2.2.3 Enhanced Integrated Climatic Model (EICM)

Environmental effects influence the behavior of pavement materials and pavement performance. Environmental effects on pavement structure can be categorized into (1) direct effect based on thermal contraction and/or expansion, and (2) indirect environmental effects on material properties

resulting from variations in moisture and temperature with depth of the pavement structure (NCHRP, 2004).

The EICM model accounts for moisture and temperature variations within the flexible pavement structural layers over the design life. Hourly weather-related data, such as precipitation, air temperature, percent sunshine, wind speed, and relative humidity are required as inputs into the EICM for climatic analysis over the pavement design life. These weather-related data are obtained from weather stations in close proximity to the pavement location. The EICM predicted temperature for flexible pavements significantly influences the stiffness of the HMA layer, as such pertinent for rutting and thermal cracking predictions (Saha et al. 2014).

2.2.2.4 Pavement ME Implementation Status Across North America

The full implementation of the MEPDG procedure involves various aspects ranging from material characterization, local calibration and validation, traffic characterization to running parallel designs. Since the release of the MEPDG, various studies have documented implementation efforts by different highway agencies across North America. NCHRP synthesis 457 conducted by Pierce and McGovern (2014) documented the implementation strategies and lesson learned based on the experience of different highway agencies. Pierce and McGovern (2014) also reported that three state DOT's: Indiana DOT in 2009, Missouri DOT in 2009, and Arizona DOT in 2014 have fully implemented the MEPDG procedure. In addition, 30 other state DOT's and several Canadian provinces indicated they are currently evaluating the MEPDG procedure and planned to implement within the next 5 years. A recent Federal Highway Administration (FHWA) report based on the AASHTO MEPDG Regional Peer Exchange Meetings also summarizes the MEPDG

implementation status (Pierce and Smith, 2015). Figure 2.3 shows the implementation status for asphalt pavements by different state across North America.

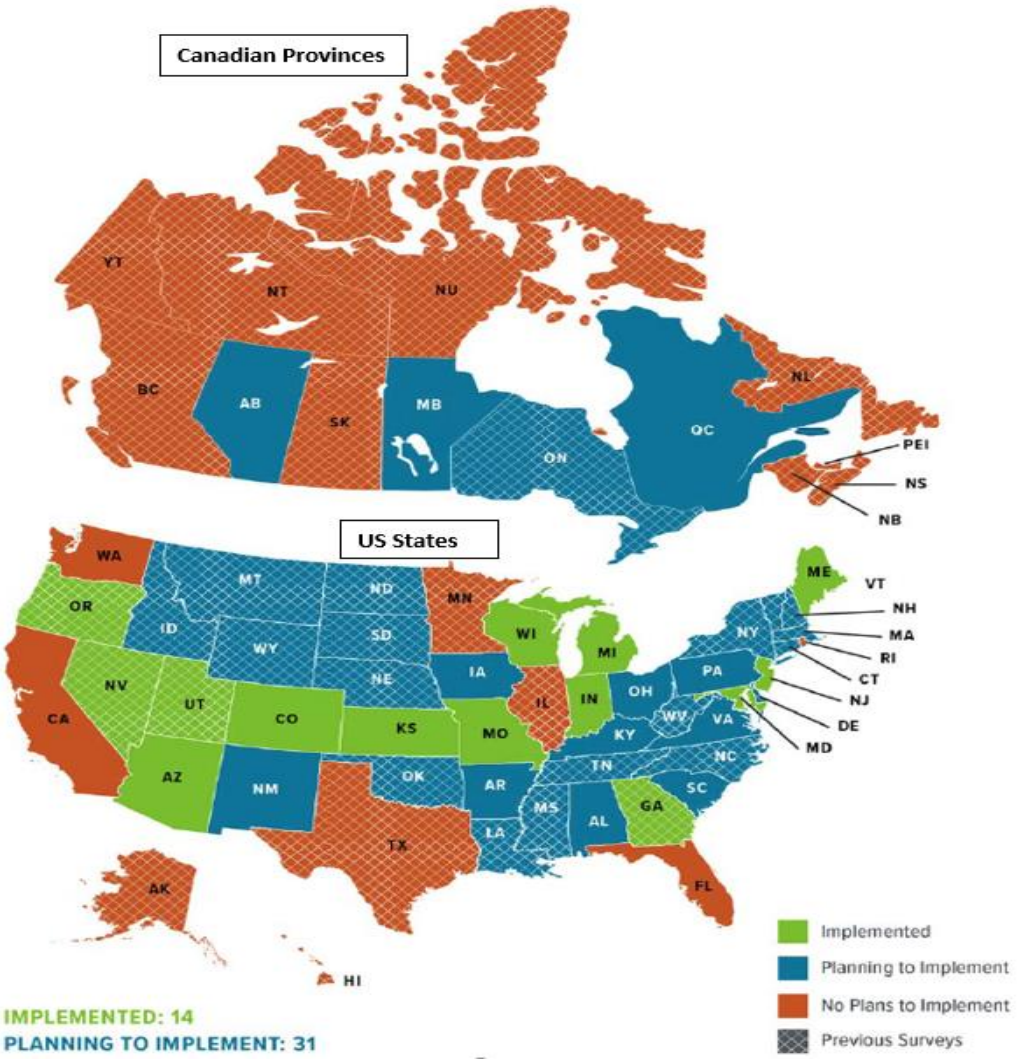

Figure 2.3: Asphalt pavement MEPDG implementation status across North America (Applied Pavement Technology. Inc., 2017)

2.3 Material Property Models for Flexible Pavements

This section presents the fundamental principles, previous assessment and local calibration studies on the HMA, unbound granular base and subgrade layer predictive models used for design of flexible pavement structures.

2.3.1 HMA Layer Material Input Predictive Models

2.3.1.1 Dynamic Modulus |E*|

Rutting and fatigue cracking are common distresses associated with flexible pavement structures. The dynamic modulus, |E*| is a primary stiffness material property which is utilized to evaluate the fatigue cracking and rutting potential of the time and temperature dependent HMA mixture. (Bayomy et al. 2012; Georgouli, et al. 2016).

|E*| can be defined as: "*the absolute value of the complex modulus calculated by dividing the maximum (peak to peak) stress by the recoverable (peak-to-peak) axial strain for a material subjected to sinusoidal (repeated vertical) loading"* (Mallick and El-Korchi, 2017).

The complex modulus comprises two components: 1) the real, and 2) the imaginary component. The real component of the complex modulus describes the elastic stiffness (storage modulus) of the HMA mixture, while the imaginary component of the complex modulus describes the viscous behavior (loss) of the HMA mixture (Huang, 2004). This can be further illustrated as shown in equations 2.1 to 2.3 (Huang, 2004). Figure 2.4 shows a typical stress-strain behavior of a viscoelastic material subjected to repeat vertical loading.

$$E^* = E' + iE'' \quad (2.1)$$

$$E^* = |E^*| \cos(\delta) + i\,|E^*| \sin(\delta) \quad (2.2)$$

where: E′= elastic modulus or storage modulus, and E″ = viscous modulus.

The dynamic modulus, |E*| can, therefore, be mathematically expressed as shown in equation 2.3 (Mallick and El-Korchi, 2017)

$$|E^*| = \frac{\sigma_0}{\varepsilon_o} \quad (2.3)$$

Where |E*| = dynamic modulus, σ_0 = maximum stress, ε_o = maximum strain.

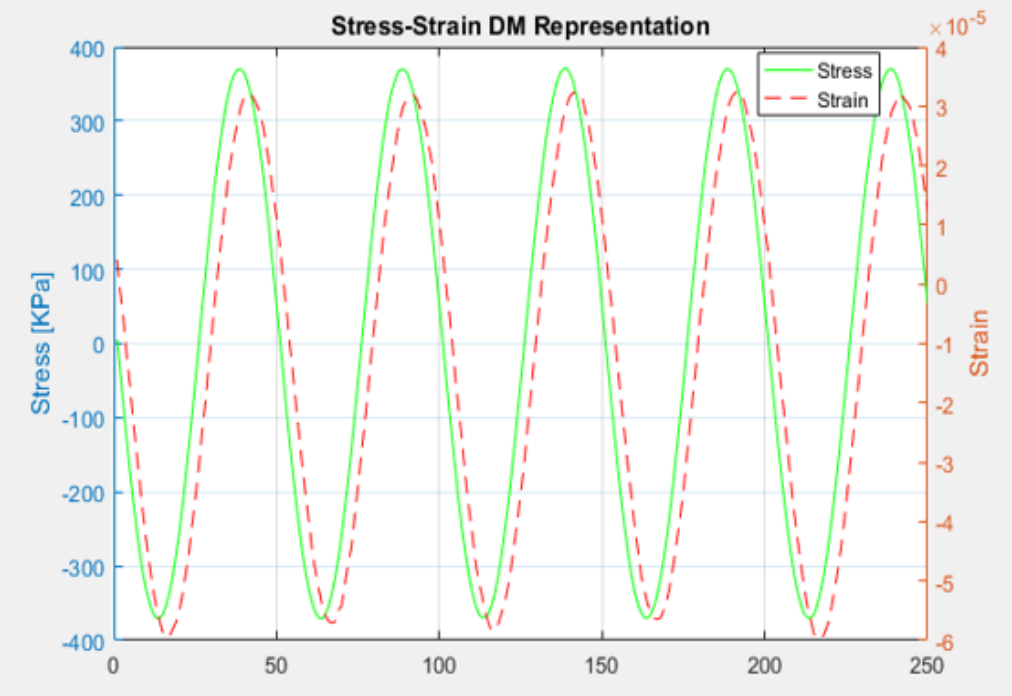

Figure 2.4: Stress-strain relationship of a viscoelastic material under dynamic modulus loading

It has been reported that material mixture properties (binder stiffness, aggregate gradation, air voids, binder content), and non-material properties such as rate of loading, temperature, specimen geometry are factors that affect the dynamic modulus of asphalt concrete (Elangovan, 2008; El-Badawy et al. 2012). As such, Table 2.1 presents various evaluation studies of the dynamic modulus of AC mixtures.

Table 2.1: Summary of research studies on the evaluation of |E*|

Source Author (Year)	Investigated material property on |E*|	Investigated field performance of |E*|	Findings
Kim et al. (2005)	Aggregate gradation, asphalt grade, and asphalt content	NP	➢ Dynamic modulus is fairly affected by binder PG, asphalt content and binder source. ➢ Aggregate gradation and sources for NCDOT[1] mixtures were found to have an insignificant effect on dynamic modulus.
Tarefder et al. (2007)	Aggregate gradation, air voids, asphalt type, and asphalt content.	Rutting	➢ Increase in air voids resulted to decrease in dynamic modulus. ➢ Effect of asphalt content on dynamic modulus did not seem to produce a clear trend. ➢ Increase in air voids and asphalt content likely leads to an increase in the rutting potential ➢ Higher stability and interlocking of coarser aggregate gradation produced lower rut potential ➢ Rutting is affected by PG grade at medium and low temperatures
Mohammad et al. (2007)	Aggregate gradation, RAP contents	Rutting	➢ Dynamic modulus values showed high sensitivity to the nominal maximum aggregate size (NMAS). Dynamic modulus values
Esfandiarpour (2017)	Percentage of RAP and RAS content	Rutting	➢ Increase in RAP and RAS content can increase rutting potential of HMA mixes

Note[1]: NCDOT = North Carolina Department of Transportation, NP = not provided

2.3.1.1.1 Review of Dynamic Modulus Predictive Models

In years past, numerous regression equations have been developed to estimate the stiffness of asphalt concrete mixes from basic mix volumetric and material properties (Biligiri and Way, 2014; Georgouli et al. 2016; Kim et al. 2011; Mohammad et al. 2014). The Van der Poel model, dating back to 1945 was one of the earliest prediction models used to estimate the stiffness from mix properties (Georgouli et al. 2016; Poel and Der, 1954).

These predictive equations were derived to relate temperature, loading frequency, basic mixture and asphalt binder properties to the stiffness of asphalt mixtures using linear and/or nonlinear mathematical regression (Biligiri and Way, 2014). Table 2.2 presents the different |E*| predictive regression models available in the literature.

Table 2.2: |E*| predictive regression models

Source	Model
Andrei et al. (1999)	Viscosity based Witczak model (NCHRP 1-37A)
Bari and Witczak (2006)	G* based Bari and Witczak model
(Witczak, El-Basyouny, and El-Badawy, 2007)	Revised G* based Witczak and Bari model NCHRP 1-40D model
(Christensen et al. 2003)	Hirsch model
(Al-Khateeb et al. 2006)	Law of mixtures parallel model

2.3.1.1.2 Pavement ME Dynamic Modulus Predictive Models

Dynamic modulus in the Pavement ME design software can be obtained using three hierarchical approaches. Level 1 dynamic modulus values are obtained from laboratory testing under a minimum of three test temperatures and three loading frequencies. Users can obtain Level 2 or

Level 3 dynamic modulus values at the temperatures of interest, using regression equations from basic material gradations and volumetric properties in the absence of Level 1 data (laboratory testing). Although several |E*| predictive models have been presented in Table 2.2, NCHRP 1-37A, and NCHRP 1-40D dynamic modulus predictive models are currently incorporated in the Pavement ME design software for Level 2 and Level 3 |E*| predictions. These models are of particular interest and are relevant to this research study. The models are briefly presented as follows:

NCHRP 1-37A: Witczak |E*| predictive model

Andrei et al. (1999) developed the NCHRP 1-37A |E*| predictive model from 2750 data points based on correlations with aggregate gradations, mix volumetric properties, binder stiffness (viscosity) and loading frequency. The model takes a sigmoidal form and is presented in equation 2.4 (NCHRP, 2004; Andrei et al. 1999)

$$\log_{10}|E^*| = -1.249937 + 0.02932\rho_{200} - 0.001767(\rho_{200})^2 - 0.002841\rho_4 - 0.058097V_a - 0.802208\left(\frac{V_{beff}}{V_{beff}+V_a}\right) + \frac{3.871977 - 0.0021\rho_4 + 0.003958\rho_{38} - 0.000017(\rho_{38})^2 + 0.00547\rho_{34}}{1+e^{(-0.603313-0.313351(\log f) - 0.393532(\log\eta))}} \quad (2.4)$$

where: |E*| = HMA dynamic modulus, psi (1 psi = 6.89 kPa); η =binder viscosity, (10^6 poise); f = sample loading frequency, in Hz; Va = % air voids in the mix, by volume; V_{beff} = % effective binder content, by volume; ρ_{34} = % cumulative retained weight on the 3/4-in (19 mm) sieve; ρ_{38} = % cumulative retained weight on the 3/8-in (9.5mm) sieve; ρ_4 = % cumulative retained weight on the No. 4 sieve (4.75 mm); and ρ_{200} = % passing No. 200 sieve (0.075 mm).

NCHRP 1-40 D: Revised Witczak |E*| predictive model

Bari and Witczak (2006) revised the NCHRP 1-37A model using 7400 data points from 346 mixes to incorporate binder characterization based on dynamic shear modulus |G*| and phase angle (δ) for |E*| predictions. The revised |E*| predictive model is presented in equation 2.5 (Bari and Witczak 2006).

$$\log_{10}|E^*| = -0.349+0.754(|G_b^*|^{-0.0052})*(6.65-0.032\,\rho_{200}+0.0027(\rho_{200})^2+0.011\,\rho_4 - 0.0001(\rho_4)^2+0.006\,\rho_{38}-0.00014(\rho_{38})^2-0.08V_a-1.06\left(\frac{V_{beff}}{V_{beff}+V_a}\right)) + \frac{2.558+0.032Va+0.713\left(\frac{V_{beff}}{V_{beff}+V_a}\right)+0.0124\,\rho_{38}-0.0001(\rho_{38})^2-0.0098\rho_{34}}{1+e^{(-0.7814-0.5785log|G_b^*|+0.8834log\delta_b)}} \quad (2.5)$$

Under the NCHRP 1-40D project, Bari and Witczak (2007) further revised the |E*| predictive model to be implemented in the Pavement ME design procedure. The revised NCHRP 1-40D |E*| predictive model currently utilized in the Pavement ME software is shown in equation 2.6

$$\log_{10}|E^*| = -0.02+0.758(|G_b^*|^{-0.0009})*(6.8232-0.03274\,\rho_{200}+0.00431(\rho_{200})^2+0.0104\,\rho_4 -0.00012(\rho_4)^2+0.00678\,\rho_{38}-0.00016(\rho_{38})^2-0.0796\,V_a-1.1689\left(\frac{V_{beff}}{V_{beff}+V_a}\right)) + \frac{1.437+0.03313Va+0.6926\left(\frac{V_{beff}}{V_{beff}+V_a}\right)+0.00891\,\rho_{38}-0.00007(\rho_{38})^2-0.0081\rho_{34}}{1+e^{(-4.5868-0.8176\,log|G_b^*|+3.2738log\delta_b)}} \quad (2.6)$$

where: |E*| = HMA dynamic modulus, in psi (1 psi = 6.89 kPa); $|G_b^*|$ = complex binder shear modulus, in psi; δ_b = binder phase angle, in degree; V_a = % air voids in the mix, by volume; V_{beff} = % effective binder content, by volume; ρ_{34} = % cumulative retained weight on the 3/4-in. sieve (19 mm); ρ38 = % cumulative retained weight on the 3/8-in. sieve (9.5mm); ρ4 = % cumulative retained weight on the No. 4 sieve (4.75 mm); and ρ200 = % passing No. 200 sieve (0.075 mm).

2.3.1.2 Creep Compliance and IDT Strength Predictive Model

Thermal cracking or low-temperature cracking is a severe pavement distress commonly observed on asphalt pavements in cold climates. Thermal cracks occur when accumulated thermal stresses in the pavement, induced by extreme low temperature or large daily temperature variations, exceed the tensile strength of the asphalt mixture (Dave and Hoplin, 2015; Shalaby, et al. 1996). With the intrusion of moisture, dust and other foreign materials into these cracks, coupled with the combined effect of freeze-thaw cycles and heavy traffic loading, the structural and functional integrity of the pavement is undermined. This leads to the occurrence of more severe pavement distresses, poor quality of ride, reduced pavement serviceability and early pavement maintenance (Marasteanu and Cannone Falchetto, 2018).

The Pavement ME incorporates a thermo-viscoelastic thermal cracking model, which is used to predict the thermal cracking performance of asphalt pavements over its lifetime (Roque et al. 1995; Witczak et al. 2004). The creep compliance and IDT strength of are pertinent mechanical properties inputs for thermal cracking predictions of HMA mixtures.

2.3.1.2.1 Pavement ME Creep Compliance Predictive Model

The Pavement ME design program utilizes a globally calibrated regression model to estimate the creep compliance values of HMA mixtures. 714 data points from 32 mixtures were used to develop the creep compliance model (NCHRP, 2004). Equation 2.7 presents the creep compliance model utilized in the Pavement ME software (AASHTO, 2015).

$$D(t) = D_1 t^m \quad (2.7)$$

According to AASHTO (2015), D_1 and m represent the regression constants which are obtained from the mix volumetric properties. D_1 and m are further illustrated in Equations 2.8 and 2.9.

$$\log (D_1) = -8.5241 + 0.01306\,T + 0.7957 \log (V_a) + 2.0103 \log (VFA) - 1.923 \log (A) \quad (2.8)$$

$$m = 1.1628 - 0.00185\,T - 0.04596\,V_a - 0.01126\,VFA + 0.00247\,Pen_{77} + 0.001683\,(Pen_{77})^{0.4605T} \quad (2.9)$$

where: D_1 and m are regression, coefficients obtained from volumetric properties, t = loading time in seconds, V_a = air voids (%), VFA = voids filled with asphalt (%), A = intercept of asphalt binder viscosity-temperature relationship, T = test temperature, VTS = regression slope of viscosity temperature susceptibility. Pen_{77} = penetration at 77°F (25°C), mm/10.

The penetration value of the asphalt binder at 77°F (25°C), which serves as a pertinent input into the creep compliance model is predicted using equation 2.10.

$$Pen_{77} = 10^{290.5013 - \sqrt{81177.288 + 257.0694 * 10^{(A + 2.72973 * VTS)}}} \quad (2.10)$$

where: Pen_{77} = binder penetration at 77°F (25°C), mm/10, A = asphalt viscosity-temperature susceptibility intercept, and VTS= regression slope of the binder viscosity-temperature relationship.

2.3.1.2.2 Indirect Tensile Strength Prediction Model

Thermal crack initiation in asphalt pavements is significantly influenced by the indirect tensile (IDT) strength of the mixture (Zhang et al. 2015). The IDT strength of the mixture directly relates to the low-temperature cracking pavement performance expected in the field (Krcmarik et al. 2016). Consequently, highway agencies rely on the low-temperature IDT strength as a fundamental HMA material property input into the Pavement ME design software for thermal cracking analysis.

The Pavement ME design program utilizes a globally calibrated regression model to estimate the IDT strength values. The prediction model for IDT strength, at -10°C, is based on correlations with binder penetration at 77°F (25°C), the intercept of the viscosity-temperature susceptibility intercept obtained for the rolling thin film oven (RTFO) conditioned binder, voids filled with asphalt, and air voids of the HMA mixture. The globally calibrated Pavement ME IDT strength predictive model is presented in Equation 2.11 (NCHRP, 2004):

$$TS = 7416.712 - 114.016\,V_a - 0.304\,V_a{}^2 - 122.592\,VFA + 0.704\,VFA^2 + 405.71\log_{10}(Pen_{77}) - 2039.296\log_{10}(A) \quad (2.11)$$

where: TS = indirect tensile strength at -10°C, (psi), V_a = air voids in the mixture, (%), VFA = voids filled with asphalt in the mixture, (%), Pen_{77} = binder penetration at 77°F (25°C), mm/10, A = asphalt viscosity-temperature susceptibility intercept.

The Pavement ME IDT strength regression model presented in Equation 2.11 was globally calibrated and achieved a satisfactory goodness-of-fit statistics of 0.535 and 0.686 for R^2 and Se/Sy, respectively. R^2 defines the regression model's coefficient of determination, while Se/Sy is defined as the ratio between the predicted IDT strength standard error and the measured IDT strength standard deviation (AASHTO, 2015).

2.3.1.2.3 Asphalt Binder Characterization

Schwartz et al. (2011) inferred that the asphalt binder PG affects thermal cracking. Therefore, it is considered a pertinent parameter that contributes to thermal cracking analysis. Manitoba, Canada is located in a cold climatic region, in which some locations may experience extreme low air temperature of -40°C in the winter (Esfandiarpour and Shalaby, 2017a).

The global Pavement ME IDT global model requires binder penetration input values at 77°F (25°C) for IDT strength predictions. When penetration test results of the recovered binders are not readily available, penetration values can either be estimated by Level 2 or Level 3 binder grade characterization.

For Level 2 asphalt binder characterization, the binder properties (aged at RTFO condition) in terms of the complex shear modulus (G*) and phase angle (δ) were obtained in the laboratory using the Dynamic Shear Rheometer (DSR) test. The DSR test for the extracted binder was conducted at the preferred intermediate to high-temperature ranges in accordance with AASHTO T 315-12 (2012). The DSR obtained G* and δ at different temperatures were then used to estimate the binder viscosity using Equation 2.12 (Bari, 2005).

$$\eta = \frac{G^*}{10}\left(\frac{1}{Sin\,(\delta)}\right)^{4.8628} \quad (2.12)$$

where: η = viscosity of binder, cP; G* = binder complex shear modulus, Pa; δ = binder phase angle, degrees.

After obtaining the viscosity of the binder at the preferred temperatures, the regression-based viscosity-temperature relationship using Equation 2.13 was then used to determine A and VTS regression coefficients (ASTM, 2009).

$$\log(\log \eta) = A + VTS \log T_R \quad (2.13)$$

where: η = viscosity, cP; T_R = temperature in Rankine at which the viscosity was estimated; A= regression intercept and VTS = regression slope of the viscosity-temperature susceptibility.

For Level 3 asphalt binder inputs, A and VTS parameters can be obtained as default values from the Pavement ME design software by selecting the binder PG. The default parameters are then used to estimate the binder penetration at 77°F (25°C).

For both the Level 2 and Level 3 asphalt binder inputs, the penetration values at 77°F (25°C) for the extracted binders are estimated based on A and VTS regression constants using Equation 2.10.

2.3.1.2.4 Previous Assessment and Local Calibration Efforts of the IDT strength model

In Wisconsin, Bonaquist (2011) reported that Level 3 global Pavement ME IDT strength model tends to overestimate IDT strength values. In another study carried out in Michigan, Krcmarik et al. (2016b) found that Level 3 global Pavement ME IDT strength model tends to underestimate IDT strength values. These inconsistencies in the prediction accuracy of the IDT strength global model could lead to under-designed or over-designed pavements, both of which have cost and pavement performance implications to highway agencies.

It is, therefore, imperative to calibrate the IDT strength global model to local materials, traffic, and environmental conditions to improve the reliability of Level 3 thermal-cracking predictions, and establish confidence in the design procedure.

2.3.2 Unbound Granular and Subgrade Layer Material Input Predictive Models

Resilient Modulus (M_R)

The resilient modulus (M_R) or elastic modulus is an important mechanical property of UGM and subgrade material which characterizes the stress-strain relationship under repeated traffic loading (Xiao et al. 2017). A typical stress-strain relationship of the UGM and subgrade soil subjected to

one cycle of traffic loading is diagrammatically represented in Figure 2.5.

The M_R can be defined as:

"*the ratio of the amplitude of the repeated axial stress to the amplitude of the resultant axial strain*" (Mallick and El-Korchi, 2017).

The M_R is mathematically expressed as shown in Equation 2.14 (Soliman, 2015):

$$M_R = \frac{\sigma_d}{\varepsilon_r} \tag{2.14}$$

where: M_R = resilient or elastic modulus, σ_d = deviator stress or axial stress under a repeated load triaxial test, ε_r = resilient of recoverable strain.

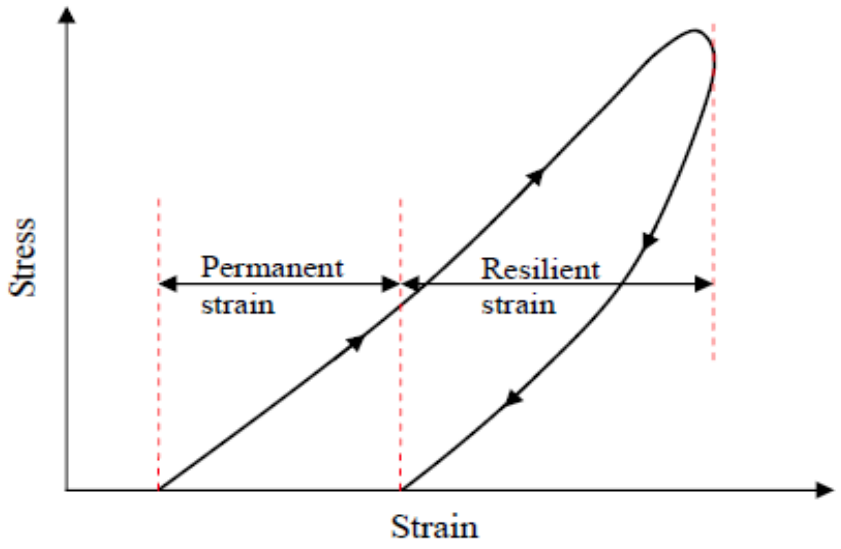

Figure 2.5: Stress-strain relationship of UGM and Subgrade soil under once repetition of traffic loading (Soliman, 2015)

Impact of Unbound Granular and Subgrade layer M_R on flexible pavement performance.

Several literature (Ahammed et al. 2013; Luo et al. 2017) have indicated that the predicted pavement performance based on Pavement ME design software shows minimal or no sensitivity

to the thickness and modulus of the unbound and subgrade layers of flexible and rigid pavements. As such, Luo et al. (2017) carried out an extensive literature review on recent studies to determine the key unbound and subgrade layer properties that affect pavement performance. It was reported that for flexible pavements, the shear strength, moisture dependency resilient modulus and permanent deformation are critical factors. M_R models developed by Luo et al. (2017), incorporating these critical factors yielded better performance predictions when compared to the Pavement ME models. However, Luo et al. (2017) stated that further calibration and validation of the developed models are required prior to implementation.

2.3.2.1 Pavement ME UGM and Subgrade M_R Predictive Models

Several predictive models, ranging from empirical regression models to non-linear stress-dependent models to stress for unbound have been developed for estimating the resilient modulus of unbound granular and subgrade soils. The resilient modulus is highly dependent on state of stress. For M-E design, the resilient modulus of subgrade and unbound materials at any given state of stress is normally predicted from the generalized universal constitutive model (NCHRP 1-28A, 2004) using regression constants k_1, k_2 and k_3 presented in Equation 2.15.

$$M_R = K_1 P_a \left[\frac{\theta}{P_a}\right]^{K_2} \left[\frac{\tau_{oct}}{P_a} + 1\right]^{K_3} \quad (2.15)$$

where:

M_R = Resilient Modulus in MPa;

$\theta = \sigma_1 + \sigma_2 + \sigma_3$ = bulk stress in kPa;

τ_{oct}= octahedral shear stress, kPa;

$$\tau_{oct} = \left(\frac{1}{3}\right)\sqrt{(\sigma_1 - \sigma_2)^2 + (\sigma_1 - \sigma_3)^2 + (\sigma_2 - \sigma_3)^2}$$

σ_1,σ_2, σ_3 = Principal stresses in kPa, and the confining pressure ($\sigma_2 = \sigma_3$) for resilient modulus test on cylindrical specimen.

P_a = atmospheric pressure at sea level (101.35 kPa);

k_1, k_2, and k_3 = regression coefficients (typically estimated by fitting Equation 2.15 to laboratory tested resilience modulus data).

2.4 Need for Local Calibration

The Pavement ME predictive models are representative of global level conditions, which do not necessarily represent local materials, traffic, climatic, and construction practices specific to each local jurisdiction (Robbins et al. 2017). As such, the local calibration guide, (AASHTO, 2010) highly recommends the evaluation of the Pavement ME prediction models to assess bias in predictions and determine if local calibration is warranted. This has led several highway agencies to investigate the reliability of the global Pavement ME predictive model to support the implementation of the Pavement ME design procedure in their jurisdiction and establish confidence in the design procedure.

Local calibration is a methodical process, which involves the elimination of bias and minimizing the standard error of estimate between the predicted and measured values (AASHTO, 2010; Esfandiarpour and Shalaby, 2017). A biased prediction model can significantly lead to under- or over–prediction of the pavement performance. The increase in precision accuracy of predictive models can also be accomplished through local calibration.

Local calibration can be achieved by adjusting the calibration parameters/coefficients in the prediction model in order to reduce the difference associated with the predicted and measured values (AASHTO, 2010). The effect of local calibration to improve bias and precision of prediction models is illustrated in Figure 2.6.

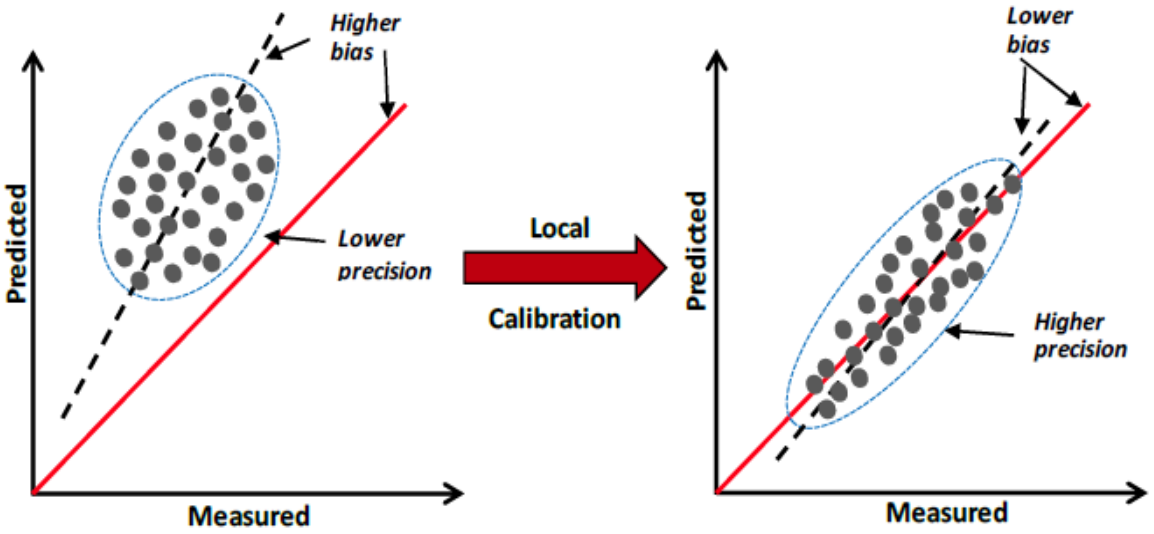

Figure 2.6: Improvement of bias and Precision through local calibration (Robbins et al. 2017)

Ideally, the term "local calibration" involves three main processes: 1) local verification of the existing global predictive model, 2) calibration of the existing global predictive model and 3) validation of the newly calibrated predictive model.

Local verification involves the assessment of the internal consistency and reasonableness of the Pavement ME global predictive model by comparing the predictions using the globally calibrated coefficients to the measured values for the desired material property. Agencies adopt the global predictive model coefficients if the variation between the measured and predicted material property values are within acceptable limits. Else, calibration of the global predictive models to

local conditions and materials by adjusting the model coefficients is necessary (Robbins et al. 2017). Validation of the locally calibrated predictive models involves a systematic process of applying independent dataset (validation dataset), which was not used in the local calibration process to re-examine if the prediction accuracy is robust and similar to the accuracy obtained from locally calibrated model.

2.4.1 Review of Local Calibration-Validation Methods

Generally, the split sample (traditional approach) and the jack-knife testing approach are two local calibration-validation methods which can be utilized to improve the accuracy of the Pavement ME global prediction models for both materials and distresses. These methods are briefly described in this subsection.

2.4.1.1 Split Sample (Traditional approach)

Split sample approach involves the random division of the dataset into two sets of samples. The dataset can be divided into half or more depending on size of the dataset. The larger portion of the divided sample is typically used for model calibration to obtain the calibrated coefficients, while the rest is used to validate the prediction accuracy of the predictive model (AASHTO, 2010).

A drawback to the use of split sample approach is the generation of misleading indicators of model accuracy when a small sample size is utilized (AASHTO, 2010). As such, the jackknife calibration-validation approach is recommended to address the drawback of the traditional split-sample approach by providing a more reliable assessment of the accuracy of prediction models. (AASHTO, 2010).

2.4.1.2 Jack-Knife Testing Approach

The jack-knife approach can be used with a small sample size of measured values. Jack-knifing process involves the random division of a data matrix of *n* sets of measured values into two groups (AASHTO, 2010). First group for model calibration and the other group for prediction. One set of measurements is removed from the data matrix and the remaining *n-1* set of measurements is used for model calibration. Thereafter, the first set of measurements initially removed is replaced and a new set of measurements is removed from the data matrix and the new *n-1* set of measurements is used to recalibrate the model. This process is repeated until the entire *n* measurements is utilized for predictions (AASHTO, 2010).

A major advantage of the jack-knifing approach is the goodness-of-fit statistics of the predictive model are developed from separate data which are not used for model calibration (AASHTO, 2010).

2.4.1.3 Calibration Methods by Different Highway Agencies

The local calibration and verification of the global Pavement ME models was evaluated by several DOT's (Ceylan et al. 2009; Darter et al. 2014; Glover and Mallela, 2009; Mallela et al. 2009; Mallela et al. 2013; Momin, 2011; Zhou, 2013).

For Colorado DOT, Advanced Research Associate (ARA) conducted local calibration and verification studies on new and overlay asphalt pavements containing modified and neat binders (Mallela et al. 2013). Dynamic modulus, creep compliance and IDT strength of the mixtures were characterized at Level 2. In addition, other mix volumetric properties were characterized at Level 3. A nonlinear optimization tool was used to calibrate the global Pavement ME models. The model accuracy criteria used for Colorado condition is presented in Table 2.3.

Table 2.3: Colorado DOT model accuracy criteria (Mallela et al. 2013)

Criterion	Test Statistics	R^2 Range/Model SEE	Rating
Goodness of Fit	R^2, percent (for all models)	81-100 Very Good 64-81 Good 49-64 <49	Very Good Good Fair Poor
	Global HMA Alligator Cracking model SEE	<5 percent 5-10 percent >10 percent	Good Fair Poor
	Global HMA Total Rutting model SEE	<0.1 in 0.1-0.2 in >0.2 in	Good Fair Poor
	Global HMA IRI model SEE	<19 in/mi 19-38 in/mi >38 in/mi	Good Fair Poor
Bias	Global HMA IRI model SEE	p-value	Reject if p-value is <0.05
	Paired t-test between measured and predicted distress/IRI	p-value	Reject if p-value is <0.05

Washington State DOT (WSDOT) utilized the traditional split sample, together with the Jack-knife method for local calibration (Li et al. 2009). Local calibration was conducted on the global alligator cracking, rutting, longitudinal cracking and fatigue cracking distress models. Li et al. (2009) also reported that the combined use of both calibration methods was done in an effort to yield accurate and stable results due to small sample size. The least root mean square error (RMSE) was used as the model accuracy indicator for the calibrated model coefficients.

Chapter 3: Progress on Local Calibration of Material Models

3.1 Introduction

One of the major steps in the local calibration process is the development of a database of laboratory-measured values to characterize the properties of local construction materials used in a particular jurisdiction. Various transportation agencies spend a lot of time and effort to obtain such pertinent information. The existing local models developed for HMA, base and subgrade materials for Manitoba are discussed in this section.

3.1.1 HMA Layer Locally Calibrated Material Characterization Models

To characterize the response of AC mixtures, Esfandiarpour and Shalaby (2017a, 2017b) tested the dynamic modulus, creep compliance and indirect tensile strength of local mixes in the laboratory. The tested mixes represent the current practices for HMA mixtures in Manitoba. A summary of the HMA material characterization database developed by the University of Manitoba's Pavement Research Group for local mixes in Manitoba is presented in Appendix A. The following subsections present the local characterization models developed for Manitoba.

3.1.1.1 HMA Dynamic Modulus Local Model (Esfandiarpour and Shalaby, 2017b)

The AC mixtures tested by Esfandiarpour and Shalaby (2017a) for characterization consisted of HMA containing RAP, and HMA containing recycled asphalt shingles (RAS). 51 samples in total from 17 types of HMA mixes were tested in accordance with AASHTO T 342-11 (2011) to obtain their dynamic modulus values. Mixes contained 0 to 50% RAP contents.

The dynamic modulus testing is normally conducted at six frequencies (25Hz, 10Hz, 5Hz, 1Hz, 0.5Hz, and 0.1 Hz) and five temperature levels (-10°C, 5°C, 25°C, 40°C, and 54°C) (AASHTO 2011). However, since soft binders are used for Manitoba mixes to minimize the impact of rutting

at high temperature (up to 35) and thermal cracking at low temperature, not all mixes were tested at 54°C.

Consequently, 576 dynamic modulus measurements were obtained for twenty-four samples tested at four temperatures and 810 dynamic modulus measurements were obtained for twenty-seven samples tested at all five temperatures. In summary, 1386 E* measurements were used to evaluate the reliability of the NCHRP 1-37A and NCHRP 1-40D models in predicting E* values for Manitoba mixes.

Figure 3.1 and Figure 3.2 present comparison between the dynamic modulus values predicted using NCHRP 1-37A and NCHRP 1-40D models and the laboratory measured values for Level 2 and Level 3 predictions. This comparison was carried out on a logarithmic scale.

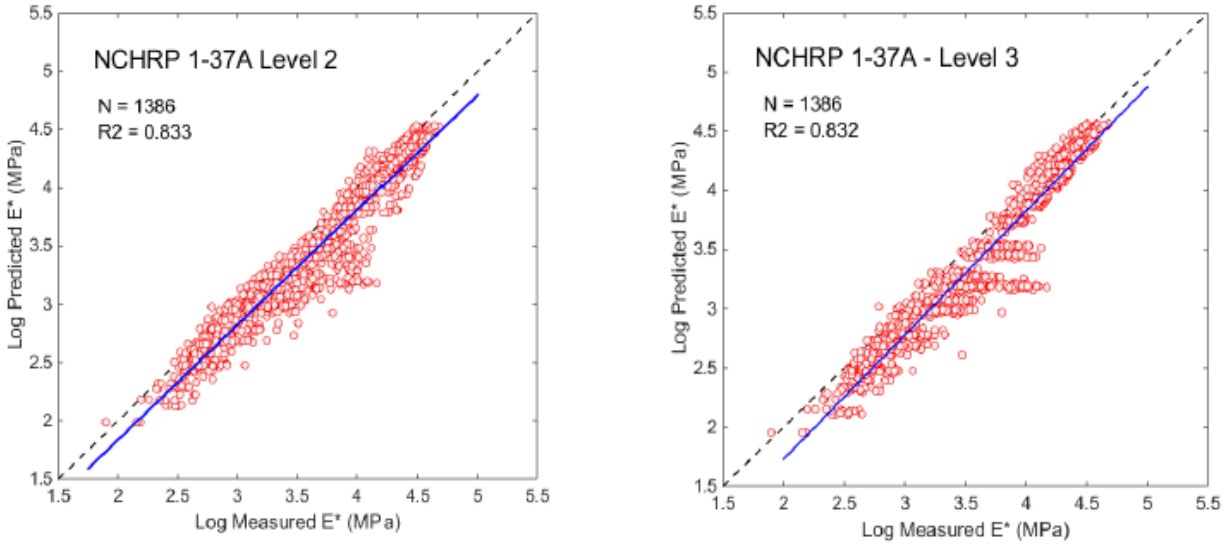

Figure 3.1: NCHRP 1-37A predicted E* values versus laboratory-measured E* for Level 2 and Level 3 asphalt binder inputs on a log-log scale (Esfandiarpour, 2017)

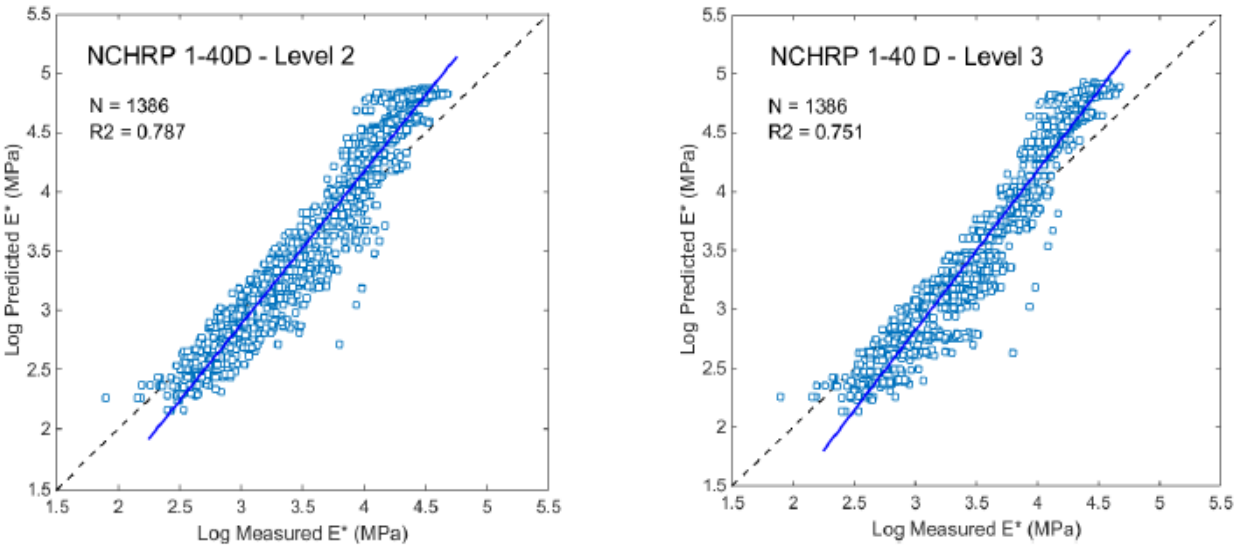

Figure 3.2: NCHRP 1-40D predicted E* values versus laboratory-measured E* for Level 2 and Level 3 asphalt binder inputs on a log-log scale (Esfandiarpour, 2017)

As seen in Figure 3.1, results from the laboratory evaluation show that at all range of temperatures, the NCHRP 1-37A model underestimates the |E*| values. On the other hand, Figure 3.2 shows that the NCHRP 1-40D model underestimate the |E*| predictions at high temperature and overestimates E* predictions at low temperature.

Consequently, local calibration on the NCHRP 1-37A and NCHRP 1-40D dynamic modulus prediction models for Level 2 and Level 3 predictions was proposed to improve the reliability of |E*| predictions for Manitoba mixes. Two local calibration alternative methods were considered to improve the reliability of the dynamic modulus global prediction models. Firstly, Esfandiarpour and Shalaby (2017a) applied an exponential fit of the NCHRP 1-37A and NCHRP 1-40D global model outputs to measured E* models. Secondly, an update of the NCHRP 1-37A and NCHRP 1-40D global models achieved using nonlinear multiple regression. Furthermore, the authors contrasted an exponential fit of the NCHRP 1-37A and NCHRP 1-40D global model output versus

an update of model coefficient using nonlinear regression and found nonlinear regression calibration technique to produce more reliable predictions of dynamic modulus values.

Results from the local calibration of each global model for Level 2 and Level 3 using exponential fit of model outputs to measured values is presented in Table 3.1. The summary statistics are also shown in Table 3.2.

Table 3.1: Exponential fit for each model in Level 2 and Level 3 (Esfandiarpour and Shalaby, 2017a)

Model	Level 2	Level 3
NCHRP 1-37A	$\log(E^*_{Calibrated}) = 0.938\log(E^*_{Predicted}) + 0.398$	$\log(E^*_{Calibrated}) = 0.893 \log(E^*_{Predicted}) + 0.563$
NCHRP 1-40D	$\log(E^*_{Calibrated}) = 0.727 \log(E^*_{Predicted}) + 0.947$	$\log(E^*_{Calibrated}) = 0.695 \log(E^*_{Predicted}) + 1.077$

Table 3.2: Summary statistics of Case 2: exponential fit of model outputs (Esfandiarpour and Shalaby, 2017a)

Scale	NCHRP 1-37A		NCHRP 1-40D	
	Level 2	Level 3	Level 2	Level 3
SSE (MPa)	39.649	32.175	33.422	29.912
R^2	0.940	0.940	0.938	0.945
Se/Sy	0.271	0.244	0.249	0.235
Slope	0.932	0.940	0.938	0.945
Intercept	0.252	0.220	0.229	0.203

SSE= sum of squared errors, R^2 = coefficient of determination, *Se* = Predicted dynamic modulus standard error, *Sy* = measured dynamic modulus standard deviation

The Pavement ME globally calibrated NCHRP 1-37A and NCHRP 1-40D dynamic modulus prediction equation are presented in Equation 3.1 and Equation 3.2 respectively. The updated

coefficients after applying nonlinear regression local calibration to these models are presented in Table 3.3 and Table 3.4.

$$\text{Log}_{10}|E^*| = -(C1) + (C2)\rho_{200} - (C3)(\rho_{200})^2 - (C4)\rho_4 - (C5)V_a - (C6)\frac{V_{beff}}{V_{beff}+V_a} + \frac{(C7)-(C8)\rho_4+(C9)\,\rho_{38}-(C10)(\rho_{38})^2+(C11)\rho_{34}}{1+e^{(-(C12)-(C13)(logf)-(C14)(log\eta))}} \quad (3.1)$$

where:

$|E|^*$ = HMA dynamic modulus, in 689 MPa (105 psi); η =binder viscosity, in poise; f = sample loading frequency, in Hz; Va = % air voids in the mix, by volume; V_{beff} = % effective binder content, by volume; ρ_{34} = % cumulative retained weight on the 3/4-in. sieve; ρ_{38} = % cumulative retained weight on the 3/8-in. sieve; ρ_4 = % cumulative retained weight on the No. 4 sieve; and ρ_{200} = % passing No. 200 sieve.

$$\text{Log}_{10}|E^*| = -(D1)+(D2)(|G_b^*|^{-(D3)})^*((D4)-(D5)\,\rho_{200} + (D6)(\rho_{200})^2 + (D7)\,\rho_4 - (D8)(\rho_4)^2 + (D9)\,\rho_{38} - (D10)(\rho_{38})^2 - (D11)V_a - (D12)\,(\frac{V_{beff}}{V_{beff}+V_a})) + \frac{(D13)+(D14)Va+(D15)\left(\frac{V_{beff}}{V_{beff}+V_a}\right)+(D16)\rho_{38}-(D17)(\rho_{38})^2-(D18)\rho_{34}}{1+e^{(-(D19)-(D20)\left(\log\left(\left|G_b^*\right|\right)\right)+(D21)(log(\delta_b)))}} \quad (3.2)$$

where: $|E^*|$ = HMA dynamic modulus, in psi; $|G_b^*|$ = complex binder shear modulus, in psi; δ_b = binder phase angle, in degree; V_a = % air voids in the mix, by volume; V_{beff} = % effective binder content, by volume; ρ_{34} = % cumulative retained weight on the 3/4-in. sieve; ρ_{38} = % cumulative retained weight on the 3/8-in. sieve; ρ_4 = % cumulative retained weight on the No. 4 sieve; and ρ_{200} = % passing No. 200 sieve.

Table 3.3: NCHRP-1-37A global and locally calibrated dynamic modulus coefficients (Esfandiarpour and Shalaby, 2017a)

Parameter	Global coefficients	Locally calibrated coefficients
C_1	1.249937	-4.81235
C_2	0.029230	0.42 905
C_3	0.001767	0.05349
C_4	0.002841	0.01998
C_5	0.058097	0.43028
C_6	0.822080	6.29353
C_7	3.871977	4.15346
C_8	0.002100	0.03492
C_9	0.003958	-0.02127
C_{10}	0.000017	-0.00168
C_{11}	0.005470	0.00547
C_{12}	0.603313	0.64591
C_{13}	0.313351	0.45174
C_{14}	0.393532	0.47811

Table 3.4: NCHRP 1-40D model default and locally calibrated dynamic modulus coefficients (Esfandiarpour and Shalaby, 2017a)

Parameter	Global coefficient	Locally calibrated coefficient
D_1	0.34900	3.70917
D_2	0.75400	2.80833
D_3	0.00520	0.02046
D_4	6.65000	2.00973
D_5	0.03200	-0.24978
D_6	0.00270	-0.03214
D_7	0.01100	0.11355
D_8	0.00010	0.00200
D_9	0.00600	-0.05228
D_{10}	0.00014	-0.00181
D_{11}	0.08000	0.24776
D_{12}	1.06000	3.87083
D_{13}	2.55800	6.75482
D_{14}	0.03200	-0.02249
D_{15}	0.71300	-0.19306
D_{16}	0.01240	-0.04551
D_{17}	0.00010	-0.00123
D_{18}	0.00980	0.09800
D_{19}	0.78140	2.24101
D_{20}	0.57850	-6.44E-08
D_{21}	0.88340	0.01588

3.1.1.2 HMA Creep Compliance Local Model (Esfandiarpour and Shalaby, 2017b)

Another study by Esfandiarpour and Shalaby (2017), reported the inaccuracy of the Pavement ME creep compliance model in predicting creep compliance values of mixes used especially in cold climates like Manitoba. This generalized model uses the binder and mix volumetric properties for Level 3 creep compliance predictions. In summary, 41 samples from 14 types of HMA mixes were tested in accordance with AASHTO T 322-07 (2011) to obtain the creep compliance values of the local mixes. The creep compliance testing was conducted at three temperatures (0°C, -10°C, and -20°C). 861 creep compliance measurements were obtained and used to evaluate the reliability of the Pavement ME globally calibrated creep compliance model. Two alternatives, nonlinear regression, and artificial neural nets (ANN) were considered for local calibration of creep compliance model. The Pavement ME globally calibrated predictive model is presented in Equation 2.7 (AASHTO 2015). The updated locally calibrated model coefficient based on nonlinear regression calibration method for the Pavement ME creep compliance model at three test temperatures is presented in Table 3.5.

Table 3.5: Default and locally calibrated creep compliance coefficients (Esfandiarpour and Shalaby, 2017b)

Parameter	Default coefficients (Level 3)	Locally calibrated coefficients		
		0°C	-10°C	-20°C
b_1	-8.5240	15.9607	-8.4431	-2.5344
b_2	0.0131	19.4842	-0.7962	0.1810
b_3	0.7957	-1.9350	-0.1614	-0.3353
b_4	2.0103	-3.7781	-0.8346	0.0129
b_5	-1.9230	-13.2820	-3.9940	-0.1763
b_6	1.1628	-1.4878	1.0927	1.1595
b_7	-0.0019	28.7711	0.6952	0.0929
b_8	-0.0460	0.1484	0.2249	0.0295
b_9	-0.0113	0.0221	0.0272	0.0001
b_{10}	0.0025	-0.0049	-0.1146	-0.0086
b_{11}	0.0016	1.7498	-0.0657	-0.0092
b_{12}	0.4605	2.0298	0.6717	0.4629

In summary, the reliability of laboratory-based inputs, default input values, and locally calibrated models inputs was compared. It was reported that the locally calibrated models showed excellent results, and are therefore a viable and efficient alternative to extensive laboratory testing.

3.1.2 Unbound Granular Base and Subgrade Layer Material Characterization Models

Further calibration and validation studies to support the implementation of the Pavement ME design method in Manitoba were carried out by Soliman and Shalaby (2014, 2015, 2016). The resilient modulus prediction models developed to improve the reliability of Level 2 design inputs of available local subgrade and unbound granular materials is discussed and presented in the subsequent sections.

3.1.2.1 Subgrade Layer Local Models (Soliman and Shalaby, 2014; Soliman, 2015)

Soliman and Shalaby (2014, 2015) characterized the subgrade materials by testing the resilient modulus of three common types of soil: high plastic clay, sandy clay, and silty sand/sandy silt. The research investigated the behavior of the tested soils under various stress states and levels of moisture content. The locations of samples collected, moisture content and AASHTO classification considered for M_R testing in the study is shown in Table 3.6. The M_R tests were performed in accordance with the NCHRP Project 1-28A test protocol developed for testing UGM and subgrade soils (Harrigan and Witczak, 2004).

The test protocol for estimating the resilient modulus of subgrade soils recommends utilizing a confining stress (σ_3) = 14 kPa and a cyclic stress ($\sigma_1 - \sigma_3$) = 41 kPa which represents the traffic induced stress states for calculating the resilient modulus (Harrigan and Witczak, 2004).

Table 3.6: AASHTO classification and moisture contents for M_R tests (Soliman and Shalaby, 2014)

Sample ID	AASHTO classification	Plasticity index (PI)	Optimum moisture content (%)	Moisture contents for M_R tests (%)
PTH 59	A-7-6 High plastic clay	56	28.2	26.0, 28.0, 30.0, 32.0
PTH 75	A-7-6 High plastic clay	27	20.4	18.0, 20.0, 22.0, 24.0
PTH 16	A-6 Sandy clay	15	14.1	12.0, 13.5, 15.5, 17.0
PTH 1-West	A-6 Sandy clay	17	13.4	10.0, 12.0, 14.0, 15.5
PTH 34	A-4 Sandy silt	0	13.0	8.0, 10.5, 13.0, 14.5
PTH 1-Portage	A-2-4 Silty sand	0	10.8	7.0, 9.0, 12.5, 15.0

The resilient modulus test results, together with the regression constants obtained for the typical Manitoba subgrade soils (high plastic clay, sandy clay, and silty sand/sandy silt) at different moisture content levels are presented in Table 3.7 through 3.9.

Table 3.7: Values of MR and Regression Constants for High Plastic Clay Soil Samples (Soliman, 2015)

Sample ID	MC (%)	γ_{dry} (kg/m^3)	k_1	k_2	k_3	M_R (MPa)	St.Dev (MPa)	CV (%)
PTH 59	28.0	1397	0.971	0.140	-2.313	63.9	0.2	0.3
	28.3	1452	1.014	0.091	-2.755	62.4	10.0	16.0
	31.0	1434	0.725	0.094	-3.415	39.7	3.1	7.9
	32.6	1409	0.588	0.094	-3.546	31.5	1.3	4.2
PTH 75	18.8	1593	1.558	0.250	-1.889	108.0	2.1	1.9
	20.4	1618	1.336	0.234	-2.842	78.7	6.4	8.1
	23.0	1484	0.788	0.271	-3.358	42.1	4.7	11.4
	23.8	1587	0.694	0.239	-3.760	34.8	2.5	7.3

Note: St.Dev = standard deviation, CV = coefficient of variation

Table 3.8: Values of MR and Regression Constants for Sandy Clay Soil Samples (Soliman, 2015)

Sample ID	MC (%)	γ_{dry} (kg/m^3)	k_1	k_2	k_3	MR (MPa)	St.Dev (MPa)	CV (%)
PTH 16	12.4	1790	1.65	0.387	-2.396	101.9	0.5	0.5
	13.6	1845	1.081	0.368	-2.73	63.2	3.9	6.1
	15.4	1819	0.581	0.635	-3.719	32.3	3.9	12.1
	16.9	1792	0.305	0.696	-3.187	15.4[a]	1.0	6.3
PTH 1-West	10.6	1787	1.521	0.405	-1.713	105.4	15.2	14.4
	12.5	1859	1.315	0.426	-2.955	73.1	8.6	11.7
	14	1836	0.811	0.491	-3.086	43.5	4.9	11.2
	15.2	1849	0.466	0.67	-3.907	20.9[a]	0.9	4.1

Note: St.Dev = standard deviation, CV = coefficient of variation

Table 3.9: Values of MR and Regression Constants for Silty Sand/Sandy Silt Soil Samples (Soliman, 2015)

Sample ID	MC (%)	γ_{dry} (kg/m^3)	k_1	k_2	k_3	MR (MPa)	St.Dev (MPa)	CV (%)
PTH 34	8.5	1757	1.1400	1.036	-1.965	66.6	2.0	2.9
	10.9	1825	1.0823	1.074	-1.970	62.8	4.9	7.8
	12.8	1851	1.1220	0.942	-2.062	65.7	3.4	5.1
	14.9	1818	1.0370	1.020	-2.346	56.9[a]	7.7	13.4
PTH 1-Portage	7.7	1773	0.929	0.913	-1.689	58.4	2.0	3.4
	7.5	1834	0.834	0.997	-1.657	51.9	0.9	1.7
	12.4	1837	0.817	0.979	-1.800	49.7	1.7	3.5
	14.0	1799	0.672	1.048	-1.925	39.5[a]	1.5	3.7

Note: St.Dev = standard deviation, CV = coefficient of variation

Locally calibrated models that relate material type, density and moisture content to the resilient modulus were developed based on tested resilient modulus for the subgrade soils. The developed

equations for the local model regression coefficients for the three types of soils (Soliman and Shalaby, 2014) are presented in Equations 3.3 through 3.11.

High plastic clay soils

$$k_1 = 1.0039 - 4.9992\ LI \tag{3.3}$$

$$k_2 = 0.2885 - 2.2575\ \frac{MC}{\%\ Silt * OMC} \tag{3.4}$$

$$k_3 = 4.0740 - 0.0690\ \frac{MC * P200}{OMC} \tag{3.5}$$

Silty sand/sandy silt soils

$$k_1 = 1.2999 - 10.766\frac{MC}{\%\ Silt * OMC} \tag{3.6}$$

$$k_2 = 0.9184 + 0.0020\ \frac{MC * P200}{OMC} \tag{3.7}$$

$$k_3 = -1.2209 - 0.0176\ \frac{MC * P200}{OMC} \tag{3.8}$$

Sandy clay soils

$$k_1 = 0.5364 - 4.2647\ LI \tag{3.9}$$

$$k_2 = 0.6059 + 1.1482\ LI \tag{3.10}$$

$$k_3 = 0.7567 - 105.35\ \frac{MC}{\%\ Silt * OMC} \tag{3.11}$$

where:

LI = liquidity index; MC = specimen moisture content, (%); OMC = optimum moisture content, (%); % clay = percentage of clay in the soil sample % silt = percentage of silt in the soil sample, (%); % P200 = percentage passing sieve no. 200.

Manitoba infrastructure has incorporated these models into their designs using both conventional empirical design tools and Pavement ME, AASHTO (2015).

3.1.2.2 Unbound Base Local Model (Soliman, 2015; Soliman and Shalaby, 2016)

In addition to the developed local models for subgrade resilient modulus prediction, the response of unbound granular materials (UGM) was also investigated by Soliman and Shalaby (2015, 2016) through testing the resilient modulus, permanent deformation, and permeability of various aggregate sources including gravel, limestone, and granite.

These sources are commonly used in the five regional jurisdictions of Manitoba. For calculating the resilient modulus of UGM, the test protocol recommends utilizing a confining stress (σ_3) of 35 kPa and a cyclic stress ($\sigma_1 - \sigma_3$) of 103kPa which represents the stress state to which the base material is subjected to (Harrigan and Witczak, 2004). The resilient modulus test results, together with the regression constants obtained for the typical Manitoba UGM (Gravel, limestone and Granite) at different moisture content levels and gradations is presented in Table 3.10 through Table 3.12.

Table 3.10: MR values and Regression Constants for Gravel UGM Gradations (Soliman, 2015)

Sample ID	MC (%)	γ_{dry} (kg/m^3)	k_1	k_2	k_3	M_R (MPa)	St.Dev (MPa)	CV (%)
GA-4	5.7	2154	0.958	1.062	-0.838	150.1	5.7	3.8
	8.7	2165	0.866	1.045	-0.760	138.2	6.7	4.9
GA-9	5.3	2202	1.331	1.143	-0.952	211.3	14.2	6.7
	7.1	2213	1.085	1.088	-0.913	168.1	2.9	1.7
GA-14.5	6.4	2192	1.422	1.264	-1.172	226	26.0	11.5
	8.0	2189	0.917	1.382	-1.223	155.6	5.3	3.4

Note: St.Dev = standard deviation, CV = coefficient of variation

Table 3.11: MR values and Regression Constants for Limestone UGM Gradations (Soliman, 2015)

Sample ID	MC (%)	γ_{dry} (kg/m^3)	k_1	k_2	k_3	M_R (MPa)	St.Dev (MPa)	CV (%)
LS-4.5	5.3	2182	1.410	1.016	-0.867	211.3	13.6	6.5
	7.6	2189	1.264	1.116	-0.968	195.7	10.3	5.3
LS-10.5	4.8	2261	1.289	1.110	-1.024	194.4	14.7	7.5
	7.6	2246	0.997	0.978	-0.698	155.4	6.0	3.9
LS-16	4.0	2293	1.581	1.165	-0.970	253.4	42.6	16.7
	6.0	2291	0.934	0.986	-0.645	149.3	5.4	3.6

Note: St.Dev = standard deviation, CV = coefficient of variation

Table 3.12: MR values and Regression Constants for Granite UGM (Soliman, 2015)

Sample ID	MC (%)	γ_{dry} (kg/m^3)	k_1	k_2	k_3	M_R (MPa)	St.Dev (MPa)	CV (%)
GR-9	4.6	2284	1.262	0.979	-0.646	200.7	26.0	13.8
	7.2	2189	0.946	1.301	-0.982	166.3	29.6	17.8

Note: St.Dev = standard deviation, CV = coefficient of variation

Locally calibrated models for UGM in Manitoba were developed for resilient modulus and compared to LTPP models. Soliman (2015) found that the proposed models provide more reliable predictions with lower root mean square error. Equations 3.12 through 3.17 show the developed models for unbound granular material in Manitoba (Soliman 2015):

Gravel

$$k_1 = 0.9804 - 0.1349\,(MC - OMC), \quad (3.12)$$

$$k_2 = 3.4675 - 0.0571\,\frac{\gamma opt}{P4} \quad (3.13)$$

$$k_3 = -4.4656 + 0.0860\,\frac{\gamma opt}{P4} \quad (3.14)$$

Limestone

$k_1 = 1.2087 – 0.1067 (MC – OMC),$ (3.15)

$k_2 = 5.1153 – 0.0949 \frac{\gamma opt}{P4}$ (3.16)

$k_3 = -5.0141 + 0.0975 \frac{\gamma opt}{P4}$ (3.17)

where:

MC = specimen moisture content; OMC = Optimum moisture content; γ_{opt} = maximum dry density (kg/m^3); P4 = percentage passing sieve No. 4.

Soliman and Shalaby (2014) recommended the validation of the developed resilient modulus local models with a larger set of data since only a limited set of data was utilized for local calibration process.

3.1.2.3 Locally Calibrated Distress Prediction Models

According to the MEPDG local calibration design guide (AASHTO, 2008), the distress prediction models are considered integral components of the Pavement ME analysis procedure. As such, the pavement distress prediction models, or transfer functions should be effectively calibrated and validated to improve the reliability of pavement performance predictions throughout its service life.

The calibration of the global distress prediction models to Manitoba local materials and conditions is yet to be achieved. In addition, the calibration of the global distress prediction models is very pertinent to pavement prediction reliability, but is out of the scope of this research. However, the global distress prediction models will be used for analysis later in chapter 6 of this thesis.

3.1.3 Gap Analysis and Research Need

The literature presented and discussed show good implementation efforts of the Pavement ME design procedure by several jurisdictions. However, there is limited research regarding the full integration of locally calibrated material characterization models for all pavement layers: HMA, base, and subgrade into the Pavement ME framework.

The developed HMA layer calibrated models (dynamic modulus and creep compliance) for Manitoba has been presented. A locally calibrated IDT strength model is yet to be developed for thermal cracking predictions in Manitoba. This thesis bridges that gap by developing a local IDT strength model to incorporate a complete set of calibrated HMA layer characterization models into the Pavement ME framework.

It is, therefore, necessary to apply and investigate the impact of integrating the Manitoba developed material characterization prediction models into the Pavement ME to improve the designs of flexible pavements.

Chapter 4: Research Methodology

4.1 Introduction

This research seeks to support the step-by-step implementation of the Pavement ME design method for adoption as a day-to-day design tool in Manitoba. For this purpose, this research work builds on and extends previous research studies to include the local calibration of the Pavement ME global predictive IDT strength model based on a comprehensive material characterization database of laboratory-measured values of local materials. The research also includes the integration of the HMA, base, and subgrade characterization models into the Pavement ME framework as a means of improving flexible pavement designs. As summarized in Chapter 3 of this thesis, the developed local models are a viable alternative to laboratory testing and provide more reliable estimates of Pavement ME design inputs when compared to default input values.

One of the recommendations proposed from the research work of Esfandiarpour (2017), was to evaluate the reliability of other HMA input prediction models used in the Pavement ME design software. As mentioned in the research gap, the reliability of the Pavement ME IDT strength prediction model is yet to be assessed. Therefore, this current research updates the database of laboratory-measured IDT strength values based on testing of additional local mixes. Results from testing additional mixes, together with the previously measured values provided in the database was used to conduct local calibration on the Pavement ME IDT strength global prediction model. This is vital to enhance the reliability of Level 3 low-temperature performance of local mixtures.

This chapter presents the research methodology developed in achieving the research objectives outlined in Chapter 1 of this thesis.

The research methodology was structured to comprise of three main phases: (1) conducting an extensive literature review of relevant studies to identify gaps and research needs, (2) calibrating the global Pavement ME IDT strength prediction model based on laboratory-measured data to improve the reliability of thermal cracking predictions, and (3) investigating the impact of integrating locally calibrated models into the Pavement ME to improve the design of flexible pavements.

The research methodology framework is shown in Figure 4.1

A breakdown of each research phase is described as follows:

Phase 1 of the research methodology was the review of relevant literature to assess pertinent gaps in the literature, which forms the basis for the need to conduct this research.

Since the Pavement ME IDT strength model is yet to be calibrated to Manitoba conditions, Phase 2 of the research methodology was to update the database of laboratory-measured IDT strength values through testing additional local mixtures. Bulk HMA mixtures from various projects across Manitoba were prepared by Manitoba Infrastructure and sent to the University of Manitoba for testing. These mixes contain virgin and RAP mixes. RAP mixes contained different amount of RAP contents ranging from 0% to 50%. Samples were prepared and compacted in the laboratory. IDT strength test was conducted on the samples to characterize the tensile strength of the mixes obtained.

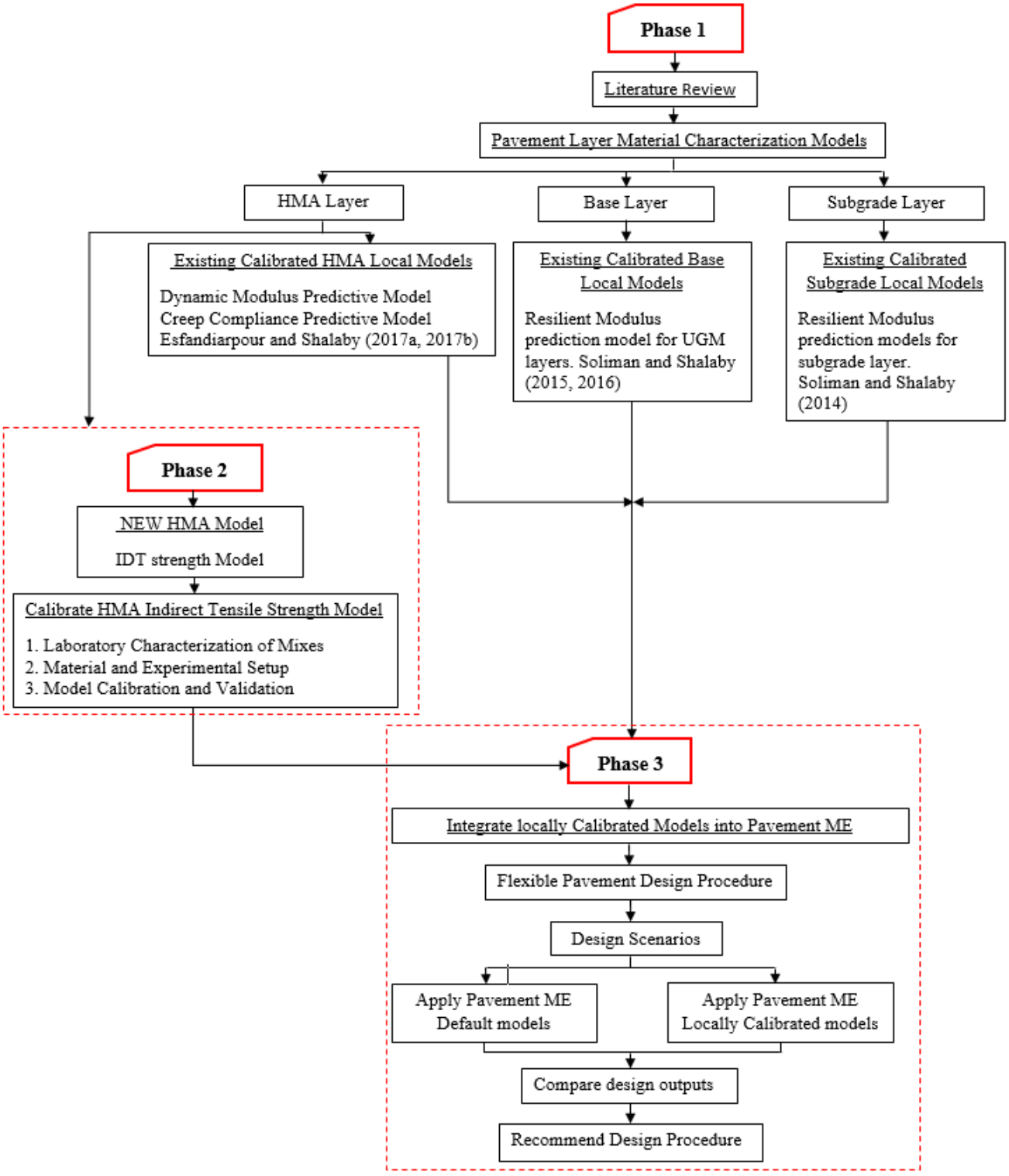

Figure 4.1: Research methodology framework

The Dynamic Shear Rheometer (DSR) asphalt binder characterization test results in terms of binder complex shear modulus (G*) and binder phase angle (δ) were obtained for local calibration of the Pavement ME IDT strength model. This data was obtained from Manitoba Infrastructure materials department. In addition, results from testing additional mixes, together with the previous laboratory-measured values contained in the database was used to conduct local calibration on the Pavement ME IDT strength predictive model. This is essential to enhance the reliability of low-temperature performance of local mixes. Simple multiple linear regression was used to update the coefficients of globally calibrated Pavement ME IDT strength prediction models to obtain more reliable strength prediction of local mixes. The IDT strength serves as an important input into the thermal cracking model (TCMODEL), which is used to simulate the initiation and propagation of thermal cracks over the pavements lifetime.

Finally, Phase 3 of the research methodology investigates the integration of the devolved locally calibrated HMA, unbound granular and subgrade material characterization models into the Pavement ME to improve the design of flexible pavements. To access the impact of the local models, a case study that comprised of different design scenarios using locally calibrated HMA, base, and subgrade material characterization models in Manitoba were compared to designs using default material values in Pavement ME. Traffic data and other pertinent default material input values were obtained from Manitoba Infrastructure. The impact of the integrated locally calibrated material models on the predicted pavement distresses for pavement sections with different traffic loadings and subgrade types were compared.

It is imperative to note that, the globally calibrated distress prediction models in the Pavement ME software was used to predict the long-term pavement performance for all design scenarios. These

globally calibrated distress prediction models are yet to be calibrated and validated to account for material, traffic and environmental conditions in Manitoba. From the obtained results of the case study, a design procedure was recommended based on the satisfactory predicted distress requirements.

4.2 Investigated Laboratory Mixes

In this study, laboratory testing was performed on 22 HMA mixtures to characterize their tensile strength. The HMA mixtures were obtained from bulk asphalt mixtures sampled from ten field projects across Manitoba. The tested mixtures were selected to represent the current practices for HMA mixtures in different regional jurisdictions of Manitoba. The field project locations are shown in Figure 4.2.

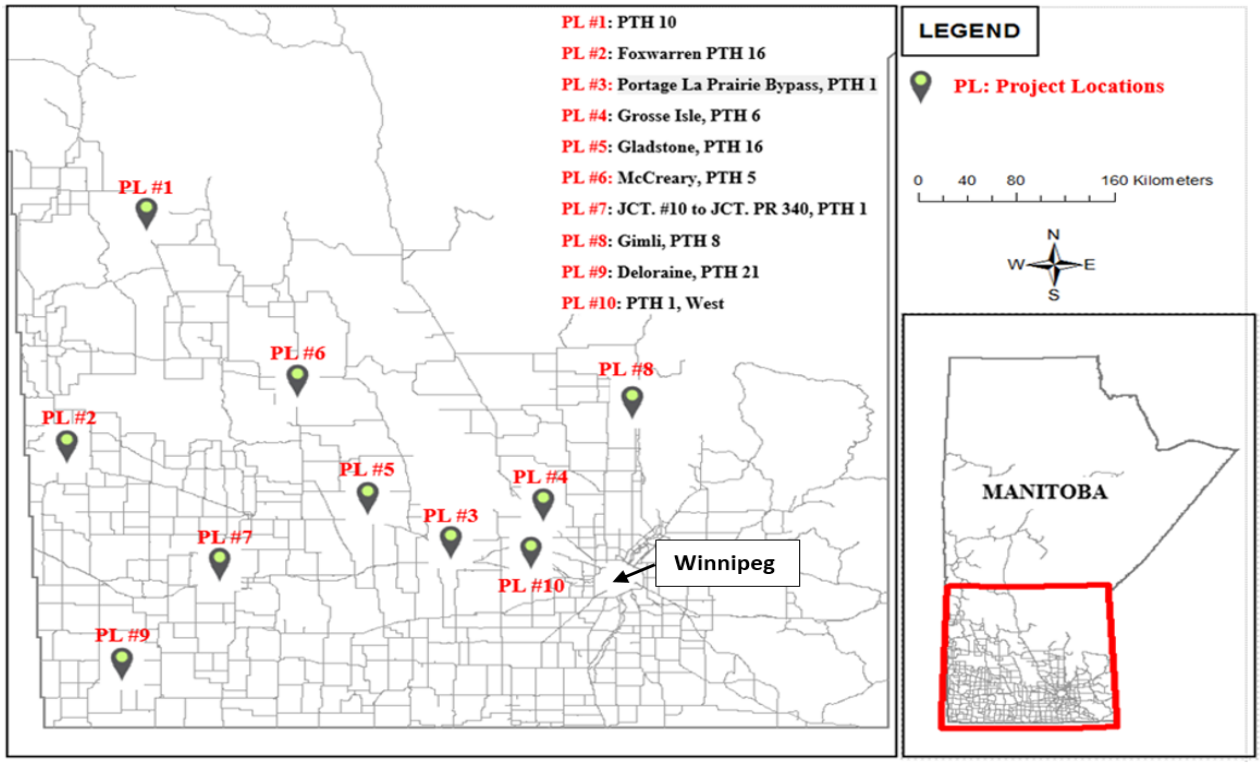

Figure 4.2: Representative field project locations used for this study.

Fifteen of the 22 HMA mixtures contain reclaimed asphalt pavement (RAP) ranging between 10% and 50%. Gyratory compaction was used to prepare three replicate samples from each investigated mixture. The mixes have a nominal maximum aggregate size of 12.5 mm and fall within specification limits. Figure 4.3 shows the aggregate gradations of the investigated mixtures. Figure 4.3 also indicates that the investigated mixes plotted with respect to the maximum density line represents a fine mix. Table 4.1 presents the standard deviation and averages of the mixture design volumetric properties used in this study. Each mix is identified by using a two-part nomenclature system. The first being an identification number, and the second is the percentage of RAP contained in the mix.

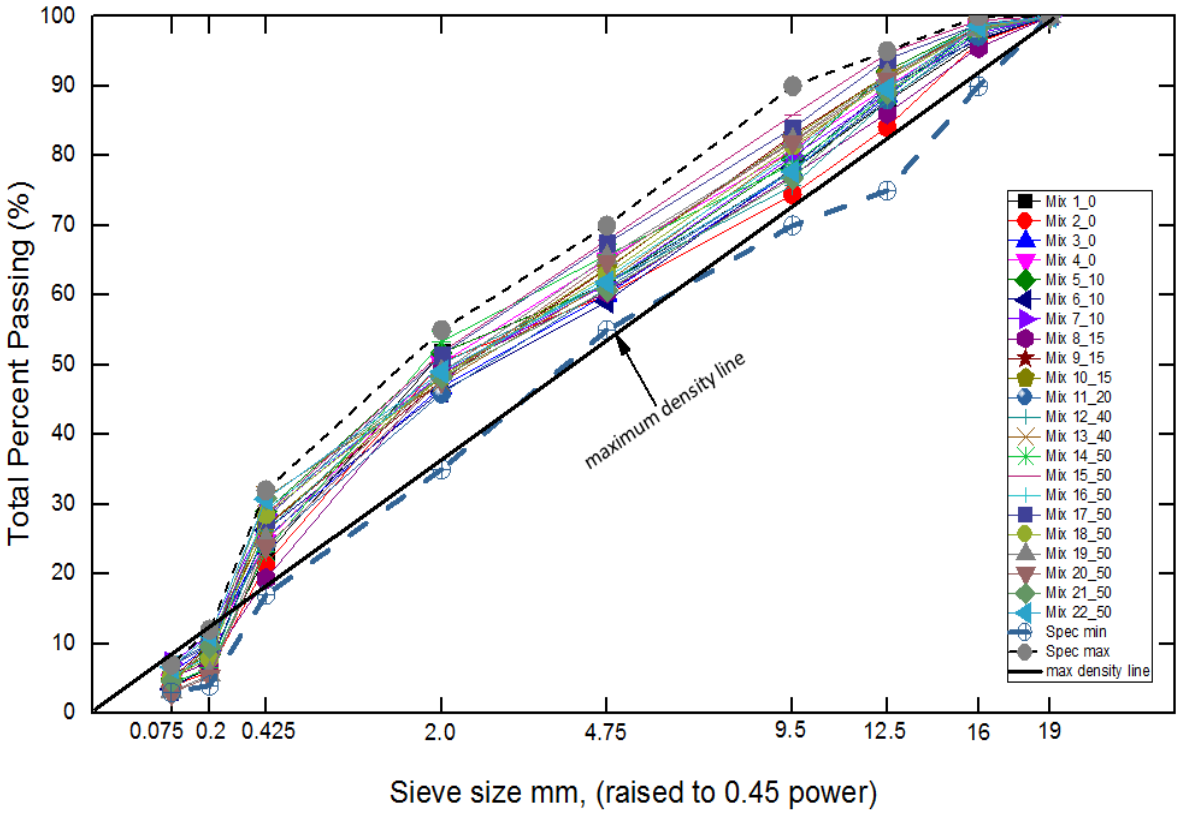

Figure 4.3: Aggregate gradations of the investigated mixtures

Table 4.1: Volumetric properties of the investigated HMA mixtures

Mix ID	RAP	AC		VMA		Va		VFA		MTSG	
	%	%	St.Dev	%	St.Dev	%	St.Dev	%	St.Dev	Avg.	St.Dev
Mix 1_15	15	5.9	0.2	15.3	0.6	3.8	0.4	75.1	2.4	2.4	0.009
Mix 2_0	0	6.4	0.1	14.3	0.4	3.3	0.5	77.0	2.8	2.4	0.007
Mix 3_10	10	6.1	0.1	14.1	0.2	3.5	0.2	75.4	1.4	2.4	0.002
Mix 4_0	0	6.1	0.2	14.5	0.2	3.4	0.3	76.7	2.0	2.4	0.004
Mix 5_40	40	6.1	0.2	13.5	0.3	3.5	0.3	73.9	1.7	2.4	0.005
Mix 6_15	15	6.2	0.3	13.8	0.3	3.6	0.5	73.8	3.0	2.4	0.007
Mix 7_40	40	4.6	0.2	12.4	0.4	4.0	0.9	67.8	6.6	2.5	0.011
Mix 8_15	15	5.6	0.3	14.3	0.3	4.0	0.1	72.4	0.9	2.5	0.003
Mix 9_20	20	5.0	0.1	13.5	0.2	3.9	0.2	70.8	1.3	2.5	0.004
Mix 10_10	10	5.5	0.1	14.0	0.2	3.7	0.2	73.8	1.0	2.5	0.004
Mix 11_40	40	5.3	0.1	11.0	0.3	3.6	0.4	67.3	2.7	2.5	0.006
Mix 12_0	0	6.6	0.2	13.6	0.3	3.4	0.3	75.3	1.9	2.4	0.003
Mix 13_15	15	6.1	0.3	14.4	0.3	3.8	0.6	73.7	4.0	2.5	0.010
Mix 14_0	0	6.9	0.2	15.9	0.4	3.3	0.5	79.3	2.7	2.4	0.012
Mix 15_40	40	5.1	0.1	12.7	0.2	4.2	0.2	66.9	1.4	2.5	0.002
Mix 16_10	10	5.4	1.1	14.1	1.0	3.7	0.6	73.6	4.6	2.5	0.016
Mix 17_50	50	5.3	0.5	12.3	0.5	3.6	0.5	70.9	3.4	2.5	0.009
Mix 18_0	0	5.2	0.3	14.1	0.5	4.1	0.7	71.0	4.8	2.5	0.011
Mix 19_0	0	6.2	0.2	14.5	0.3	3.5	0.1	75.8	0.7	2.5	0.008
Mix 20_0	0	6.2	0.3	14.6	0.2	3.8	0.3	74.0	2.0	2.5	0.007
Mix 21_15	15	5.4	0.3	13.4	0.4	3.7	0.5	72.6	3.6	2.5	0.007
Mix 22_40	40	4.8	0.3	11.6	0.4	3.3	0.2	71.6	1.7	2.5	0.006

AC = asphalt content (%); *VMA*= voids in mineral aggregates (%); *Va* = air voids (%); *VFA*= voids filled with asphalt (%)*; MTSG* = maximum theoretical specific gravity; *St.Dev* = standard deviation.

4.3 Materials and Experimental Set up

The indirect tensile strength test is a predominant test widely used to characterize the thermal-cracking behavior of HMA mixtures at low temperature. The IDT sample preparation, test procedure and test setup used to characterize and evaluate the low-temperature performance of the investigated laboratory mixes are described in the following subsections.

4.3.1 Sample Preparation

The field mixes were compacted and prepared in Manitoba Infrastructure central laboratory to meet the mix design specifications for each specific project location. These laboratory compacted samples were sawed to target a final sample thickness of approximately 50 mm and a diameter of 150 mm as shown in Figure 4.4. Three replicates samples were sent to the University of Manitoba for testing. Samples were conditioned in an environmental chamber for about 3 hours prior to testing.

Figure 4.4: Sawed IDT Strength test samples prior to environmental conditioning.

4.3.2 IDT Strength Test Procedure and Setup

The IDT strength test was conducted in accordance to testing procedure described in AASHTO T 322-07 (2011). IDT samples were tested using a servohydraulic testing machine, referred to as the

INSTRON 300 DX universal testing machine. A compressive load was applied diametrically to generate tensile stress distributions within the test sample. The tensile stress distribution occurs along the vertical diametric plane and perpendicular to the application of load, thereby, resulting in the failure of the sample by fracture (tensile failure) (Witczak et al. 1997).

According to AASHTO T 322-07 (2011), a compressive load is applied to the sample at a constant rate of 12.5 mm per minute of ram vertical displacement to failure through two loading plates. One loading plate was placed at the bottom of the sample, and the other at the top of the sample. The loading plates are necessary to allow uniform application of load across the thickness of the sample. The test was configured to stop automatically when the displacement controlled applied load decreases to 30 percent of the peak load observed from the data acquisition system. The tensile strength of each sample was calculated as a function of the observed peak failure load using Equation 4.1 (AASHTO T 322-07, 2011):

$$S_t = \frac{2\,P_f}{\pi b D} \tag{4.1}$$

where: S_t = tensile strength of sample, MPa; P_f = observed sample peak load, N; b = sample thickness, mm; D = sample diameter, mm.

Figure 4.5 shows a typical load versus displacement relationship observed during IDT strength testing of the HMA samples.

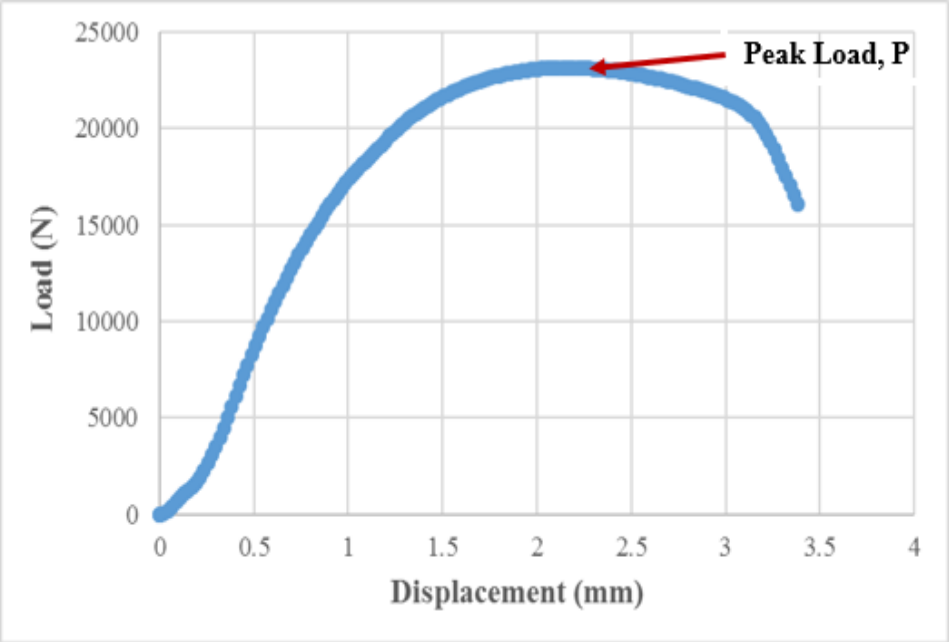

Figure 4.5: Load versus displacement relationship observed during IDT strength loading

IDT strength testing was conducted at -10°C in accordance with AASHTO T-322 (2011). IDT strength input into Pavement ME software is required at -10°C (AASHTO 2015). NCHRP 1-37A project (2004) reported that, during the Strategic Highway Research Program (SHRP) A-005 IDT strength testing program, peak strength was observed at temperatures less than -10 °C. As such, testing the IDT strength of asphalt mixes at -10°C is conservative and represents the undamaged tensile strength of the mix (Krcmarik, 2013b). Krcmarik (2013b) further defines the undamaged tensile strength as the strength of a newly constructed asphalt mixture, which has undergone no damage nor aging.

The IDT strength test is a destructive test, which could potentially lead to damage of the Linear Variable Differential Transducers (LVDTs) upon splitting (failure) of the samples. For this reason, it is also paramount to note that the LVDTs were not used to monitor horizontal and vertical

deformations of the samples during the strength test in this study. Figure 4.6 shows the testing setup used in this study.

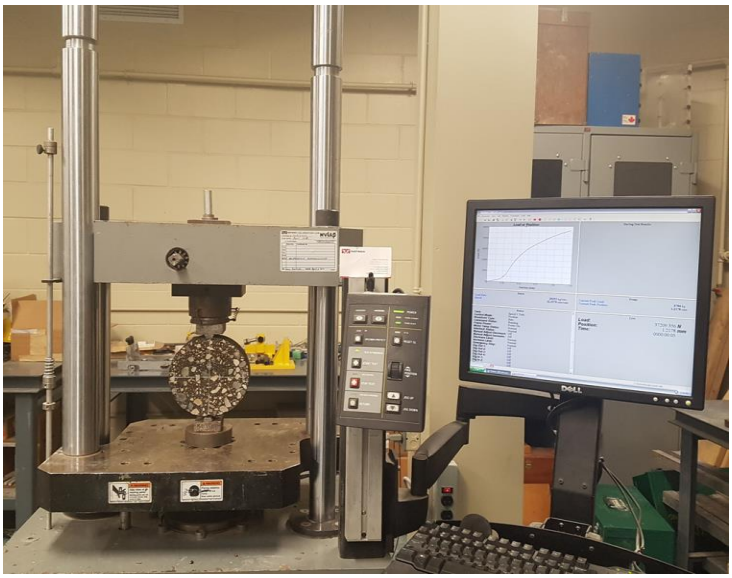

(a) Loading frame and data acquisition system

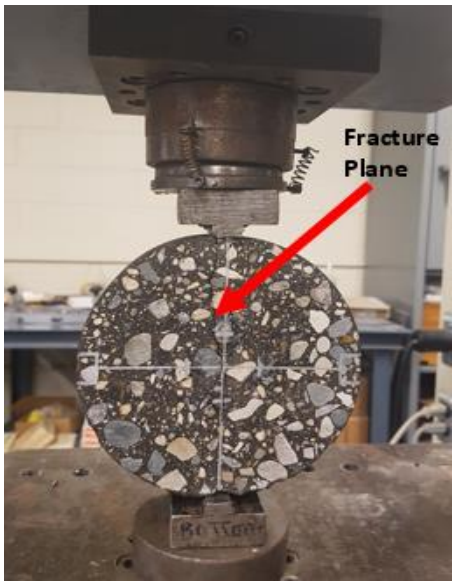

(b) Tested sample under IDT loading

Figure 4.6: IDT strength test setup and sample under indirect tensile loading.

Chapter 5: Local Calibration of IDT Strength Model of HMA Mixtures

5.1 Introduction

In Chapter 2, the global Pavement ME model utilized for estimating the IDT strength of HMA mixtures was presented and discussed. It was reported that this model produced inconsistent estimates of the IDT strength values, as such, needs to be assessed and calibrated to local HMA, if warranted.

Therefore, this chapter presents the calibration of the global Pavement ME IDT model to local HMA in Manitoba with the aim of improving the reliability of thermal-cracking predictions in the Pavement ME software. An assessment and comparison was conducted on the IDT strength predictions from the locally calibrated model, the globally calibrated Pavement ME and Michigan calibrated IDT models. In addition, a statistical analysis was conducted to validate the reliability of the global and local model prediction accuracy.

5.2 Laboratory measured IDT strength results

The IDT strength of asphalt mixtures in Manitoba were measured in the laboratory. The results from laboratory characterization were used to develop and update a database of laboratory measured IDT strength data, required to effectively assess the reliability of the global Pavement ME IDT strength model. A summary of the IDT strength material characterization database is presented in Appendix B.

Figure 5.1 presents the results of the laboratory measured IDT strength values, with varying RAP contents, used for this study.

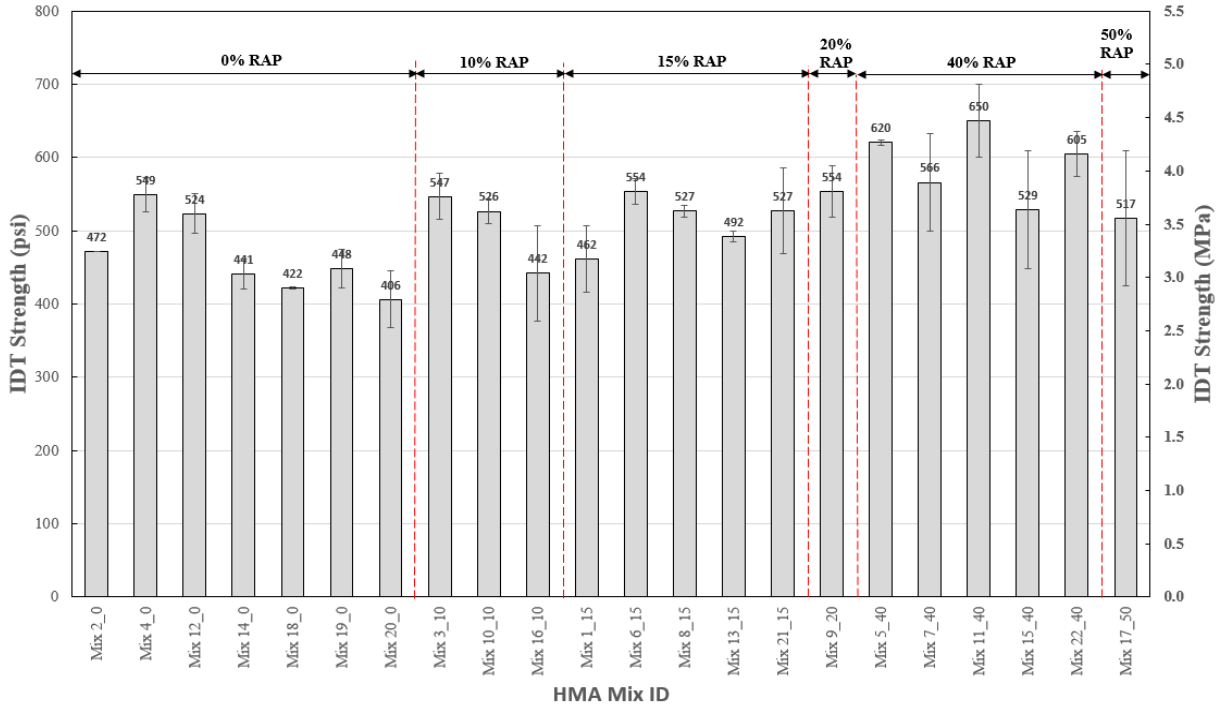

Figure 5.1: Measured IDT strength values with varying RAP contents; 1 psi = 0.00689 MPa

As seen from Figure 5.1, the measured IDT strength for the investigated mixtures were between 406 psi (2.80 MPa) to 650 psi (4.48 MPa). The average IDT strength was found to be 517 psi (3.56 MPa) with a standard deviation of 64 psi (0.44 MPa). Generally, the results show that the IDT strength values of the mixtures increased with increasing percentage of RAP contents. Similar trends were also reported in several previous studies (Huang et al. 2011; Richardson and Lusher, 2008). When the IDT strength of mixtures containing RAP contents are greater than virgin mixtures, it is generally observed that the higher percentage of RAP results in greater thermal fracture resistance of the mixtures (Zborowski and Kaloush, 2007). However, both laboratory and field assessments of mixes containing high RAP contents is recommended to evaluate the long-term impact of high percentage of RAP on not only thermal cracking performance, but other key

pavement distress performance measures such as International Roughness Index (IRI), rutting, fatigue cracking, etcetera.

5.3 Prediction of IDT strength values

5.3.1 Asphalt Binder Characterization Results.

In this study, four different extracted asphalt binders were utilized, namely; PG 58-28, PG 52-28, PG 58-34 and PG 64-16. Table 5.1 presents a summary of the predicted Level 2 and Level 3 A, VTS, and the corresponding Pen_{77} values for the binder penetration grade used in this study. In addition, Table 5.1 shows the R^2 values obtained from fitting Equation 2.13 for Level 2 binder input details. The regression fit produced high R^2 values close to one, indicating excellent fit. Since Level 3 binder inputs were obtained from default values in the Pavement ME software, no R^2 values was obtained. The Level 3 A and VTS binder regression constants were higher than those obtained for Level 2 binder inputs. This trend was also reported in previous studies, Esfandiarpour and Shalaby (2017a), and Khattab et al. (2014, 2017)

Table 5.1: Level 2 and Level 3 A and VTS coefficients for investigated recovered binders

Mix ID	Extracted Binder PG	Level 2				Level 3[1]		
		A	VTS	R^2	Pen_{77}	A	VTS	Pen_{77}
Mix 1_15	58-28	10.493	-3.512	0.999	93.490	11.010	-3.701	92.061
Mix 2_0	58-28	10.436	-3.491	0.998	93.398	11.010	-3.701	92.061
Mix 3_10	58-28	10.222	-3.414	0.999	101.960	11.010	-3.701	92.061
Mix 4_0	58-28	10.222	-3.414	0.999	101.960	11.010	-3.701	92.061
Mix 5_40	58-28	10.133	-3.385	0.999	122.477	11.010	-3.701	92.061
Mix 6_10	58-28	10.133	-3.385	0.999	122.477	11.010	-3.701	92.061
Mix 7_40	58-28	10.133	-3.385	0.999	122.477	11.010	-3.701	92.061
Mix 8_15	58-28	9.9987	-3.343	0.999	172.025	11.010	-3.701	92.061
Mix 9_20	58-28	10.369	-3.472	0.998	122.136	11.010	-3.701	92.061
Mix 10_10	58-28	9.8746	-3.294	0.999	141.258	11.010	-3.701	92.061
Mix 11_40	52-34	10.492	-3.522	0.998	159.090	10.707	-3.602	168.116
Mix 12_0	52-28	10.211	-3.413	0.999	117.787	11.010	-3.701	92.061
Mix 13_15	58-28	10.038	-3.345	0.999	91.961	11.010	-3.701	92.061
Mix 14_0	52-28	10.231	-3.311	0.999	71.723	11.010	-3.701	92.061
Mix 15_40	58-28	10.906	-3.658	0.999	70.285	11.010	-3.701	92.061
Mix 16_10	58-28	9.7438	-3.231	0.999	67.162	11.010	-3.701	92.061
Mix 17_50	64-16	10.530	-3.515	0.999	53.622	11.375	-3.822	46.229
Mix 18_0	58-28	10.110	-3.373	0.999	102.116	11.010	-3.701	92.061
Mix 19_0	58-28	10.211	-3.413	0.999	117.787	11.010	-3.701	92.061
Mix 20_0	52-34	11.047	-3.722	0.993	131.822	10.707	-3.602	168.116
Mix 21_15	58-28	10.133	-3.385	0.999	112.477	11.010	-3.701	92.061
Mix 22_40	58-28	10.133	-3.385	0.999	122.477	11.010	-3.701	92.061

Note:[1] *obtained as default values, no* R^2

A = asphalt viscosity-temperature susceptibility intercept; *VTS* = regression slope of the binder viscosity-temperature relationship*;* Pen_{77} = binder penetration at 77 °F (25°C), mm/10.

5.3.2 Assessment of Pavement ME IDT Strength Global Model

The laboratory measured IDT strength values for the investigated mixtures were plotted against the IDT strength values predicted from the global Pavement ME model in Equation 2.11, for Level 2 and Level 3 binder inputs. Figure 5.2 shows the comparison plot of the laboratory measured and global Pavement ME predicted IDT strength values for Level 2 and Level 3 asphalt binder inputs, respectively. The line of Equality (LOE) is shown in the plots.

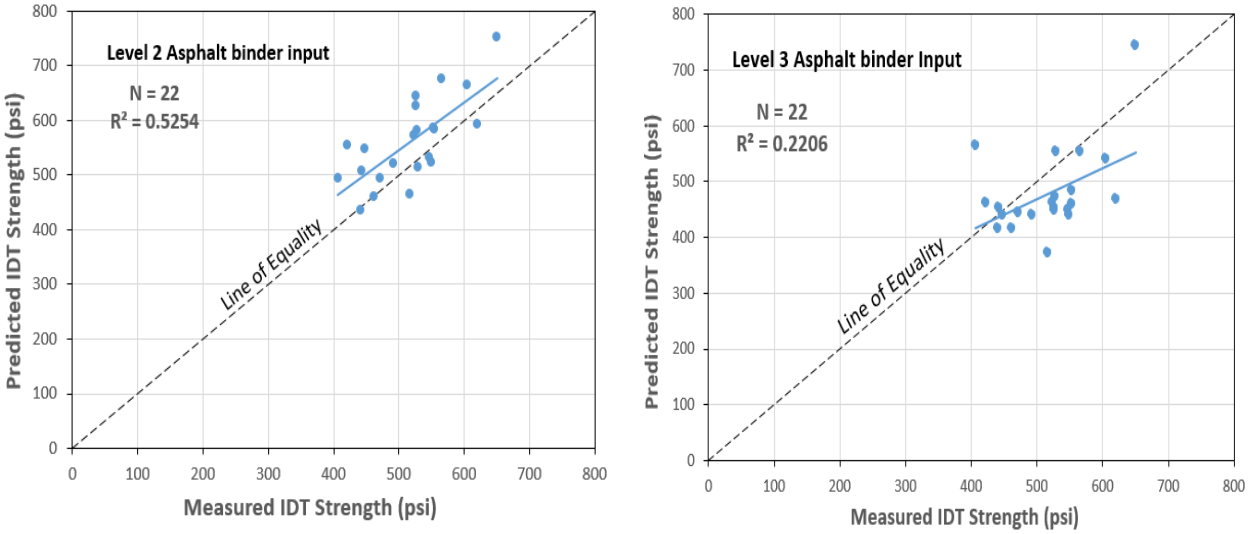

(a) Level 2 PG binder inputs (b) Level 3 PG binder inputs

Figure 5.2: Global Pavement ME model predicted IDT strength values versus laboratory measured IDT strength values of investigated mixtures; 1 psi = 0.00689 MPa

The global Pavement ME model predictions as seen in Figure 5.2, tends to overestimate the IDT strength values for Level 2 binder inputs, while the IDT strength values are generally underestimated for Level 3 asphalt binder inputs. A statistical approach, as recommended by the AASHTO local calibration guide (AASHTO, 2010), was used to determine the bias in global model predictions, assess the variability of the data and compute goodness of fit statistics. Computed prediction accuracy indicators include: (i) standard error of the predicted IDT strength values (Se), (ii) standard deviation of the laboratory measured IDT strength values about the measured mean (Sy) (iii) sum of squared errors (SSE), and (iv) R^2 values. An indication of an improvement in the model prediction accuracy is determined by the ratio between Se and Sy (Se/Sy) (Khattab et al., 2014).

Table 5.2 presents the summary of statistics for the global Pavement ME IDT model for the investigated mixes at both Level 2 and Level 3 binder inputs. The R^2 and Se/Sy values for global model Level 2 binder input were found to be 0.525 and 1.249, respectively. For Level 3 binder

input, the global model R^2 and Se/Sy values were computed as 0.221 and 1.480 respectively. As such, the R^2 value for the global Pavement ME IDT model for Level 2 binder input was higher when compared to Level 3 binder input. The Se/Sy value for Level 2 binder input was lower than Level 3 binder input. This indicates that the global Pavement ME IDT model predicts the IDT strength values more accurately for Level 2 binder inputs than for Level 3 binder inputs. However, when the intercept and slope of the linear fit for both binder inputs were calculated, it was found that the global model predicts the IDT strength values with a high bias for both binder Levels. The large values of SSE, 103.1E+3 psi and 144.9E+3 psi for Level 2 and Level 3 binder inputs respectively, further denotes high bias in IDT predicted values. These inconsistencies in the accuracy of the global Pavement ME model prediction using Level 2 and Level 3 binder inputs can have a significant impact on the thermal cracking predictions. In summary, the goodness of fit results show a poor correlation and this gives an indication that the global Pavement ME IDT model cannot be adequately relied upon in predicting the IDT strength values for Manitoba mixtures.

Table 5.2: Summary statistics of Global Pavement ME IDT model for Level 2 and Level 3 binder inputs.

Global Pavement ME model accuracy indicators	Binder Input Level	
	Level 2	Level 3
Sample size (N)	22	22
R^2	0.525	0.221
Se/Sy	1.249	1.480
Slope	0.878	0.558
Intercept	106.390	190.090
SSE (psi)	103.1E+3	144.9E+3

1 psi = 0.00689 MPa

Note: R^2 = coefficient of determination; *Se* = standard error of predicted IDT strength; *Sy* = standard deviation of measured IDT strength values about the mean; *SSE*= sum of squared errors.

5.3.3 Local Calibration of the Globally Calibrated IDT Model

Results of the assessment of the global Pavement ME IDT strength model emphasized the unreliability of the global model for thermal cracking predictions for local agencies. Krcmarik et al. (2016b) reported that due to poor estimations of IDT strength using the IDT global model, the Pavement ME design software could predict higher thermal cracking rates, which consequently results in overdesigned pavement structures. Therefore, the need for local calibration is apparent to improve the accuracy of IDT strength predictions for local agencies. Different local calibration techniques, ranging from regression (linear and nonlinear), artificial neural network (ANN) to genetic algorithms have been utilized to improve the accuracy of prediction models. In this study, multiple linear regression was conducted to update the coefficients of the global Pavement ME IDT model for Manitoba, thereby reducing the sum of the squares of the residuals between the laboratory measured and predicted IDT strength values.

The global Pavement ME IDT strength model takes a linearized form. For this reason, the same multiple linear regression model was utilized for local calibration. The global Pavement ME IDT strength model comprises of seven coefficients, a_1 to a_7 as shown in Equation 2.11. To perform local calibration, new calibrated coefficients were developed from Equation 5.1 (NCHRP, 2004), using the measured IDT values of the investigated mixtures.

$$TS = a_1 - a_2 V_a - a_3 {V_a}^2 - a_4 VFA + a_5 VFA^2 + a_6 \log_{10}(Pen_{77}) - a_7 \log_{10}(A) \quad (5.1)$$

where: TS = indirect tensile strength at -10°C, (psi), V_a = air voids in the mixture, (%), VFA = voids filled with asphalt in the mixture, (%), Pen_{77} = binder penetration at 77°F, mm/10, A = asphalt viscosity-temperature susceptibility intercept.

The laboratory-measured IDT strength data set for the twenty-two HMA mixtures were fitted to Equation 5.1 to update the model coefficients based on Level 2 and Level 3 binder inputs. The results of the locally calibrated Manitoba model IDT coefficients for Level 2 and Level 3 binder input are shown in Table 5.3 The global Pavement ME IDT strength coefficients are also for comparison.

Table 5.3: Global Pavement ME coefficients and locally calibrated Manitoba coefficients for Level 2 and Level 3 asphalt binder inputs for the investigated mixes.

Coefficient	Global Pavement ME model	Locally calibrated Manitoba model	
		Level 2 binder input	Level 3 binder input
a_1	7416.712	4704.553	683438.547
a_2	-114.016	96.435	1840.390
a_3	-0.304	-37.908	-280.576
a_4	-122.592	-77.274	-85.117
a_5	0.704	0.398	0.410
a_6	405.710	149.918	-28151.153
a_7	-2039.296	-806.968	-601417.059

Figure 5.3 shows the locally calibrated Manitoba model predicted IDT strength values versus the measured IDT strength values for Level 2 and Level 3 binder inputs, respectively. The line of Equality (LOE) is also shown in the plots. The result shows that the locally calibrated IDT strength predictions for Level 2 and Level 3 binder inputs are closer to the LOE compared to predictions from the global Pavement ME model predictions (shown in Figure 5.2). This indicates an improvement in the prediction accuracy of the locally calibrated IDT model for the investigated mixes.

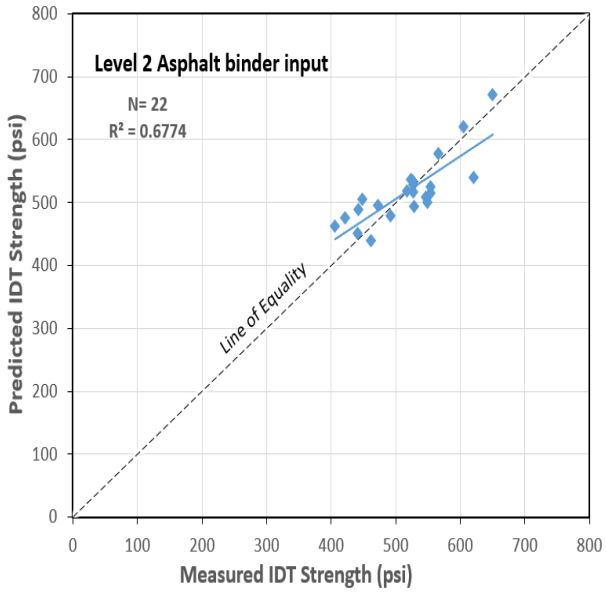

(a) Level 2 PG binder inputs

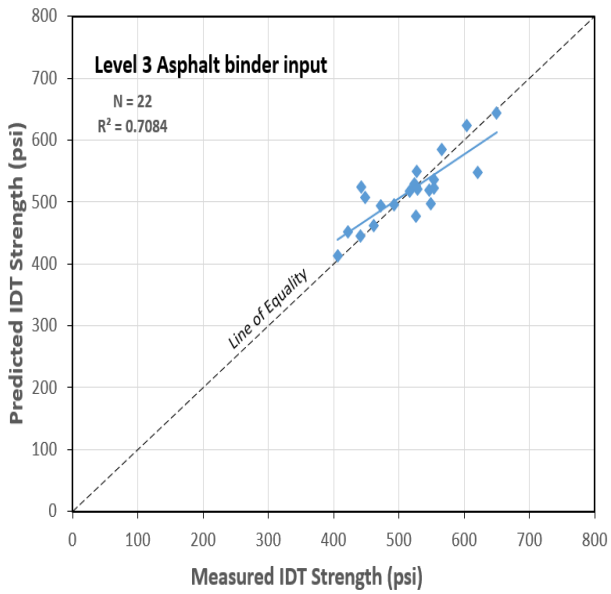

(b) Level 3 PG binder inputs

Figure 5.3: Locally calibrated Manitoba predicted IDT strength values versus laboratory measured IDT strength values of the investigated mixtures; 1 psi = 0.00689 MPa

Visual inspection alone is insufficient in examining the improvement in the accuracy of the locally calibrated Manitoba predictions. As such, an evaluation of the goodness of fit statistics was necessary. Table 5.4 presents the summary statistics for the locally calibrated Manitoba IDT strength model. The locally calibrated IDT strength model predictions produced R^2 and Se/Sy values of 0.667 and 0.651, respectively for Level 2 binder inputs. The R^2 and Se/Sy values for Level 3 binder inputs were found to be 0.708 and 0.619, respectively. The SSE of the multiple linear regression model was 28.0E+03 (psi) and 25.3E+03 (psi) for Level 2 and Level 3 binder inputs, respectively. This indicates a 72.8% reduction in SSE for Level 2 binder inputs and an 82.7% reduction in SSE for Level 3 binder inputs when compared to the global Pavement ME IDT model. Based on an overall comparison of the model accuracy indicators in Table 5.2 to those in Table 5.4, it is observed that the locally calibrated model shows good improvement for Level 2

binder inputs and significant improvement for Level 3 binder inputs over the global Pavement ME IDT strength model.

Table 5.4: Summary statistics of locally calibrated Manitoba model for Level 2 and Level 3 binder inputs for the investigated mixes.

Locally Calibrated Manitoba model accuracy indicators	Binder Input Level	
	Level 2	Level 3
Sample size (N)	22	22
R^2	0.677	0.708
Se/Sy	0.651	0.619
Slope	0.667	0.708
Intercept	167.020	151.170
SSE (psi)	28.0E+03	25.3E+03

1 psi = 0.00689 MPa

Note: R^2 = coefficient of determination, *Se* = standard error of predicted IDT strength, *Sy* = standard deviation of measured IDT strength values about the mean, *SSE*= sum of squared errors.

5.3.3.1 Effect of Multicollinearity on Locally Calibrated Model

It is pertinent to note that some of the locally calibrated coefficients of the predictor variable for Level 3 binder inputs in Table 5.3 appear to be much larger than for Level 2 binder inputs for the investigated mixes. A likely reason for the much larger predictor coefficients is the effect of multicolliearity in the calibration data set. The existence of linear dependency (high degree of correlation) between two or more predictor variables in a dataset is defined as multicollinearity (Zhang et al. 2015). A common contributing factor to multicollinearity is having a large number of predictor variables with a very small data sample size (Zhang et al. 2015). This leads to overfitting of the regression model (Hawkins, 2004).

As a result, further data exploration was conducted to determine if one or more predictor variables in the calibration data are highly correlated. To achieve this, a Pearson's correlation coefficient,

R, and a variance inflation factor (VIF) were used to examine if multicollinearity existed between predictor variables in the dataset. The VIF was computed for each predictor variable, against the other predictor variables, using Equation 5.2 (Zhang et al., 2015):

$$\text{VIF} = \frac{1}{1-R^2} \tag{5.2}$$

Where: R^2 is the coefficient of determination obtained when a predictor variable is regressed with other predictor variables in the dataset.

A predictor variable having a VIF greater than 10 indicates high multicollinearity (Zhang et al. 2015). Figure 5.4 shows the Level 2 binder input correlation matrix and the p-value significance for all predictor variables in the IDT model equation for the investigated mixes dataset. A correlation coefficient greater than 0.95 is said to have a high degree of correlation (Zhang et al. 2015). Table 5.5 presents the Level 2 binder input VIF calculation for the correlation matrix of the predictor variables in the locally calibrated Manitoba model.

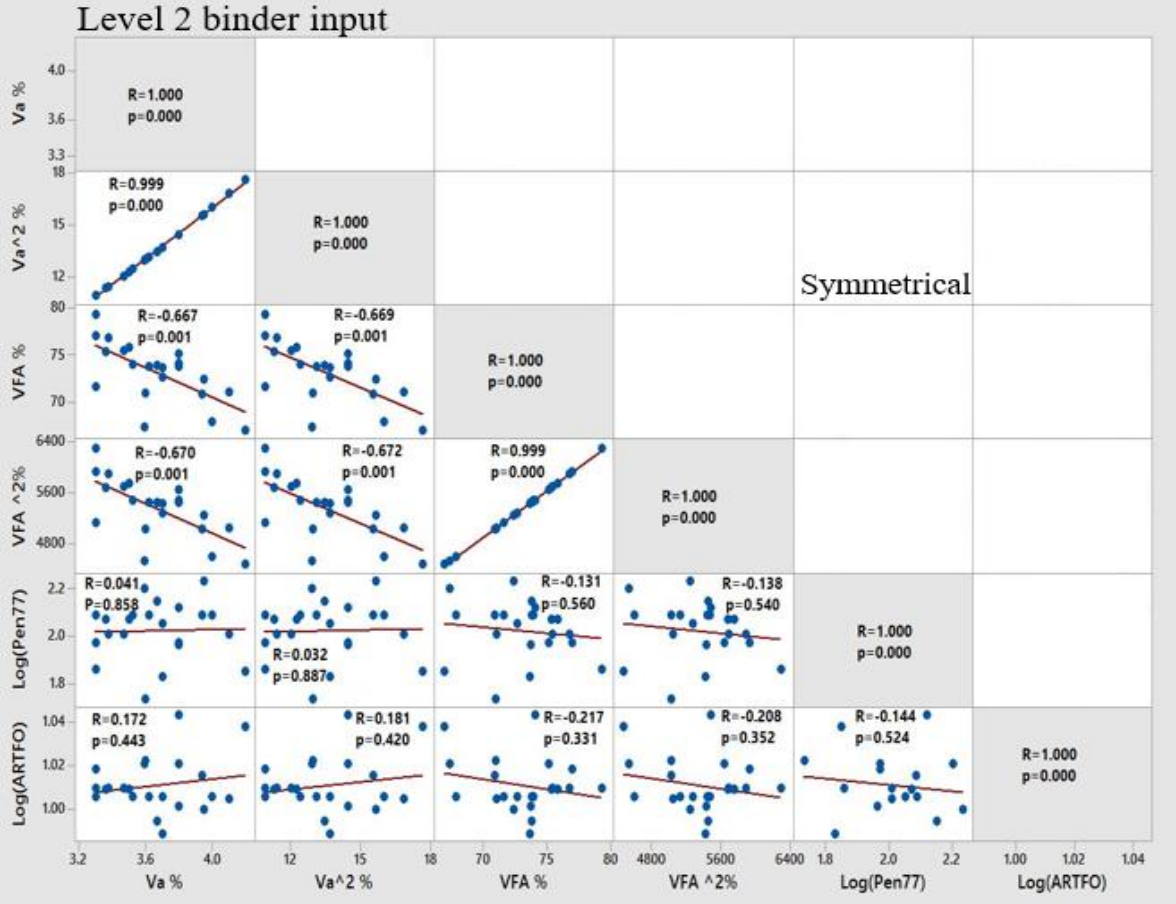

Figure 5.4: Level 2 binder input correlation matrix for the predictor variables.

Table 5.5: Level 2 binder input VIF values for predictor variable in locally calibrated Manitoba model

Term	Coefficient	Se Coefficient	T-Value	P-Value	VIF[1]	Threshold VIF >10
Constant	4705	4710	1.00	0.334		
Va%	96	1195	0.08	0.937	1130.79	High
Va^2%	-38	161	-0.24	0.817	1127.00	High
VFA%	-77	141	-0.55	0.593	2241.73	High
VFA^2%	0.398	0.976	0.41	0.689	2251.68	High
log(Pen_{77})	149.9	80.7	1.86	0.083	1.13	Low
log(ARTFO)	-807	824	-0.98	0.343	1.21	Low

Note[1]: *VIF* = variance inflation factor; *Se* = standard error; *T-value* = test statistics; *P-value* = probability value at 95% confidence level.

Figure 5.5 shows results of the Level 3 binder inputs correlation matrix and the p-value significance for all predictor variables IDT model equation for the investigated mixes dataset. Table 5.6 presents the Level 3 binder inputs VIF calculation from the correlation matrix for the predictor variables in the locally calibrated Manitoba model.

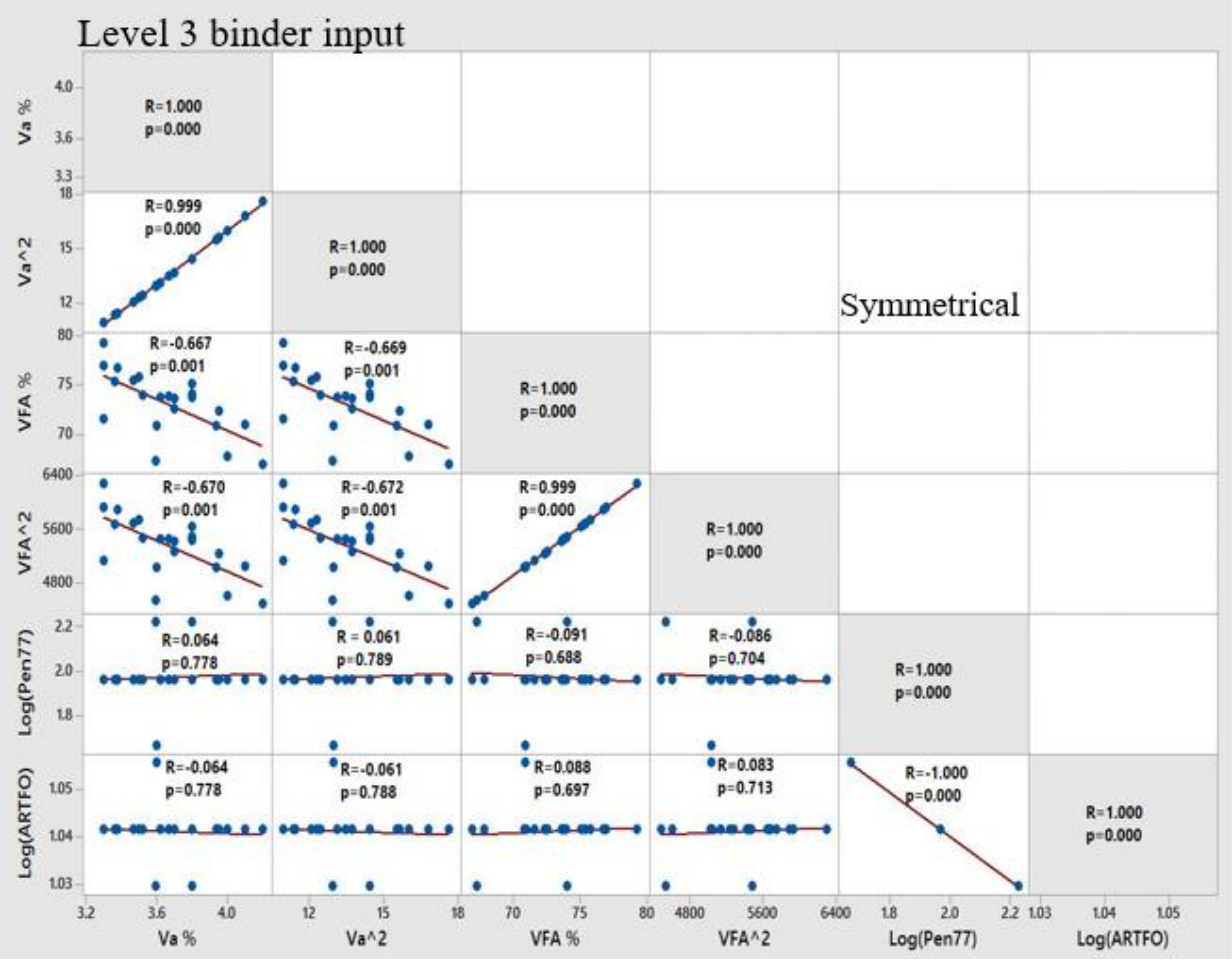

Figure 5.5: Level 3 binder input correlation matrix plot for the predictor variables

Table 5.6: Level 3 binder input VIF values for predictor variables in locally calibrated model

Term	Coefficients	SE Coefficients	T-Value	P-Value	VIF[1]	Threshold VIF > 10
Constant	683439	260726	2.62	0.019		
Va %	1840	1286	1.43	0.173	1446.96	High
Va^2	-281	174	-1.61	0.128	1455.57	High
VFA%	-85	138	-0.62	0.546	2348.59	High
VFA^2	0.410	0.947	0.43	0.671	2341.38	High
log(Pen_{77})	-28151	10752	-2.62	0.019	15367.37	High
log(ARTFO)	-601417	229693	-2.62	0.019	15333.19	High

Note[1]: *VIF* = variance inflation factor; *Se* = standard error; *T-value* = test statistics; *P-value* = probability value at 95% confidence level.

From the results, the correlation coefficient shown in Figure 5.4 and Figure 5.5, and the VIF calculations reported in Table 5.5 and 5.6, it can be observed that VIF values for most of the predictor variable were relatively high, having a VIF greater than 10, except for Level 2 log(Pen_{77}) and log(ARTFO). This confirms the existence of multicolliearity in the investigated mixes dataset.

The multicollinearity in the investigated mixes dataset could be attributed to the following reasons: (a) the lack of variability in the binder type, (b) relatively small (insufficient) data set and, (c) small range of values in the mix design properties such as air voids and voids filled with asphalt. However, it is pertinent to note that the VIF values for Level 2 binder properties, log(Pen_{77}) and log(ARTFO) have values of 1.13 and 1.21, which indicates very low level of multicollinearity. The effect of multicollinearity in the investigated mixes data, with Level 3 asphalt binder input, is more pronounced than for Level 2 asphalt binder input.

For the Level 2 binder input locally calibrated Manitoba coefficients, the increase in log(Pen_{77}) penetration value results in an increase in the IDT strength. This is reasonable, as a more flexible

HMA mixture is desired for low-temperature resistance to thermal fracture. However, the effect of multicollinearity on Level 3 binder inputs is evident as seen in Table 5.3. The Level 3 binder input coefficient associated with the log(Pen_{77}) variable changes in both magnitude and sign, which is opposite in trend to the global Pavement ME coefficients. Based on the high multicollinearity, wrong magnitude and sign of the log(Pen_{77}) coefficients, using the Level 3 binder inputs could result to inaccurate IDT strength predictions. Therefore, for this study, the results from locally calibrated Manitoba IDT model with Level 2 binder input is more reliable and is recommended.

5.3.3.2 Calibrated Michigan Pavement ME IDT Strength Model

Krcmarik et al. (2016b) performed local calibration on the Pavement ME IDT strength model to improve IDT strength predictions for Michigan mixtures. The calibrated Michigan IDT model is presented in Equation 5.3 (Krcmarik et al. 2016).

$$TS = 6377.5873 - 112.9216\,V_a - 0.3039\,{V_a}^2 - 122.5112\,VFA + 0.8589\,VFA^2 - 246.1319\log_{10}(Pen_{77}) - 346.4313\log_{10}(A) \quad (5.3)$$

where: TS = indirect tensile strength at -10°C, (psi), Va = air voids in the mixture, (%), VFA = voids filled with asphalt in the mixture, (%), Pen_{77} = binder penetration at 77°F (25°C), mm/10, A = asphalt viscosity-temperature susceptibility intercept.

The calibrated Michigan model was used to determine its applicability and reasonableness for predicting the IDT strength for the investigated HMA mixtures. Manitoba data set was applied to the calibrated Michigan IDT strength model to predict the IDT strength. The calibrated Michigan model predicted IDT strength values were plotted against the laboratory measured IDT strength for the investigated mixes. Figure 5.6 shows the comparison of the laboratory measured and

calibrated Michigan model predicted IDT strength values for Level 2 and Level 3 binder inputs, respectively for the investigated mixes.

The calibrated Michigan model, as seen in Figure 5.6, tends to overestimate the IDT strength for the Level 2 and Level 3 binder inputs. This may be attributed to the effect of the RAP contents in Manitoba mixtures and the stiffer binder grades used in Michigan.

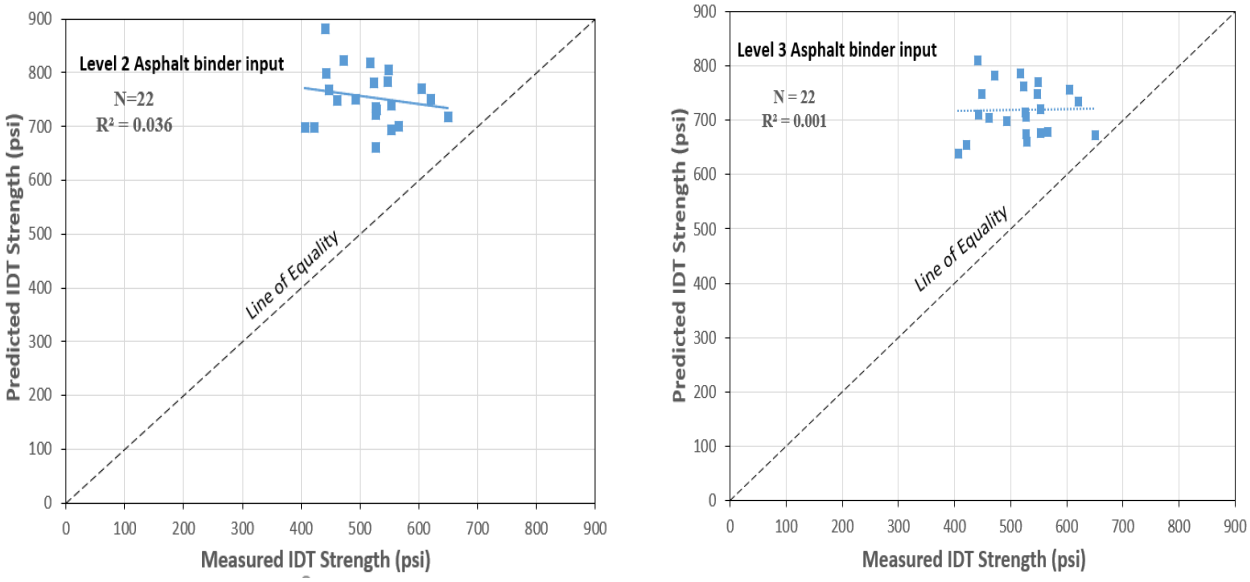

(a) Level 2 PG binder inputs (b) Level 3 PG binder inputs

Figure 5.6: Michigan calibrated IDT predicted strength for Level 2 and Level 3 binder inputs for the investigated mixes; 1 psi = 0.00689 MPa

The summary statistics from the calibrated Michigan IDT model is presented in Table 5.7. Based on the results of the summary statistics, it was found that Michigan calibrated IDT model produced very poor estimates of the IDT strength for the investigated mixes, with a very high degree of bias and inaccuracy. Although the calibrated Michigan model is suitable for mixtures used in Michigan, its overall performance showed that this model is unsuitable for use in predicting the IDT strength

for the investigated mixtures. As such, this highlights the importance of local calibration of the IDT strength model for Manitoba.

Table 5.7: Summary statistics of calibrated Michigan Pavement ME model for Level 2 and Level 3 binder inputs for the investigated mixes

Calibrated Michigan model accuracy indicators	Binder Input Level	
	Level 2	Level 3
Sample size (N)	22	22
R^2	0.036	0.001
Se/Sy	4.601	0.619
Slope	-0.153	0.708
Intercept	832.81	151.170
SSE (psi)	1.40E+06	1.02E+06

1 psi = 0.00689 MPa
Note: R^2 = coefficient of determination; *Se* = standard error of predicted IDT strength; *Sy* = standard deviation of measured IDT strength values about the mean; *SSE*= sum of squared errors.

5.4 Comparison of Global Pavement ME and Locally Calibrated IDT strength models

The global Pavement ME, the locally calibrated Manitoba, and Michigan calibrated IDT strength models were assessed using statistical performance indicators to evaluate the reliability of the models in predicting the IDT strength for the investigated mixtures. Statistical performance indications consisted of the goodness of fit parameters, R^2 and Se/Sy. In addition, the SEE, slope, and intercept of the predicted IDT strength values were also calculated and compared. The regression line, slope, and intercept of the fitted data gives an indication of possible under-prediction or over-prediction of the assessed models.

Table 5.8 presents the summary of the statistical indicators for the global Pavement ME model, locally calibrated Manitoba and Michigan calibrated IDT models, for Level 2 and Level 3 binder

inputs. The locally calibrated Manitoba IDT model showed improved performance (lower bias and increased prediction accuracy) in predicting the IDT strength at both Level 2 and Level 3 binder inputs, when compared to the global calibrated Pavement ME and calibrated Michigan models. However, since the locally calibrated Manitoba model with Level 3 asphalt binder is strongly affected by the presence of multicollinearity in the investigated mixes dataset, the locally calibrated Manitoba model with Level 2 binder input is recommended as the preferred model in predicting the IDT values for low temperature cracking analysis in Manitoba.

Table 5.8: Global Pavement ME, Locally calibrated Manitoba and Michigan calibrated IDT strength summary statistics for Level 2 and Level 3 binder inputs

IDT Prediction Models	Binder Input Level	N	R^2	Se/Sy	Slope	Intercept	SSE (psi)
Global Pavement ME model	Level 2	22	0.525	1.249	0.878	106.39	103.1E+3
	Level 3	22	0.221	1.48	0.558	190.09	144.9E+3
Locally calibrated Manitoba Model	Level 2	22	0.677	0.651	0.677	167.02	28.0E+3
	Level 3	22	0.708	0.619	0.708	151.17	25.3E+3
Michigan calibrated model	Level 2	22	0.036	4.601	-0.153	832.81	1.40E+6
	Level 3	22	0.001	3.937	0.019	709.12	1.02E+6

Note: *N* = number of data points, R^2 = coefficient of determination, *Se* = standard error of predicted IDT strength*; Sy* = standard deviation of measured IDT strength values about the mean, *SSE*= sum of squared errors.

5.5 Statistical analysis

A student's paired sample *t*-test was performed on the predictions of the global Pavement ME model, locally calibrated Manitoba model and Michigan calibrated models, versus the measured IDT strength for the investigated mixes. The *t*-test is a statistical comparison between the difference in mean and variance of the measured and predicted IDT strength values at 95% level of significance. The tested hypothesis is rejected if the t- calculated is greater than the t-critical at

0.05% level of significance. Table 5.9 shows the results of the paired *t*-test at a significance level $\alpha = 0.05\%$ for the global Pavement ME, locally calibrated Manitoba, and calibrated Michigan models.

Table 5.9: Summary of Paired t-test analysis for the assessed models

IDT Prediction Models	Binder Input Level	Two-tailed *t*-Test for variance at 95% confidence Level					Two-tailed *t*-Test for means at 95% confidence level				
		t stat	t crit	P(t stat ≤ t)	df	Accept/ Reject	t stat	t crit	P(t stat ≤ t)	df	Accept/ Reject
Global Pavement ME model	Level 2	2.016	2.018	0.050	42	Accept	3.754	2.080	0.001	21	Reject
	Level 3	1.805	2.018	0.078	42	Accept	2.463	2.080	0.023	21	Reject
Calibrated Manitoba Model	Level 2	0.008	2.018	0.994	42	Accept	0.017	2.080	0.986	21	Accept
	Level 3	0.015	2.018	0.988	42	Accept	0.036	2.080	0.972	21	Accept
Calibrated Michigan Model	Level 2	13.433	2.018	0.000	42	Reject	12.336	2.080	0.000	21	Reject
	Level 3	11.831	2.018	0.000	42	Reject	11.976	2.080	0.000	21	Reject

df = degree of freedom*; t stat* = test statistics, *t crit* = t critical.

As shown in Table 5.9, the results of the paired *t*-test show statistically significant differences between the measured and the predicted IDT strength values from the global Pavement ME model for Level 2 and Level 3 binder inputs. This confirms that the global Pavement ME model predicts the IDT strength with a significant level of bias, if used for local mixes. This factor could contribute to the poor prediction accuracy of the IDT strength for Manitoba mixtures. Interestingly, no statistical difference was found when the *t*-test for variance was conducted on global Pavement ME model with Level 3 binder inputs. This was unexpected, since the goodness of fit of the global Pavement ME model to the investigated mixes was poor. This may be attributed to the small sample size and equal variance assumption made.

The findings for the calibrated Michigan model for both Level 2 and Level 3 binder inputs show statistically significant differences between the measured and the predicted IDT strength values. In general, the results of the paired *t*-test suggest that the global Pavement ME model and the Michigan calibrated model are inaccurate in predicting the IDT strength for Manitoba mixes. As such, their utilization for thermal cracking predictions for asphalt pavements in Manitoba is unsuitable and may yield inappropriate results. One possible reason to explain the poor prediction accuracy of Michigan calibrated local model is the differences in the extracted binder PG types, mix design aggregate gradation, and mix volumetric.

Chapter 6: Effect of Integrating HMA, Base and Subgrade Local Models on Design and Performance of Flexible Pavements: Case Study

6.1 Introduction

This chapter investigates the integration of locally calibrated HMA and unbound granular material characterization models into the Pavement ME software to improve the design of flexible pavements. In this chapter, a case study using the proposed design method with the locally calibrated HMA, base, and subgrade materials characterization models were compared to a design that uses default values. Design outputs for pavement sections with different traffic levels and subgrade types were compared and are presented.

In summary, the goal of this chapter is to demonstrate the significance of developing design inputs based on locally calibrated material models as a means of improving the reliability of flexible pavement designs.

6.2 General Project Information and Analysis Parameters

Two flexible pavements, Provincial Truck Highway (PTH 1- PTH 34 to PR 350) and PTH 23 (E Jct. PTH 18 to PTH 5) located in Manitoba, Canada with varying traffic levels and subgrade types were considered in this study. PTH 1 is a four-lane divided primary arterial while PTH 23 is a two-way collector road. Figure 6.1 shows the locations of PTH 1 and PTH 23 respectively.

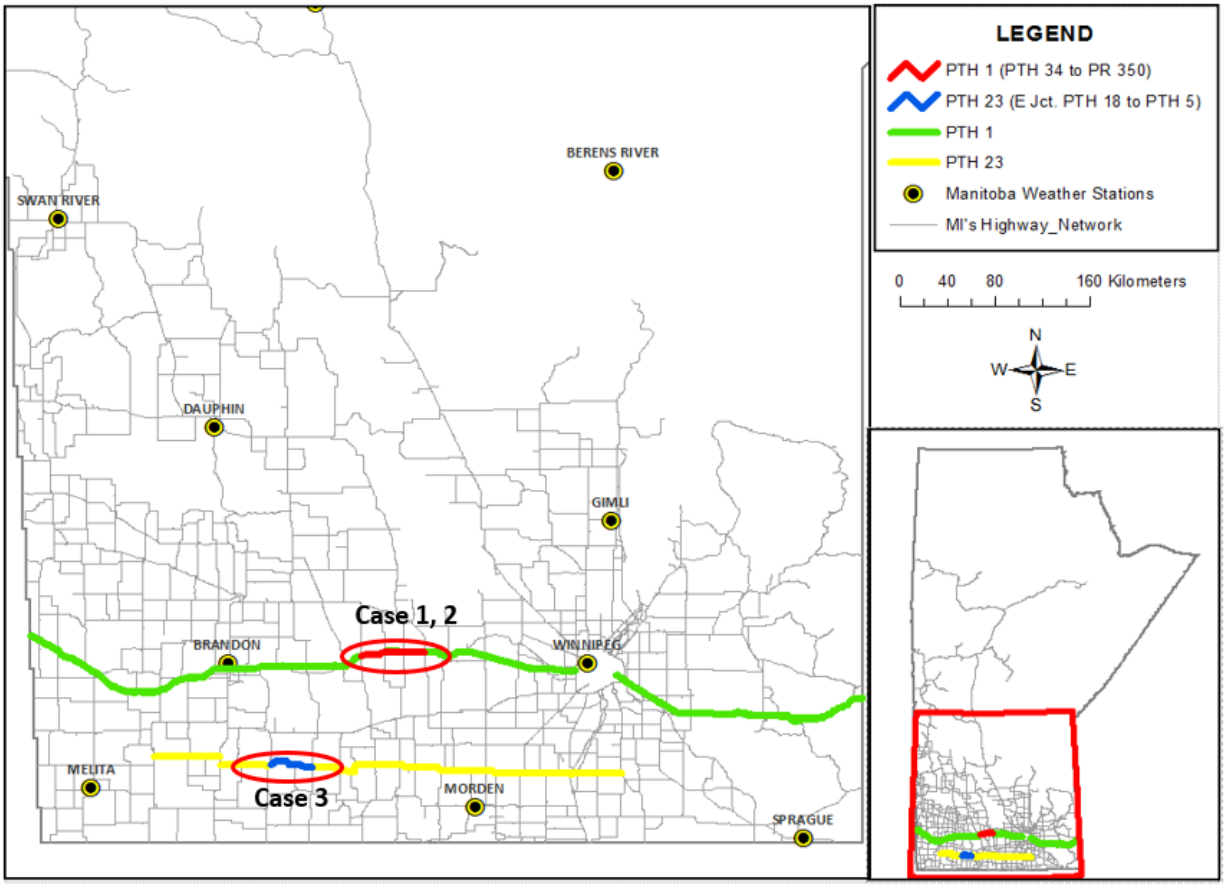

Figure 6.1: PTH 1 (PTH 34 to PR 350) and PTH 23 (E Jct. PTH 18 to PTH 5) Project locations

For this study, three design scenarios (case 1 to 3) for the two projects were established. The design scenarios were applied using default material parameters and locally calibrated material parameters into the Pavement ME design procedures. Traffic load levels were categorized into two groups: high traffic (>1000 trucks per day) and low traffic (<250 trucks per day). Two different Manitoba subgrade soils were considered in this study: weak (high plastic clay with no organics having Group Index of 20) and strong (sandy silt with Group Index of 0). The default material input parameters were selected based on recommendations from the 2016 draft Canadian MEPDG Guide while calibrated material input parameters were estimated from material characterization

models calibrated to Manitoba local conditions presented in chapter 3. A summary of the project description is presented in Table 6.1.

Table 6.1: Project description summary

Project Information	**Case 1**	**Case 2**	**Case 3**
Location	Primary Arterial PTH 1	Primary Arterial PTH 1	Collector road PTH 23
Traffic (Trucks per day)	High	High	Low
Subgrade condition	Weak	Strong	Weak
Traffic Loading	Axle Load Spectra		
Design Traffic (Trucks per day)	2420	2420	170
Lanes in design direction	2	2	1
Trucks per design direction,%	50	50	50
% Trucks in the design lane	90	90	100
Trucks on design lane	1090	1090	85
Operational speed (km/h)	100	100	90
Subgrade type	High Plastic Clay (A-7-5) GI = 20	Sandy Silt (A-4) GI=4	High Plastic Clay (A-7-5) GI = 20

The Pavement ME design software (version 2.3.1) was used to predict the pavement performance based on the globally calibrated distress prediction models. A design life of 20 years was assumed and used in the analysis for all case scenarios. From the obtained results, an improved design procedure was recommended based on the satisfactory predicted distress requirements for Manitoba. The target performance criteria for the selected projects as recommended by the local jurisdiction are presented in Table 6.2.

Table 6.2: Target Pavement Distress Performance Criteria

Distress Type	**High Traffic**	**Low Traffic**
Reliability (%)	90	90
Initial IRI (m/km)	0.9	0.9
Terminal IRI (m/km)	2.5	2.5
AC top-down fatigue cracking (m/km)	500	500
AC bottom-up fatigue cracking (%)	15	15
AC thermal cracking (m/km)	200	200
Permanent deformation -total pavement (mm)	19	19
Permanent deformation -AC only (mm)	12	12
Total cracking (Reflective + Alligator) (%)	50	50

The methodology developed for this case study is summarized in Figure 6.2

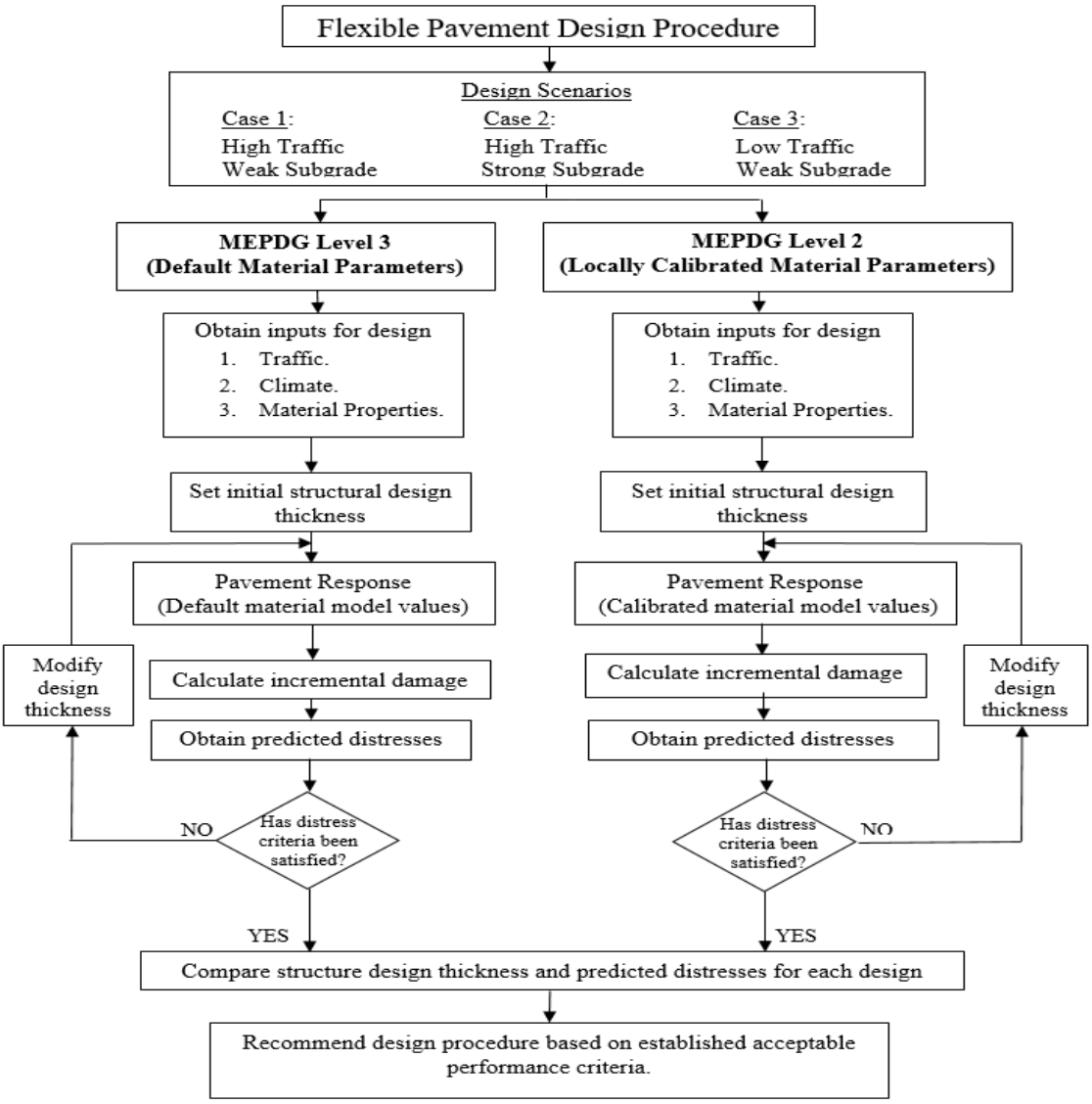

Figure 6.2: Case Study Methodology Flowchart

6.3 Pavement ME Design Inputs

6.3.1 Traffic Inputs

Traffic is an essential input for the analysis and structural design of both new and rehabilitated pavements. Traffic load levels for AASHTOWare Pavement ME analysis is expressed in terms of Axle Load Spectra (ALS). In addition to ALS, other pertinent traffic input parameters required for

AASHTOWare Pavement ME analysis and design include; Average Daily Truck Traffic (AADTT), vehicle class distribution, axles per truck traffic, traffic growth rate, and vehicle monthly distribution.

The AADTT in the design lane for PTH 1 and PTH 23 is given as 1090 and 85 trucks respectively. Manitoba Infrastructure provided the axle load distribution, vehicle classification and vehicle monthly distribution based on Weigh in Motion (WIM) station data obtained for the two project locations. The vehicle class distributions for the PTH 1 and PTH 23 is shown in Table 6.3. A comprehensive summary of the axle load distribution, axles per truck and vehicle monthly distribution for the project locations are presented in Appendix C.

Table 6.3: Vehicle class distribution for PTH 1 and PTH 23

FHWA Truck Class	**FHWA Description**	**Distribution of commercial vehicles (%)**	
		PTH 1	PTH 23
4	Two or three Axle Buses	0.8	0.2
5	Two-Axle, Six-Tire, Single-Unit Trucks	3.6	3.7
6	Three-Axle Single-Unit Trucks	3.6	3.4
7	Four or More Axle Single-Unit Trucks	0.1	0.3
8	Four or Fewer Axle Single-Trailer Trucks	2.3	9.8
9	Five-Axle Single-Trailer Trucks	46.9	50.5
10	Six or More Axle Single-Trailer Trucks	20.4	17.3
11	Five or Fewer Axle Multi-Trailer Trucks	0.3	0.3
12	Six-Axle Multi-Trailer Trucks	0.8	0.6
13	Seven or More Axle Multi-Trailer Trucks	21.2	13.8

6.3.2 Climate Inputs

Brandon's weather station located in Manitoba was selected for AASHTOWare Pavement ME analysis for all design scenarios. The historical climate data generated by Brandon's weather station was utilized by the Enhanced Integrated Climate Model (EICM) to account for moisture and temperature variations within the flexible pavement structural layers over the design life. This climate station was selected because of its close proximity to both project locations as shown in Figure 6.1.

6.3.3 Material Properties

Table 6.4 shows the material property input levels used for analysis for default (Level 3) and calibrated (Level 2) material inputs design procedures.

Table 6.4: Selected Material Design Input Levels

Structural Layer	**Mechanical Properties**	**Input Level**	
		Default parameters	Locally-calibrated parameters
HMA Layer	Dynamic Modulus |E*|	Level 3	Level 2
	Creep Compliance at -20°C,-10°C, and 0°C	Level 3	Level 2
	Indirect Tensile at -10°C	Level 3	Level 2
Base Layer	Resilient Modulus (M_R)	Level 3	Level 2
Subgrade	Resilient Modulus (M_R)	Level 3	Level 2

6.3.3.1 Default Pavement Structure Material Inputs

6.3.3.1.1 HMA Layer Default Material Inputs

In this case study, a local HMA mix was considered for analysis. Specifically, a mix containing 0% RAS and 15% RAP (Mix 0-15) was used for analysis. For default (Level 3) input data, the Pavement ME design software requires basic information about the mix properties such as

aggregate gradation, mix design properties and asphalt binder performance grade (PG) to estimate HMA layer mechanical properties based on default (Level 3) characterization models. The HMA default input data for all design scenarios (case 1 to 3) based on recommendations from the 2016 draft Canadian MEPDG Guide is summarized in Table 6.5.

Table 6.5: HMA Default (Level 3) Material Input Data for all Design Case Scenarios

Design Input		**Case 1**	**Case 2**	**Case 3**
Traffic (Trucks per day)		High	High	Low
Subgrade Condition		Weak	Strong	Weak
Volumetric Properties				
Unit Weight (Kg/m^3)		2350	2350	2350
Effective binder content by volume (%)		9.9	9.9	9.9
Air Voids		3.8	3.8	3.8
Poisson's ratio		0.35	0.35	0.35
Mechanical Properties				
Dynamic Modulus		Level 3	Level 3	Level 3
Average aggregate gradation	% passing 19-mm sieve size	100	100	100
	% passing 9.5-mm sieve size	80.2	80.2	80.2
	% passing 4.75-mm sieve size	61.2	61.2	61.2
	% passing 75- µm sieve size	3.7	3.7	3.7
G* Predictive Model		Viscosity based model (nationally Calibrated)		
Reference Temperature		21.1^0C	21.1^0C	21.1^0C
Asphalt Binder		PG 58-28	PG 58-28	PG 58-28
Indirect Tensile Strength -10 ^0C (MPa)		Default	Default	Default
Creep Compliance (1/GPa)		Input level:3	Input level:3	Input level:3
Thermal Properties (Pavement ME default values)				
Thermal Conductivity (watt/meter-Kelvin)		Default	Default	Default
Heat Capacity (joule/kg-Kelvin)		Default	Default	Default
Thermal Contraction		Default	Default	Default

6.3.3.1.2 Unbound Material Layer Default (Level 3) Inputs

The typical inputs for the base and subgrade layers used in the analysis for the design scenarios are presented in Table 6.6.

Table 6.6: Default (Level 3) Base and Subgrade Input Data for all Design Case Scenarios

Design Input	**Case 1**	**Case 2**	**Case 3**
Traffic (Trucks per day)	High	High	Low
Subgrade Condition	Weak	Strong	Weak
Unbound Granular Base Properties:			
Resilient Modulus M_R (MPa)	140	140	140
Subgrade Properties:			
Material Type	High Plastic Clay (A-7-5)	Sandy Silt (A-4)	High Plastic Clay (A-7-5)
Resilient Modulus M_R (MPa)*	30	65	30

*****Effective subgrade modulus.

6.3.3.2 Locally Calibrated (Level 2) Material Inputs

6.3.3.2.1 HMA Layer Locally-Calibrated Material Inputs

Locally calibrated HMA dynamic modulus and creep compliance models were used to establish design inputs Pavement ME analysis for this study. It is important to point out that the calibrated Manitoba IDT model using Level 2 binder input was used to predict the IDT strength for analysis of all design case scenarios

This predicted IDT strength (Level 2) value for Mix 0-15 was 3.491 MPa (506.33 psi). Furthermore, the locally calibrated dynamic modulus and creep compliance inputs values predicted for Mix 0-15 and utilized for analysis in the Pavement ME design software are presented in Table 6.7 and 6.8 respectively.

Table 6.7: Dynamic Modulus Values for all Design Case Scenarios

Mix	Dynamic Modulus |E*|, MPa						
	Temperature (°C)	Loading Frequency, Hz					
		0.1	0.5	1	5	10	25
Mix 0-15	-10	22,672	25,960	27,228	29,807	30,762	31,890
	5	9,270	12,831	14,470	18,339	19,976	22,065
	25	1,746	2,969	3,687	5,866	7,030	8,748
	40	575	990	1,255	2,166	2,718	3,629

Table 6.8: Creep compliance Values for all Design Case Scenarios

Mix	Creep Compliance, (1/GPa)			
	Loading Time (seconds)	Low Temperature (-20 °C)	Mid Temperature (-10 °C)	High Temperature (-10 °C)
Mix 0-15	1	0.0479	0.0756	0.1461
	2	0.0494	0.0802	0.1640
	5	0.0521	0.0889	0.2005
	10	0.0552	0.0978	0.2425
	20	0.0598	0.1091	0.3020
	50	0.0684	0.1307	0.4239
	100	0.0778	0.1540	0.5646

6.3.3.2.2 Unbound Material Layer Locally-Calibrated Material Inputs

The resilient modulus of subgrade and Unbound Granular Materials (UGM) at any given state of stress is normally predicted from the constitutive model (NCHRP, 2004) using regression constants k_1, k_2 and k_3. Locally calibrated models that relate material type, density and moisture content to the resilient modulus was utilized in this study. These locally calibrated prediction models were used to predict the resilient modulus for the granular base (limestone) and subgrade

materials (high plastic clay and silty/sandy silt soils) for Pavement ME analysis for all design case scenarios. The base and subgrade layer properties is presented in Table 6.9.

Table 6.9: Locally Calibrated Base and Subgrade Material Properties for all Design Case Scenarios

	Granular Base Layer	**Subgrade Layer**	
Material Type:	Limestone	Weak Subgrade (A-7-5)	Strong Subgrade (A-4)
M_R (MPa)*	181	59.4	80
OMC (%)	10.8	28.2	13
MC (%)	10.8	30	4.5
Liquidity Index (%)	0	0.00357	0
MDD, (Kg/m^3)	2170	1434	1851
% Silt	N/A	12	46
P4, %	49	N/A	N/A
P200, %	N/A	81	35

N/A = Not Applicable.
*At optimum moisture content. *MDD* =Maximum dry density, *OMC* = optimum moisture content; *P4* = percentage passing sieve No. 4; *P200* is the percentage passing sieve no. 200.

6.3.4 Predicted Pavement Distresses for Each Design Case Scenario

The Pavement ME design software was used to predict the pavement distresses, based on the material, climatic and traffic inputs from the previous Section 6.3 for Case 1, Case 2 and Case 3, based on the target performance criteria. A total of 28 runs were performed based on a combination of varying thicknesses of HMA and granular base thicknesses as shown in Table 6.10. The analysis was performed for the default (Level 3) and locally calibrated material models (Level 2) at 90% reliability.

Table 6.10: Combination of HMA and Base Trial thicknesses

Trials	HMA (mm)	Granular Base (mm)
Case 1 Combinations	150, 200, 250*	300, 600
Case 2 Combinations	150, 200, 250*	300, 600
Case 3 Combinations	75, 100	300

Note* - combined only with 600 mm granular base

Tables 6.11 to 6.16 show the detailed results of the predicted distresses, reliabilities of predicted distresses and expected service life for the combination presented in Table 6.10. Results showed that the calibrated model inputs produced better-predicted performance when compared to default model inputs.

It should be noted, however, that the predictions from both the default and calibrated material models failed to meet the IRI criterion and thermal cracking performance criterion for all design cases scenarios. The thermal cracking is highly likely due to the PG 58-28 binder used for the mix considered in this study, which does not meet the low-temperature requirements for the project site.

Table 6.11: Pavement ME Default (Level 3) Model Analysis Output for all Case 1 Combinations.

CASE 1						
High Traffic, Weak Subgrade						
HMA/Base Layer Thicknesses (mm):		150/300	150/600	200/300	200/600	250/600
Distresses		**Default Model Analysis**				
Terminal IRI	**Target (m/km)**	**2.5**	**2.5**	**2.5**	**2.5**	**2.5**
	Predicted	2.95	2.91	2.81	2.79	2.68
	Reliability Predicted (%)	69.22	71.35	76.65	77.78	82.61
	Acceptance	**Fail**	**Fail**	**Fail**	**Fail**	**Fail**
	Predicted life at 90% Reliability (%)	13	14.42	15	16.33	17.82
Permanent deformation (Total Pavement)	**Target (mm)**	**19**	**19**	**19**	**19**	**19**
	Predicted	24.13	22.74	20.83	20.03	17.45
	Reliability Predicted (%)	35.59	52.41	73.99	82.03	97.01
	Acceptance	**Fail**	**Fail**	**Fail**	**Fail**	**Pass**
	Predicted life at 90% Reliability (%)	8	11	14	17	>20
AC Bottom-Up Fatigue Cracking	**Target (%)**	**15**	**15**	**15**	**15**	**15**
	Predicted	4.47	2.45	1.81	1.67	1.52
	Reliability Predicted (%)	100	100	100	100	100
	Acceptance	**Pass**	**Pass**	**Pass**	**Pass**	**Pass**
	Predicted life at 90% Reliability (%)	>20	>20	>20	>20	>20
AC Thermal Cracking	**Target (m/km)**	**200**	**200**	**200**	**200**	**200**
	Predicted	561.24	569.55	487.73	490.39	435.7
	Reliability Predicted (%)	13.09	12.67	17.99	17.77	23.31
	Acceptance	**Fail**	**Fail**	**Fail**	**Fail**	**Fail**
	Predicted life at 90% Reliability (%)	6.42	6.42	6.5	6.5	7.3
AC Top-Down Fatigue Cracking	**Target (m/km)**	**500**	**500**	**500**	**500**	**500**
	Predicted	417.63	419.4	111.92	458.3	73.37
	Reliability Predicted (%)	93.93	93.85	100	100	100
	Acceptance	**Pass**	**Pass**	**Pass**	**Pass**	**Pass**
	Predicted life at 90% Reliability (%)	>20	>20	>20	>20	>20
Permanent deformation (AC Layer only)	**Target (mm)**	**12**	**12**	**12**	**12**	**12**
	Predicted	9.74	10.23	9.06	9.51	8.35
	Reliability Predicted (%)	98.97	98	99.67	99.27	99.93
	Acceptance	**Pass**	**Pass**	**Pass**	**Pass**	**Pass**
	Predicted life at 90% Reliability (%)	>20	>20	>20	>20	>20

Table 6.12: Pavement ME Locally-Calibrated Model Analysis Output for all Case 1 Combinations.

CASE 1						
High Traffic ,Weak Subgrade						
HMA/Base Layer Thicknesses (mm):		150/300	150/600	200/300	200/600	250/600
Distresses		**Calibrated Model Analysis**				
Terminal IRI	**Target (m/km)**	**2.5**	**2.5**	**2.5**	**2.5**	**2.5**
	Predicted	2.64	2.62	2.57	2.56	2.52
	Reliability Predicted (%)	84.38	85.57	87.28	87.8	89.32
	Acceptance	**Fail**	**Fail**	**Fail**	**Fail**	**Fail**
	Predicted life at 90% Reliability (%)	17.33	18.75	19.42	19.67	19.97
Permanent deformation (Total Pavement)	**Target (mm)**	**19**	**19**	**19**	**19**	**19**
	Predicted	12.31	11.26	9.75	9.22	7.7
	Reliability Predicted (%)	100	100	100	100	100
	Acceptance	**Pass**	**Pass**	**Pass**	**Pass**	**Pass**
	Predicted life at 90% Reliability (%)	>20	>20	>20	>20	>20
AC Bottom-Up Fatigue Cracking	**Target (%)**	**15**	**15**	**15**	**15**	**15**
	Predicted	1.53	1.5	1.47	1.46	1.45
	Reliability Predicted (%)	100	100	100	100	100
	Acceptance	**Pass**	**Pass**	**Pass**	**Pass**	**Pass**
	Predicted life at 90% Reliability (%)	>20	>20	>20	>20	>20
AC Thermal Cracking	**Target (m/km)**	**200**	**200**	**200**	**200**	**200**
	Predicted	491.04	491.04	491.04	491.04	491.04
	Reliability Predicted (%)	0.24	0.24	0.24	0.24	0.24
	Acceptance	**Fail**	**Fail**	**Fail**	**Fail**	**Fail**
	Predicted life at 90% Reliability (%)	0.42	0.42	0.42	0.42	0.42
AC Top-Down Fatigue Cracking	**Target (m/km)**	**500**	**500**	**500**	**500**	**500**
	Predicted	59.86	66.85	53	54.22	54.61
	Reliability Predicted (%)	100	100	100	100	100
	Acceptance	**Pass**	**Pass**	**Pass**	**Pass**	**Pass**
	Predicted life at 90% Reliability (%)	>20	>20	>20	>20	>20
Permanent deformation (AC Layer only)	**Target (mm)**	**12**	**12**	**12**	**12**	**12**
	Predicted	1.24	1.29	1.19	1.24	1.13
	Reliability Predicted (%)	100	100	100	100	100
	Acceptance	**Pass**	**Pass**	**Pass**	**Pass**	**Pass**
	Predicted life at 90% Reliability (%)	>20	>20	>20	>20	>20

Table 6.13: Pavement ME Default (Level 3) Model Analysis Output for all Case 2 Combinations

CASE 2						
High Traffic, Strong Subgrade						
HMA/Base Layer Thicknesses (mm):		**150/300**	**150/600**	**200/300**	**200/600**	**250/600**
Distresses		**Default Model Analysis**				
Terminal IRI	**Target (m/km)**	**2.5**	**2.5**	**2.5**	**2.5**	**2.5**
	Predicted	2.89	2.87	2.75	2.75	2.65
	Reliability Predicted (%)	72.76	73.77	79.37	79.81	84.23
	Acceptance	**Fail**	**Fail**	**Fail**	**Fail**	**Fail**
	Predicted life at 90% Reliability (%)	14	15.08	16.33	17	18
Permanent deformation (Total Pavement)	**Target (mm)**	**19**	**19**	**19**	**19**	**19**
	Predicted	21.73	21.05	18.88	18.55	16.14
	Reliability Predicted (%)	64.15	72.22	90.74	92.58	99.25
	Acceptance	**Fail**	**Fail**	**Pass**	**Pass**	**Pass**
	Predicted life at 90% Reliability (%)	12.5	15	>20	>20	>20
AC Bottom-Up Fatigue Cracking	**Target (%)**	**15**	**15**	**15**	**15**	**15**
	Predicted	3.57	2.4	1.76	1.66	1.51
	Reliability Predicted (%)	100	100	100	100	100
	Acceptance	**Pass**	**Pass**	**Pass**	**Pass**	**Pass**
	Predicted life at 90% Reliability (%)	>20	>20	>20	>20	>20
AC Thermal Cracking	**Target (m/km)**	**200**	**200**	**200**	**200**	**200**
	Predicted	561.24	569.55	487.73	490.39	435.7
	Reliability Predicted (%)	13.09	12.67	17.99	17.77	23.31
	Acceptance	**Fail**	**Fail**	**Fail**	**Fail**	**Fail**
	Predicted life at 90% Reliability (%)	6.42	6.42	6.58	6.58	7.42
AC Top-Down Fatigue Cracking	**Target (m/km)**	**500**	**500**	**500**	**500**	**500**
	Predicted	515.52	490.41	177.86	217.76	84.01
	Reliability Predicted (%)	89.22	90.47	99.99	99.85	100
	Acceptance	**Fail**	**Pass**	**Pass**	**Pass**	**Pass**
	Predicted life at 90% Reliability (%)	19	>20	>20	>20	>20
Permanent deformation (AC Layer only)	**Target (mm)**	**12**	**12**	**12**	**12**	**12**
	Predicted	9.82	10.24	9.16	9.52	8.36
	Reliability Predicted (%)	98.84	97.99	99.6	99.26	99.93
	Acceptance	**Pass**	**Pass**	**Pass**	**Pass**	**Pass**
	Predicted life at 90% Reliability (%)	>20	>20	>20	>20	>20

Table 6.14: Pavement ME Locally-Calibrated Model Analysis Output for all Case 2 Combinations

CASE 2						
High Traffic, Strong Subgrade						
HMA/Base Layer Thicknesses (mm):		**150/300**	**150/600**	**200/300**	**200/600**	**250/600**
Distresses		**Calibrated Model Analysis**				
Terminal IRI	**Target (m/km)**	**2.5**	**2.5**	**2.5**	**2.5**	**2.5**
	Predicted	2.59	2.58	2.54	2.53	2.5
	Reliability Predicted (%)	86.45	87.11	88.66	88.92	90.15
	Acceptance	**Fail**	**Fail**	**Fail**	**Fail**	**Pass**
	Predicted life at 90% Reliability (%)	18.42	19	19.58	19.67	>20
Permanent deformation (Total Pavement)	**Target (mm)**	**19**	**19**	**19**	**19**	**19**
	Predicted	10.5	9.85	8.39	8.1	6.79
	Reliability Predicted (%)	100	100	100	100	100
	Acceptance	**Pass**	**Pass**	**Pass**	**Pass**	**Pass**
	Predicted life at 90% Reliability (%)	>20	>20	>20	>20	>20
AC Bottom-Up Fatigue Cracking	**Target (%)**	**15**	**15**	**15**	**15**	**15**
	Predicted	1.52	1.49	1.46	1.46	1.45
	Reliability Predicted (%)	100	100	100	100	100
	Acceptance	**Pass**	**Pass**	**Pass**	**Pass**	**Pass**
	Predicted life at 90% Reliability (%)	>20	>20	>20	>20	>20
AC Thermal Cracking	**Target (%)**	**200**	**200**	**200**	**200**	**200**
	Predicted	491.04	491.04	491.04	491.04	491.04
	Reliability Predicted (%)	0.24	0.24	0.24	0.24	0.24
	Acceptance	**Fail**	**Fail**	**Fail**	**Fail**	**Fail**
	Predicted life at 90% Reliability (%)	0.42	0.42	0.42	0.42	0.42
AC Top-Down Fatigue Cracking	**Target (m/km)**	**500**	**500**	**500**	**500**	**500**
	Predicted	62.31	68.83	53.31	54.53	54.77
	Reliability Predicted (%)	100	100	100	100	100
	Acceptance	**Pass**	**Pass**	**Pass**	**Pass**	**Pass**
	Predicted life at 90% Reliability (%)	>20	>20	>20	>20	>20
Permanent deformation (AC Layer only)	**Target (mm)**	**12**	**12**	**12**	**12**	**12**
	Predicted	1.28	1.32	1.23	1.27	1.16
	Reliability Predicted (%)	100	100	100	100	100
	Acceptance	**Pass**	**Pass**	**Pass**	**Pass**	**Pass**
	Predicted life at 90% Reliability (%)	>20	>20	>20	>20	>20

Table 6.15: Pavement ME Default (Level 3) Model Analysis Output for all Case 3 Combinations

CASE 3			
Low Traffic, Weak Subgrade			
HMA/Base Layer Thicknesses (mm):		75/300	100/300
Distresses		**Default Model Analysis**	
Terminal IRI	**Target (m/km)**	**2.5**	**2.5**
	Predicted	2.7	2.68
	Reliability Predicted (%)	80	96.9
	Acceptance	**Fail**	**Pass**
	Predicted life at 90% Reliability (%)	>20	>20
Permanent deformation (Total Pavement)	**Target (mm)**	**19**	**19**
	Predicted	15	13.11
	Reliability Predicted (%)	100	100
	Acceptance	**Pass**	**Pass**
	Predicted life at 90% Reliability (%)	>20	>20
AC Bottom-Up Fatigue Cracking	**Target (%)**	**25**	**25**
	Predicted	2	1.67
	Reliability Predicted (%)	100	100
	Acceptance	**Pass**	**Pass**
	Predicted life at 90% Reliability (%)	>20	>20
AC Thermal Cracking	**Target (m/km)**	**200**	**200**
	Predicted	608.57	608.57
	Reliability Predicted (%)	10.96	10.96
	Acceptance	**Fail**	**Fail**
	Predicted life at 90% Reliability (%)	6.42	5.33
AC Top-Down Fatigue Cracking	**Target (m/km)**	**500**	**500**
	Predicted	248.61	256.87
	Reliability Predicted (%)	99.53	99.4
	Acceptance	**Pass**	**Pass**
	Predicted life at 90% Reliability (%)	>20	>20
Permanent deformation (AC Layer only)	**Target (mm)**	**12**	**12**
	Predicted	3.62	3.41
	Reliability Predicted (%)	100	100
	Acceptance	**Pass**	**Pass**
	Predicted life at 90% Reliability (%)	>20	>20

Table 6.16: Pavement ME Locally-Calibrated Model Analysis Output for all Case 3 Combination

CASE 3			
Low Traffic, Weak Subgrade			
HMA/Base Layer Thicknesses (mm):		150/300	150/600
Distresses		**Calibrated Model Analysis**	
Terminal IRI	**Target (m/km)**	**2.5**	**2.5**
	Predicted	2.6	2.54
	Reliability Predicted (%)	87	98.56
	Acceptance	**Fail**	**Pass**
	Predicted life at 90% Reliability (%)	>20	>20
Permanent deformation (Total Pavement)	**Target (mm)**	**19**	**19**
	Predicted	9.86	8.2
	Reliability Predicted (%)	100	100
	Acceptance	**Pass**	**Pass**
	Predicted life at 90% Reliability (%)	>20	>20
AC Bottom-Up Fatigue Cracking	**Target (%)**	**25**	**25**
	Predicted	1.0	1.46
	Reliability Predicted (%)	100	100
	Acceptance	**Pass**	**Pass**
	Predicted life at 90% Reliability (%)	>20	>20
AC Thermal Cracking	**Target (m/km)**	**200**	**200**
	Predicted	491.04	491.04
	Reliability Predicted (%)	0.24	0.24
	Acceptance	**Fail**	**Fail**
	Predicted life at 90% Reliability (%)	0.42	0.42
AC Top-Down Fatigue Cracking	**Target (m/km)**	**500**	**500**
	Predicted	118.22	62.07
	Reliability Predicted (%)	100	100
	Acceptance	**Pass**	**Pass**
	Predicted life at 90% Reliability (%)	>20	>20
Permanent deformation (AC Layer only)	**Target (mm)**	**12**	**12**
	Predicted	0.62	0.5
	Reliability Predicted (%)	100	100
	Acceptance	**Pass**	**Pass**
	Predicted life at 90% Reliability (%)	>20	>20

6.3.5 Pavement Structural Design Thickness Output for the Different Case Scenarios.

A comparison of the predicted distresses, reliabilities of the predicted distresses and the expected service life obtained using default (Level 3) and locally calibrated (Level 2) material characterization models were performed for all case scenarios. The pavement structural thicknesses, that satisfied the target performance criteria for each case scenario, were selected and summarized in Table 6.17.

As shown in Table 6.17, for Case 1 high traffic truck on weak subgrade, the Default (Level 3) materials model yielded a pavement structure that consisted of 250 mm HMA and 600 mm of granular base, while the calibrated (Level 2) materials model yielded a relatively smaller pavement section consisting of 150 mm HMA and 300mm granular base. The calibrated materials model produces a 40% and 50% reduction of HMA and granular base layers, respectively.

For Case 2 high truck traffic on strong subgrade, the Default (Level 3) materials model yielded a pavement structure of 200 mm HMA and 300 mm of granular base, while the calibrated (Level 2) materials model yielded a smaller pavement consisting of 150mm HMA and 300mm granular base. The calibrated materials model produced a 20% and 0% reduction of HMA and granular base layers, respectively. The lack of change in the granular base thickness is likely a result of the strong subgrade. For Case 3 low truck traffic on weak subgrade, the Default (Level 3) materials model yielded a pavement structure of 75 mm HMA and 300 mm of granular base, while the calibrated (Level 2) materials model yielded a smaller pavement consisting of 75 mm HMA and 300mm granular base. There was no difference in the HMA and granular base layers thicknesses for the default and calibrated materials models at low traffic and weak subgrade.

Table 6.17: Pavement ME Outputs for Selected Thicknesses by Case Scenario

	CASE 1		**CASE 2**		**CASE 3**	
Traffic (Trucks per day)	High		High		Low	
Subgrade Type	Weak		Strong		Weak	
Material Model	Default	Calibrated	Default	Calibrated	Default	Calibrated
HMA/Base Thicknesses (mm)	250/600	150/300	200/300	150/300	75/300	75/300
Terminal IRI						
Target (m/km)	**2.5**	**2.5**	**2.5**	**2.5**	**2.5**	**2.5**
Predicted	2.7	2.6	2.8	2.6	2.7	2.6
Reliability Predicted (%)	83	84	79	86	80	87
Acceptance	Fail	Fail	Fail	Fail	Fail	Fail
Predicted life (years)	18	17	16	18	17	18
Permanent Deformation (Total Pavement)						
Target (mm)	**19**	**19**	**19**	**19**	**19**	**19**
Predicted	17	12	19	11	15	10
Reliability Predicted (%)	97	100	91	100	100	100
Acceptance	Pass	Pass	Pass	Pass	Pass	Pass
Predicted life (years)	>20	>20	>20	>20	>20	>20
AC Bottom-Up Fatigue Cracking						
Target (%)	**15**	**15**	**15**	**15**	**15**	**15**
Predicted	2	2	2	2	2	1
Reliability Predicted (%)	100	100	100	100	100	100
Acceptance	Pass	Pass	Pass	Pass	Pass	Pass
Predicted life (years)	>20	>20	>20	>20	>20	>20
AC Thermal Cracking						
Target (m/km)	**200**	**200**	**200**	**200**	**200**	**200**
Predicted	436	491	488	491	609	491
Reliability Predicted (%)	23	0	18	0	11	0
Acceptance	Fail	Fail	Fail	Fail	Fail	Fail
Predicted life (years)	7	0	7	0	6	0
AC Top-Down Fatigue Cracking						
Target (m/km)	500	500	500	500	500	500
Predicted	73	60	178	62	249	118
Reliability Predicted (%)	100	100	100	100	100	100
Acceptance	Pass	Pass	Pass	Pass	Pass	Pass
Predicted life (years)	>20	>20	>20	>20	>20	>20
Permanent deformation (AC Layer only)						
Target (mm)	12	12	12	12	12	12
Predicted	8	1	9	1	4	1
Reliability Predicted (%)	100	100	100	100	100	100
Acceptance	Pass	Pass	Pass	Pass	Pass	Pass
Predicted life (years)	>20	>20	>20	>20	>20	>20

The above comparison indicates that for high truck traffic volumes, the structural layer thicknesses determined using the default (Level 3) material model are significantly higher as compared to that obtained using calibrated (level 2) material model. This outcome emphasizes the significance of using locally calibrated material characterization models to arrive at more reliable optimized pavement designs. Conversely, for low truck volumes, the effect of using calibrated material inputs was not significant. Figure 6.3 illustrates the final pavement design thicknesses obtained using the default (level 3) and locally calibrated (level 2) material characterization models at 90% design reliability as shown in Table 6.17.

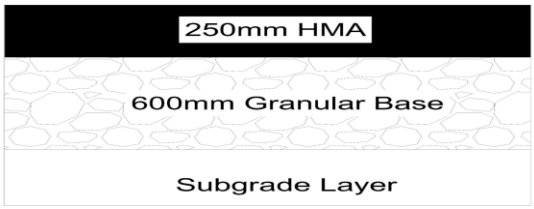

(a) Case 1 – Default Model

(b) Case 1 - Calibrated Model

(c) Case 2 – Default Model

(d) Case 2 - Calibrated Model

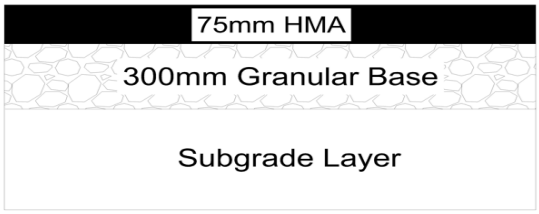

(e) Case 3 – Default Model

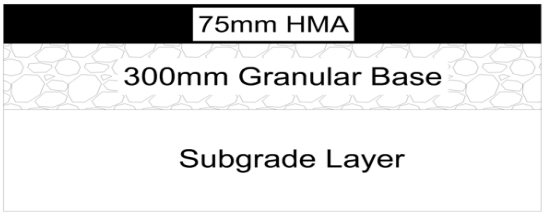

(f) Case 3 - Calibrated Model

Figure 6.3: Selected Default and Calibrated design thickness for Case 1, Case 2 and Case 3

Chapter 7: Conclusions and Recommendations

7.1 Summary and Conclusions

The primary objectives of this study were to calibrate the global predictive model to local HMA in Manitoba and integrate locally calibrated HMA, base and subgrade material characterization models into the Pavement ME design procedure to improve the design of flexible pavements.

The study developed a locally calibrated IDT model and compared the predictions to the global Pavement ME and Michigan calibrated models for the investigated HMA mixtures with Level 2 and Level 3 binder inputs. The IDT strengths of twenty-two HMA mixtures containing virgin and varying percentages of RAP were used for the local calibration IDT model. The performance of the calibrated IDT models at Level 2 and Level 3 binder input levels was evaluated and compared.

Furthermore, the impact of integrating locally calibrated HMA, unbound granular base and subgrade layer material characterization models for the design of two flexible pavements located in Manitoba were investigated. Pavements with high and low traffic, and weak and strong subgrade, for three cases (Case 1, Case 2 and Case 3) were analyzed. A local HMA mix and granular base were considered for the analysis. The design thicknesses resulting from the predicted distress criteria, using the default (Level 3) and locally calibrated (Level 2) models were compared.

Based on the analysis and results, the findings and conclusions are the following:

Local Calibration of Pavement ME IDT Strength Model

1. The global Pavement ME IDT strength model, if used without local calibration, produced inaccurate predictions of the IDT strength for the investigated mixtures. With respect to the investigated mixes dataset used in this analysis, the global Pavement ME IDT model

overestimates the IDT strength when Level 2 binder input is used, and underestimates the IDT strength for Level 3 binder. The R^2 values obtained for Level 2 and Level 3 asphalt binder input were unacceptably low at 0.525 and 0.221 respectively. The Se/Sy values obtained for Level 2 and Level 3 asphalt binder inputs were 1.249 and 1.480, respectively.

2. Assessment of the calibrated Michigan model predictions showed poor correlations with the measured IDT strength for the investigated Manitoba mixtures.
3. IDT binder characterization methods can significantly impact the accuracy of IDT strength predictions. For the investigated mixtures, Level 2 binder input is more reliable over Level 3 input.
4. The locally calibrated Manitoba IDT model improved the prediction performance for Level 2 and Level 3 binder inputs. However, local calibration results with Level 2 asphalt binder input is more reliable over Level 3 asphalt binder input and is preferred for adoption and implementation in Manitoba. The R^2 and Se/Sy values obtained for Level 2 asphalt binder input were 0.677 and 0.651 respectively.
5. While local calibration improves the predictive ability of the IDT model, it should be noted that the model can only be used for the range of materials tested.

Effect of Integrating Local HMA, Base, and Subgrade Models on design and Performance of flexible pavements

1. The use of a complete set of calibrated materials characterization models is a first for Manitoba. Results demonstrate potential optimized thicknesses due to improved pavement designs.

2. Locally calibrated material model inputs are a viable alternative to laboratory testing and provide more reliable estimate of Pavement ME design inputs when compared to default values.
3. For high traffic truck volumes, the structural layer thicknesses determined using the default (Level 3) material model are significantly higher as compared to that obtained using calibrated (Level 2) material model. For Case 1, high traffic truck on weak subgrade, the calibrated (Level 2) materials model produces a 40% and 50% reduction of HMA and granular base layers, respectively, compared to the default (Level 3) materials model. For Case 2 high truck traffic on strong subgrade, the calibrated materials model produces a 20% and 0% reduction of HMA and granular base layers, respectively, compared to the default (Level 3) materials model. The lack of change in the granular base thickness is likely a result of the strong subgrade.
4. For low truck volume roads, the effect of using calibrated material design procedure is not as crucial as compared to high truck volume roads. For Case 3 low truck traffic on the weak subgrade, there was no difference in the HMA and granular base layers thicknesses for the default and calibrated materials models at low traffic and weak subgrade.
5. The calibrated material design procedure produced lower predicted distresses with higher reliability in the predicted distresses resulting to thinner pavement sections for all design case scenarios.

7.2 Limitations and Recommended Future Work

The following are recommended for future research work

1. The IDT model can be inproved by incoperating a larger dataset with sufficient variability in the binder types for local calibration.
2. The calibrated Manitoba IDT model can only be used for the ranges of materials tested, therefore, a wider array of mixture volumetrics is required for further calibration and validation.
3. With a larger dataset, a more rigorous calibration optimization technique, such as artificail neural networks (ANN) and genetic algorithm may be used to enhance the accuracy and precison of the IDT predictive model for better low temperature cracking predictions.
4. The calibrated material design procedure is highly recommended for highway designs with high traffic volumes. Highway agencies should consider the calibrated material procedure due to better reliability levels.

Contributions to Literature

This master's thesis is a culmination of research work carried out during 2016 to 2018, at the Pavement Research Group, Civil Engineering Department, University of Manitoba, Canada. The following papers are the contributions to knowledge:

1. Afuberoh, A., Shalaby, A., and Kavanagh, L., (2018). Integrating Locally-Calibrated Characterization Models for Design of Flexible Pavements: A Case Study. International Conference on Transportation and Development. Pittsburg, Philadelphia. (Accepted) https://doi.org/10.1061/9780784481554.026
2. Afuberoh, A., Kavanagh, L., and Shalaby, A., (2018). Local Calibration of Indirect Tensile Strength of Hot-Mix Asphalt Mixtures. Journal Paper (Work in Progress)
3. Kavanagh, L., Afuberoh A., and Shalaby, A., (2018). Harmonizing Road Construction Specifications and Standards: Manitoba Experience. The 2018 Annual Conference of the Transportation Association of Canada, Saskatoon, Canada

References

AASHTO. (2015). Mechanistic-Empirical Pavement Design Guide: A Manual of Practice. AASHTO Designation: MEPDG-1. Washington, D.C

AASHTO. (2010). Guide for the local calibration of the mechanistic-empirical pavement design guide. American Association of State Highway and Transportation Officials. Washington DC

AASHTO. (1993). Guide for design of pavement structures. American Association of State Highway, and Transportation Officials. Washington, D.C

AASHTO T 322-07. (2011). Determining the creep compliance and strength of hot mix asphalt (HMA) using the indirect tensile test device. American Association of State Highway and Transportation Officials. Washington D.C

AASHTO T 315-12. (2012). Determining the rheological properties of asphalt binder using a dynamic shear rheometer (DSR). American Association of State Highway and Transportation Officials. Washington D.C

AASHTO, (2008). Mechanistic-empirical pavement design guide-A manual of practice. AASHTO Designation: MEPDG-1. Washington, DC

Ahammed, M., Kass, S., and Hilderman, S. (2013). Implementing the AASHTOWare pavement ME Design guide: Manitoba issues and proposed approaches. Paper presented at the 2013 Conference and Exhibition of the Transportation Association of Canada-Transportation: Better-Faster-Safer.

Al-Khateeb, G., Shenoy, A., Gibson, N., and Harman, T. (2006). A new simplistic model for dynamic modulus predictions of asphalt paving mixtures. Journal of the Association of Asphalt Paving Technologists, 75E(November), 1-40

Andrei, D., Witczak, M. W., and Mirza, M. W. (1999). "Development of a revised predictive model for the dynamic (complex) modulus of asphalt mixtures." Inter Team Technical Rep. prepared for the NCHRP 1-37A Project, Dept. of Civil Engineering, University of Maryland, College Park, MD

ASTM. (2009). Standard viscosity-temperature chart for asphalts. D2493M-09. American Society for Testing and Materials. West Conshohocken, PA

Bari, J. (2005). Development of a new revised version of the Witczak E* predictive models for hot mix asphalt mixtures. Doctoral dissertation, Arizona State University.

Bari, J., and Witczak, M. W. (2006). Development of a new revised version of the Witczak E* predictive models for hot mix asphalt mixtures. Journal of the Association of Asphalt Paving Technology 75, 381–417.

Bayomy, F., El-Badawy, S., and Awed, A. (2012). Implementation of the MEPDG for Flexible Pavements in Idaho. Research Report, Report No. FHWA-ID-12-193. Idaho transportation Department. Boise, Idaho.

Biligiri, P., and Way, B. (2014). Predicted E* dynamic moduli of the Arizona mixes using asphalt binders placed over a 25-year period. Construction and Building Materials, 54, 520-532. https://doi.org/10.1016/j.conbuildmat.2013.12.069

Bonaquist, R. (2011). Characterization of Wisconsin Mixture Low Temperature Properties for the AASHTO Mechanistic-Empirical Pavement Design Guide. Final Report. Report No. WHRP 11-12. Advanced Asphalt Technologies, LLC, Sterling, VA

Boone, J. (2013). Comparison of Ontario pavement designs using the AASHTO 1993 empirical method and the Mechanistic-Empirical Pavement Design Guide method. Master's thesis, University of Waterloo, Ontario, Canada

Carvalho, R. L., (2006). Mechanistic-empirical design of flexible pavements: A sensitivity study. Master's Thesis Dissertation, University of Maryland

Ceylan, H., Kim, S., Gopalakrishnan, K., and Smadi, O. (2009). Validation of Pavement Performance Curves for the Mechanistic-Empirical Pavement Design Guide. (No. CTRA Project 06-274). Iowa State University. Institute for Transportation

Christensen Jr, D., Pellinen, T., and Bonaquist, R. (2003). Hirsch model for estimating the modulus of asphalt concrete. Journal of the Association of Asphalt Paving Technologists, 72, 97-121.

Darter, M. I., Titus-Glover, L., Von Quintus, H., Bhattacharya, B. B., and Mallela, J. (2014). Calibration and Implementation of the AASHTO Mechanistic-Empirical Pavement Design Guide in Arizona. Report FHWA-AZ-14-606. Arizona Department of Transportation, Phoenix, Arizona.

Dave, E.V., and Hoplin, C. (2015). Flexible pavement thermal cracking performance sensitivity to fracture energy variation of asphalt mixtures. Road Materials and Pavement Design, 16, 423-441. https://doi.org/10.1080/14680629.2015.1029697

Elangovan, M. A. (2008). Dynamic Modulus Test: Laboratory Investigation and Future Implementation in the State of Washington, (Doctoral dissertation), Washington State University.

El-Badawy, S., Bayomy, F., and Awed, A. (2012). Performance of MEPDG dynamic modulus predictive models for asphalt concrete mixtures: Local calibration for Idaho. Journal of Materials in Civil Engineering, 24(11), 1412-1421.

Esfandiarpour, S. (2017). Calibrating MEPDG inputs prediction models for asphalt mixes containing reclaimed asphalt pavement. (Doctoral dissertation), University of Manitoba, Canada

Esfandiarpour, S., and Shalaby, A. (2017a). Alternatives for calibration of dynamic modulus prediction models of asphalt concrete containing RAP. International Journal of Pavement Research and Technology, 10(3), 203-218.

Esfandiarpour, S., and Shalaby, A. (2017b). Local calibration of creep compliance models of asphalt concrete. Construction and Building Materials, 132, 313-322.

Georgouli, K., Plati, C., and Loizos, A. (2016). Assessment of dynamic modulus prediction models in fatigue cracking estimation. Materials and Structures, 49(12), 5007-5019. https://doi.org/10.1617/s11527-016-0840-6.

Glover, L., and Mallela, J. (2009). Guidelines for implementing NCHRP 1-37A ME design procedures in Ohio: Volume 4-MEPDG models validation and recalibration. Final Report: FHWA/OH-2009/9D, Ohio Department of Transportation, Columbus, Ohio.

Haas, R., and Transportation Association of Canada. (1997). Pavement design and management guide Transportation Association of Canada Waterloo, ON, Canada.

Harrigan, E., and Witczak, M. (2004). Laboratory determination of resilient modulus for flexible pavement design. National Cooperative Highway Research Program: Research results digest, no. 285. Transportation Research Board of the National Academies, Washington, DC.

Hawkins, D. M. (2004). The Problem of Overfitting. Journal of Chemical Information and Computer Sciences, Vol. 44, 2004, pp. 1–12.

Huang, B., Shu, X., and Vukosavljevic, D. (2011). Laboratory investigation of cracking resistance of hot-mix asphalt field mixtures containing screened reclaimed asphalt pavement. Journal of Materials in Civil Engineering, 23(11), 1535-1543.

Huang, Y. H. (2004). Pavement analysis and design. New Jersey. Pearson Education, Inc.

Kavanagh, L. N. (2013). Mechanistic-Empirical Failure Prediction Models for Spring Weight Restricted Flexible Pavements in Manitoba using Manitoba and MnROAD Instrumented Test Sites. Doctoral dissertation, University of Manitoba, Canada.

Khattab, A. M., El-Badawy, S. M., and Elmwafi, M. (2014). Evaluation of witczak E* predictive models for the implementation of AASHTOWare-pavement ME design in the kingdom of saudi arabia. Construction and Building Materials, 64, 360-369.

Khattab, A. M., El-Badawy, S. M., and Elmwafi, M. (2017). Comparison of Witczak NCHRP 1-40D and Hirsh dynamic modulus models based on different binder characterization methods: A case study. Paper presented at the MATEC Web of Conferences, (Vol 120, p. 07003). EDP Sciences. https://doi.org/10.1051/matecconf/201712007003

Kim, Y. R., Underwood, B., Far, M. S., Jackson, N., and Puccinelli, J. (2011). LTPP Computed Parameter: Dynamic Modulus. Final Report No. FHWA-HRT-10-035, Report No. 1240.10, McLean, VA.

Kim, Y., King, M., and Momen, M. (2005). Typical dynamic moduli values of hot mix asphalt in North Carolina and their prediction. Paper presented at the 84th Annual Meeting of the Transportation Research Board. Washington, D.C

Krcmarik, M. (2013). Characteristics and prediction of the low temperature indirect tensile strengths of Michigan asphalt mixtures. Master's Thesis, Michigan State University, Michigan

Krcmarik, M., Varma, S., Emin Kutay, M., and Jamrah, A. (2016). Development of predictive models for low-temperature indirect tensile strength of asphalt mixtures. Journal of Materials in Civil Engineering, 28(11), 04016139.

Li, J., Pierce, L., and Uhlmeyer, J. (2009). Calibration of flexible pavement in mechanistic-empirical pavement design guide for washington state. Transportation Research Record: Journal of the Transportation Research Board, (2095), 73-83.

Luo, X., Gu, F., Zhang, Y., Lytton, R. L., and Zollinger, D. (2017). Mechanistic-empirical models for better consideration of subgrade and unbound layers influence on pavement performance. Transportation Geotechnics. 13, 52-68. https://doi.org/10.1016/j.trgeo.2017.06.002.

Mallela, J., Titus-Glover, L., Von Quintus, H., Darter, M., Stanley, M., and Rao, C. (2009). Implementing the AASHTO mechanistic-empirical pavement design guide in Missouri volume II: MEPDG model validation and calibration. Missouri Department of Transportation, Jefferson City, Missouri.

Mallela, J., Titus-Glover, L., Sadasivam, S., Bhattacharya, B., Darter, M., and Von Quintus, H. (2013). Implementation of the AASHTO Mechanistic-Empirical Pavement Design Guide for Colorado. Report CDOT-2013-4. Colorado Department of Transportation, Denver, Colorado.

Mallick, R. B., and El-Korchi, T. (2017). Pavement Engineering: Principles and practice CRC Press.

Marasteanu, M.O., and Cannone Falchetto, A. (2018). Review of experimental characterisation and modelling of asphalt binders at low temperature. International Journal of Pavement Engineering, 19(3), 279-291. https://doi.org/10.1080/10298436.2017.1347436

Mohammad, L. N., Saadeh, S., Obulareddy, S., and Cooper, S. (2007). Characterization of louisiana asphalt mixtures using simple performance tests. Journal of Testing and Evaluation, 36(1), 5-16.

Mohammad, L. N., Kim, M., Raghavendra, A., and Obulareddy, S. (2014). Characterization of Louisiana Asphalt Mixtures using Simple Performance Tests and MEPDG. FHWA Report No. FHWA/LA.11/499. Louisiana Transportation Research Center, Baton Rouge.

Momin, S. A. (2011). Local calibration of mechanistic empirical pavement design guide for North Eastern United States. Master's Thesis. University of Texas at Arlington.

NCHRP (2004). Design guide: Design of New and Rehabilitated Pavement Structures. NCHRP 1-37A Project, National Cooperative Highway Research Program, National Research Council, Washington, DC.

Pierce, L. M., and McGovern, G. (2014). NCHRP Synthesis Report 457: Implementation of the AASHTO mechanistic-empirical pavement design guide and software. Transportation Research Board. National Research Council, Washington, D.C, pp. 8.

Pierce, L., and McGovern, G. (2015). AASHTO MEPDG Regional Peer Exchange Meetings. Publication No. FHWA-HF-15-021. Federal Highway Administration, Washington, DC.

Poel, V., and Der, C. (1954). A general system describing the visco-elastic properties of bitumens and its relation to routine test data. Journal of Chemical Technology and Biotechnology, 4(5), 221-236.

Richardson, D. N., and Lusher, S. M. (2008). Determination of creep compliance and tensile strength of hot-mix asphalt for wearing courses in missouri.

Robbins, M. M., Rodezno, C., Tran, N., and Timm, D. (2017). Pavement ME Design–A Summary of Local Calibration Efforts for Flexible Pavements. National Center for Asphalt Technology Report. (No. NCAT Report 17-07)

Roque, R., Hiltunen, D.R., and Buttlar, W.G. (1995). Thermal cracking performance and design of mixtures using Superpave. Journal of the Association of Asphalt Paving Technologists, Volume 64, Association of Asphalt Paving Technologists (AAPT), p. 718-735.

Saha, J., Nassiri, S., Bayat, A., and Soleymani, H. (2014). Evaluation of the effects of canadian climate conditions on the MEPDG predictions for flexible pavement performance. International Journal of Pavement Engineering, 15(5), 392-401.

Schwartz, C. W., and Carvalho, R. L. (2007). Implementation of the NCHRP 1-37A design guide. Final Report Volume 1: Summary of Findings and Implementation Plan. University of Maryland.

Schwartz, C. W., Li, R., Kim, S., Ceylan, H., and Gopalakrishnan, K. (2011). Sensitivity evaluation of MEPDG performance prediction. Final report of NCHRP 1-47 Project, University of Maryland and Iowa State University.

Shalaby, A., El Halim, A., and Easa, S. (1996). Low-temperature stresses and fracture analysis of asphalt overlays. Transportation Research Record: Journal of the Transportation Research Board (1539), 132-139. https://doi.org/10.3141/1539-18

Soliman, H. (2015). Modelling of the resilient and permanent deformation behaviour of subgrade soils and unbound granular materials. (Doctoral dissertation), University of Manitoba.

Soliman, H., and Shalaby, A. (2014). Characterising the elastic behaviour of fine-grained subgrade soils under traffic loading. International Journal of Pavement Engineering, 15(8), 698-707.

Soliman, H., and Shalaby A. (2015). Permanent deformation behavior of unbound granular base materials with varying moisture and fines content. Transportation Geotechnics.4:1-12.

Soliman, H., and Shalaby, A. (2016). Validation of long-term pavement performance prediction models for resilient modulus of unbound granular materials. Transportation Research Record: Journal of the Transportation Research Board, (2578), 29-37.

Su, N., Xiao, F., Wang, J., and Amirkhanian, S. (2017). Characterizations of base and subbase layers for mechanistic-empirical pavement design. Construction and Building Materials, 152, 731-745.

Tarefder, R. A., Stormont, J. C., and Zaman, M. M. (2007). Evaluating Laboratory Modulus and Rutting of Asphalt Concrete. Transportation Research Board 86th Annual Meeting, Washington, DC.

Timm, D. H., Robbins, M. M., Tran, N., and Rodezno, C. (2014). Flexible Pavement Design-State of the Practice. National Center for Asphalt Technology Report. (No. NCAT Report 14-04).

Von Quintus, H., Hall, K. D., Fee, F., Coleri, E., Heitzman, M., May, R., and Hajj, E. Y. (2016). Integrating asphalt mixture design, structural design, and construction quality control. Transportation Research Circular, (E-C209).

Witczak, M., Andrei, D., and Houston, W. (2004). Guide for mechanistic-empirical design of new and rehabilitated pavement structures. Transportation Research Board of the National Research Council, 1-91.

Witczak, M., El-Basyouny, M., and El-Badawy, S. (2007). Incorporation of the new (2005) E* predictive model in the MEPDG. NCHRP 1-40D Inter-Tea, Technical Rep., Arizona State University, Tempe, AZ.

Witczak, M., Von Quintus, H., and Schwartz, C. (1997). Superpave support and performance models management: Evaluation of the SHRP performance models system. Paper presented at the Eighth International Conference on Asphalt Pavements. Federal Highway Administration, (Volume III), Seattle, Washington.

Zborowski, A., and Kaloush, K. E. (2007). Predictive equations to evaluate thermal fracture of asphalt rubber mixtures. Road Materials and Pavement Design, 8(4), 819-833.

Zhang, W., Shen, S., Basak, P., Wen, H., Wu, S., Faheem, A., and Mohammad, L. N. (2015). Development of predictive models for initiation and propagation of field transverse cracking.

Transportation Research Record: Journal of the Transportation Research Board: Vol. 2524, 92-99. https://doi.org/10.3141/2524-09.

Zhou, C. (2013). Investigation into key pavement materials and local calibration on MEPDG. (Doctoral dissertation). University of Tennessee, Knoxville.

APPENDIX

APPENDIX A: Summary of HMA material characterization database developed for Manitoba

As stated in previous chapters of this thesis, an important step to support the implementation of the Pavement ME design procedure was to develop a comprehensive HMA material characterization database based on laboratory testing. Appendix A presents a general summary on the status of asphalt concrete characterization database developed for Manitoba, which includes characterization tests and obtained test results.

A.1 HMA Samples and Characterization Tests

The advanced HMA material characterization project involved the testing of 247 asphalt mix samples under 14 contracts since 2010. 197 laboratory compacted samples and 50 extracted field core samples were sent by Manitoba Infrastructure Central laboratory to the University of Manitoba for testing. The characterization tests conducted on the HMA samples include dynamic modulus test, resilient modulus test, creep compliance test and IDT strength test. Dynamic modulus test was conducted on samples having a diameter of 4 inches and a height of 6 inches at four different temperatures (-10, 5, 25, 40 °C) and six loading frequencies (25Hz, 10Hz, 5 Hz, 1 Hz, 0.5 Hz and 0.1 Hz). The main aim of the dynamic modulus test was to evaluate the rutting and fatigue cracking potential of the HMA mixes under traffic loading. The creep compliance, resilient modulus, and IDT strength test were conducted on samples having a thickness of 2 inches and a diameter of 6 inches.

Table A.1 presents a summary of the HMA characterization test executed for all contract projects. The test temperatures, test frequency and test protocol used for each characterization test are also presented.

Table A.1**:** HMA Characterization tests and test protocol

Tests	**Purpose**	**Test Temperature**	**Test Frequency**	**Test Protocol**
Dynamic Modulus |E*|	Evaluate the rutting and fatigue cracking performance of the mixes	-10 °C	0.1 Hz	AASHTO T 342-11
		5°C	0.5 Hz	
		25°C	1 Hz	
		40°C	5Hz	
			10 Hz	
			25 Hz	
Creep Compliance	Characterize Low-Temperature thermal cracking resistance	0 °C	None	AASHTO 322-07 (2011)
		-10 °C		
		-20 °C		
Resilient Modulus	Evaluate HMA stiffness parameters used for design	5°C	None	LTPP Protocol P07/ASTM D7369
		25°C		
		40°C		
IDT Strength	Characterize Low-Temperature thermal cracking resistance of the mixes	-10 °C	None	AASHTO 322-07 (2011)

Figure A1 shows typical HMA samples used for dynamic modulus, creep compliance, resilient modulus, and IDT strength tests. Figure A2 through Figure A3 depicts the HMA characterization test setup at the University of Manitoba.

(a) (4"diameter x 6 " height) dynamic modulus test samples

(b) (2" thick x 6" diameter) Creep compliance, resilient modulus, and IDT strength test samples

Figure A.1: Typical samples used for HMA material characterization tests

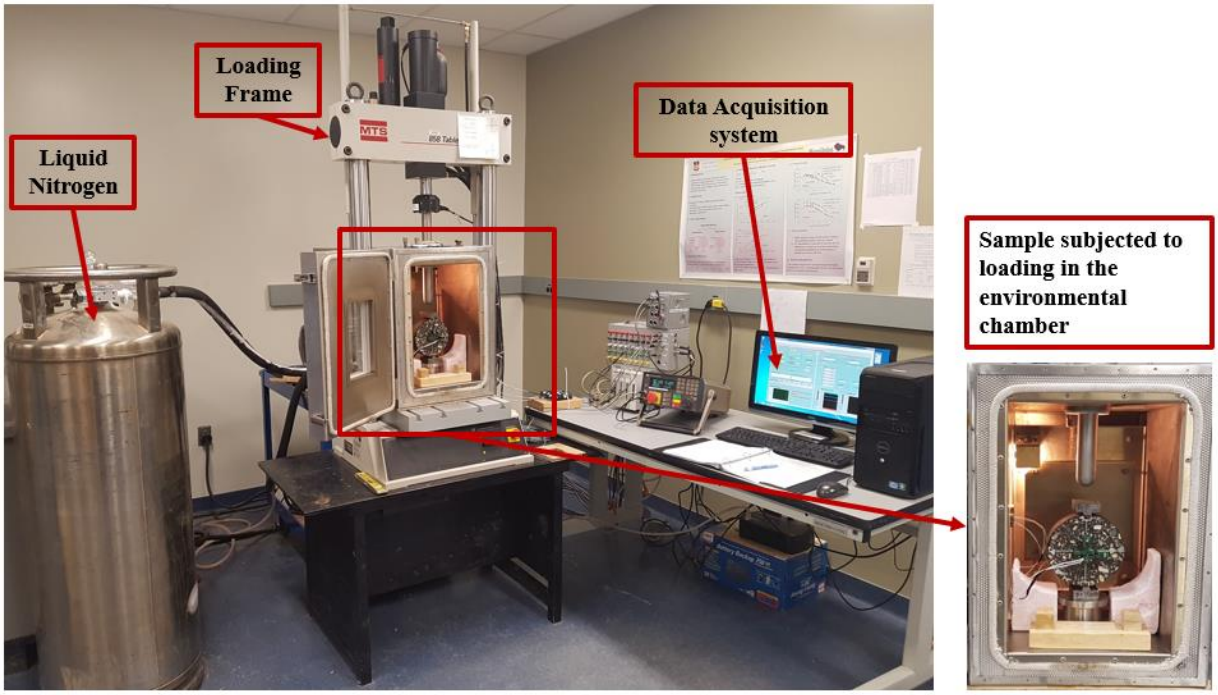

Figure A.2: Creep compliance and resilient modulus test setup

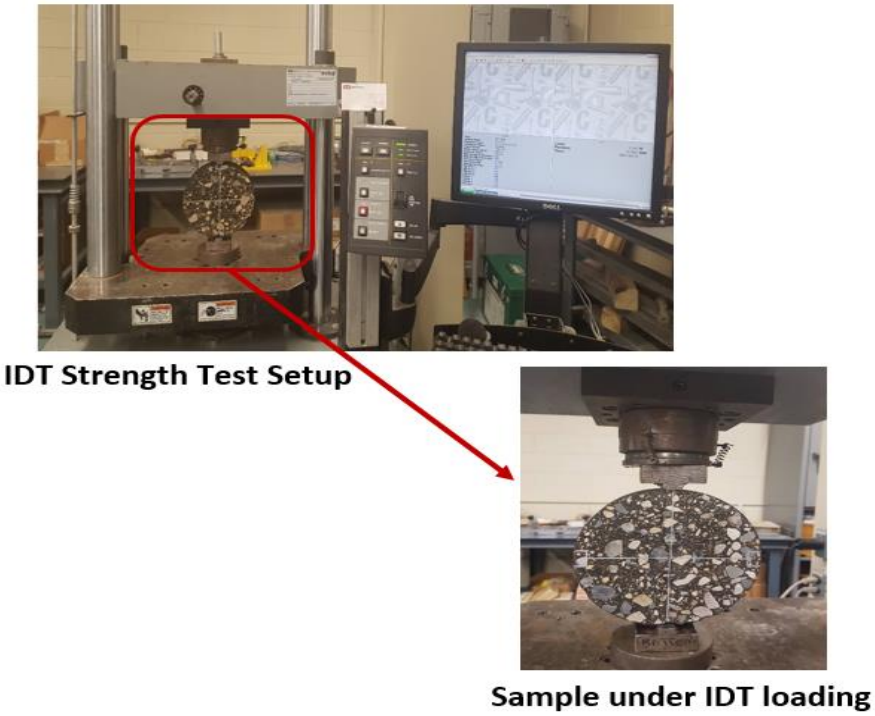

Figure A.3: IDT Strength test setup

A total number of 3642 asphalt characterization tests were conducted on the 247 HMA samples between 2010 and 2017. This is further illustrated in Figure A.4. Furthermore, Table A.2 and A.3 present a breakdown of the number of characterization tests conducted by year under each job contract.

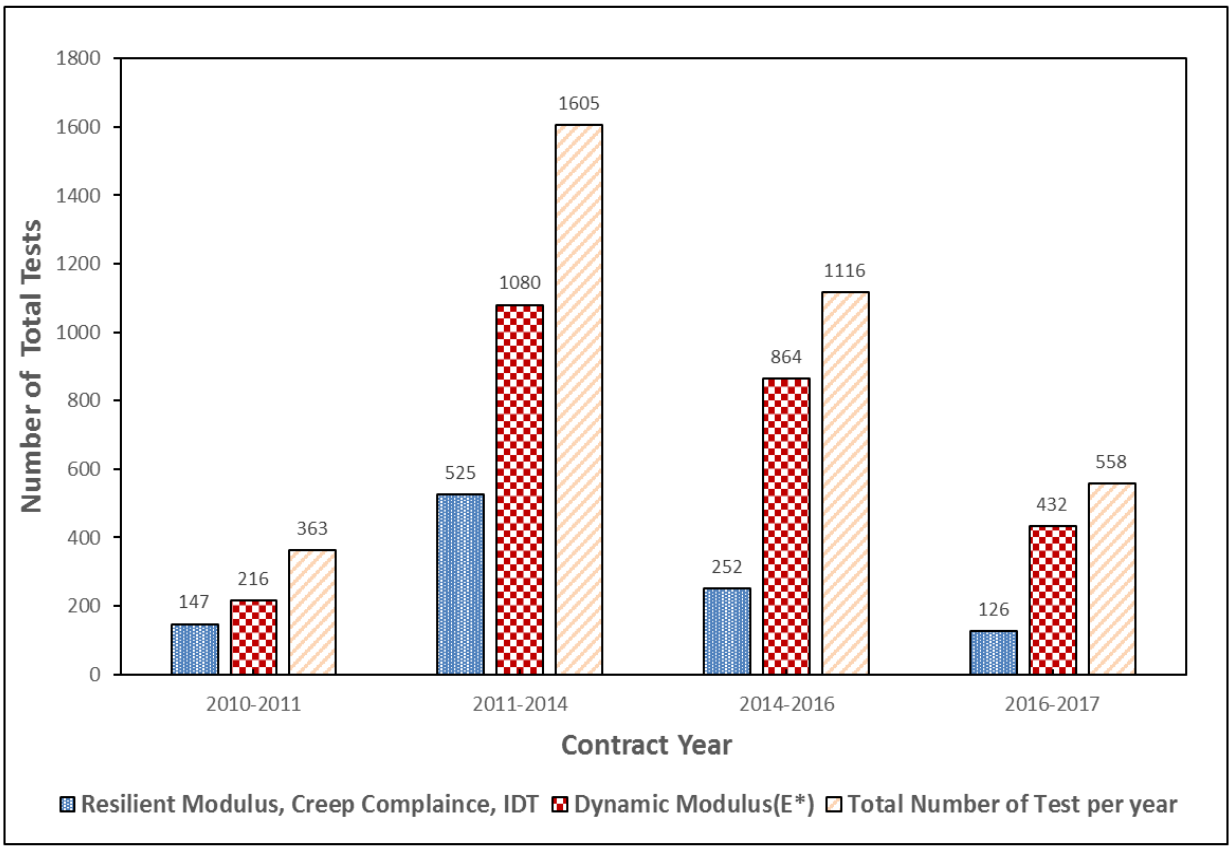

Figure A.4: Number of total tests per year

Table A.2**:** Number of samples and Percentage tested.

Year	Contracts	Number of Samples for dynamic modulus test |E*|	Number of Samples for Resilient Modulus, Creep compliance and IDT tests	Percentage Tested and analysis completed
2016-2017	6341	18	18	100%
	6298			
2014-2016	6131	36	36	100%
	6152			
	6168			
	6224			
	6135			
	6133			
2011-2014	6045	36	73	100%
	6022			
	6017			
	5895			
	5888			
2010-2011	5918	9	21	100%
	6017			
Total:		**99**	**148**	**100%**

Table A.3**:** Breakdown by sample type and Contract number

Year	**Contract number**	**RAP Content (%)**	**Dynamic Modulus |E*|Tests**		**Resilient Modulus, Creep compliance, IDT tests**			
			Laboratory Compacted Samples		**Laboratory Compacted Samples**		**Field Core Samples**	
			Bit B	Bit C	Bit B	Bit C	Bit B	Bit C
2016-2017	6341	0	12	-	12	-	-	-
	6298*	15,40	6	-	6	-	-	-
	Total:		**18**	**0**	**18**	**0**	**0**	**0**
2014-2016	6131*	0,15,	6	-	6	-	-	-
	6152*	15,40	6	-	6	-	-	-
	6168*	10,20	6	-	6	-	-	-
	6224*	0,40	6	-	6	-	-	-
	6135*	15,40	6	-	6	-	-	-
	6133*	0,10	6	-	6	-	-	-
	Total:		**36**	**0**	**36**	**0**	**0**	**0**
2011-2014	6045	n/a	6	-	6	-	6	-
	6022	n/a	6	-	6	-	6	-
	6017	n/a	3	-	3	-	3	-
	5895*	0,10,40,50	12	3	11	3	15	3
	5888	n/a	3	3	3	3	5	-
	Total:		**30**	**6**	**29**	**6**	**35**	**3**
2010-2011	5918	n/a	3	3	3	6	6	6
	6017	n/a	3	-	-	-	-	-
	Total:		**6**	**3**	**3**	**6**	**6**	**6**
Grand Total:			**99**		**148**			

Note: *contracts containing high RAP contents

A.2 Test Result Summary

A.2.1 Dynamic modulus |E*| test results

Table A.4 presents the average dynamic modulus values of the laboratory, compacted samples obtained over all contract years. In addition, Figures A.5 (a) to (d) shows the breakdown of the average dynamic modulus values obtained at each test temperature per contract year. Table A. 4 shows that the dynamic modulus values increase with increase in test frequency. In addition, it was generally observed that the increase of test temperature resulted in a decrease of dynamic modulus values.

Table A.4**:** Average Dynamic Modulus |E*| values for all contract years

Dynamic Modulus |E*|, GPa						
Test Temperature, °C	0.1 Hz	0.5 Hz	1 Hz	5 Hz	10 Hz	25 Hz
-10	17.82	21.47	23.12	26.5	27.71	29.1
5	7.08	9.98	11.35	14.85	16.42	18.24
25	1.62	2.48	3.08	4.94	5.98	7.36
40	0.48	0.72	0.91	1.54	1.98	2.7

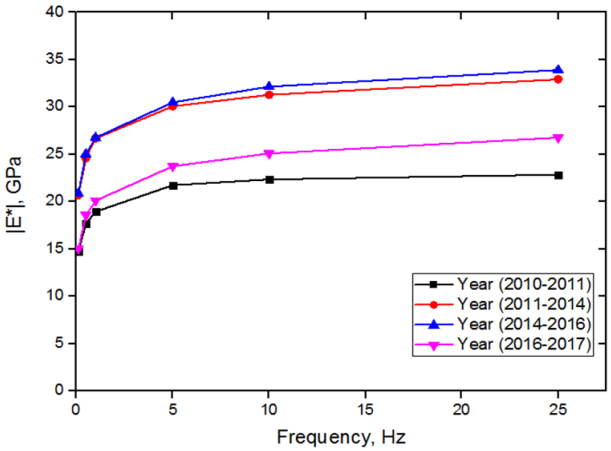

(a) Dynamic modulus values by year at (-10 °C)

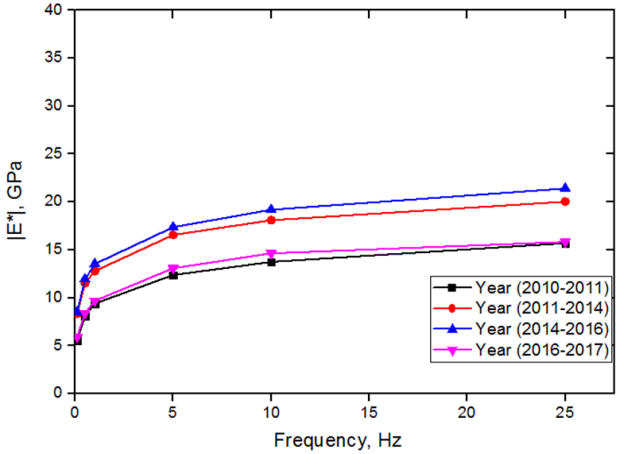

(b) Dynamic modulus values by year at (5 °C)

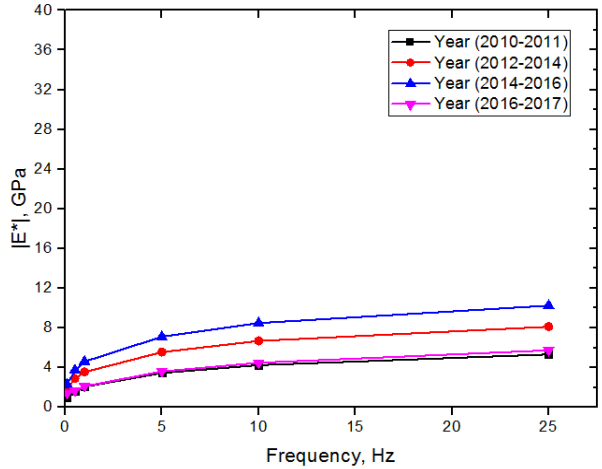

(c) Dynamic modulus values by year at (25 °C)

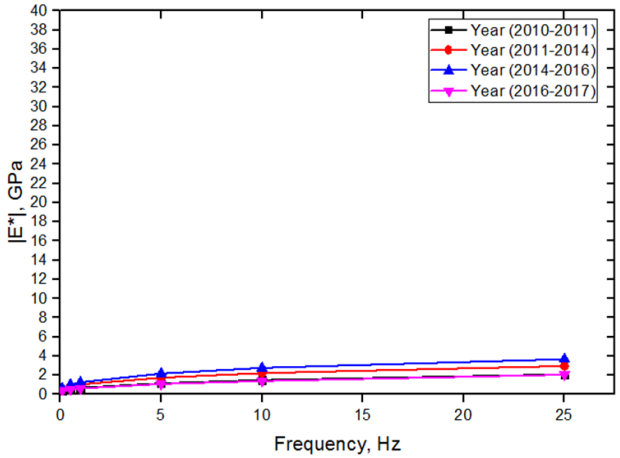

(d) Dynamic modulus values by year at (40 °C)

Figures A.5 Comparison of dynamic modulus values by temperature for each year

A.2.2 Creep compliance test results

Table A.5 presents the average creep compliance values obtained over all contract years. Also, Figures A.6 (a) to (c) show the breakdown of the average creep compliance values obtained at each test temperature per contract year.

Table A.5**:** Average creep compliance values for all contract years

Creep Compliance, (1/GPa)			
Loading Time (seconds)	Low Temperature (-20°C)	Mid Temperature (-10°C)	High Temperature (0°C)
1	0.051016	0.089929	0.180363
2	0.053251	0.095989	0.200425
5	0.057733	0.108678	0.24536
10	0.062413	0.123652	0.298613
20	0.068708	0.144832	0.377462
50	0.08025	0.18708	0.539773
100	0.092541	0.23387	0.727722

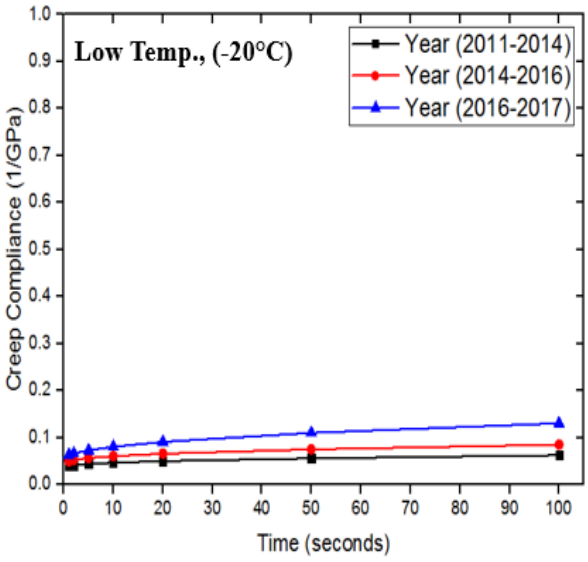

(a) Average creep compliance values (-20 °C)

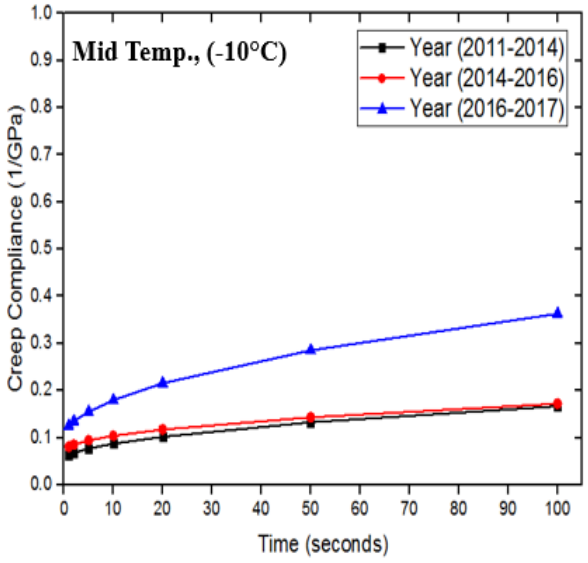

(b) Average creep compliance values (-10 °C)

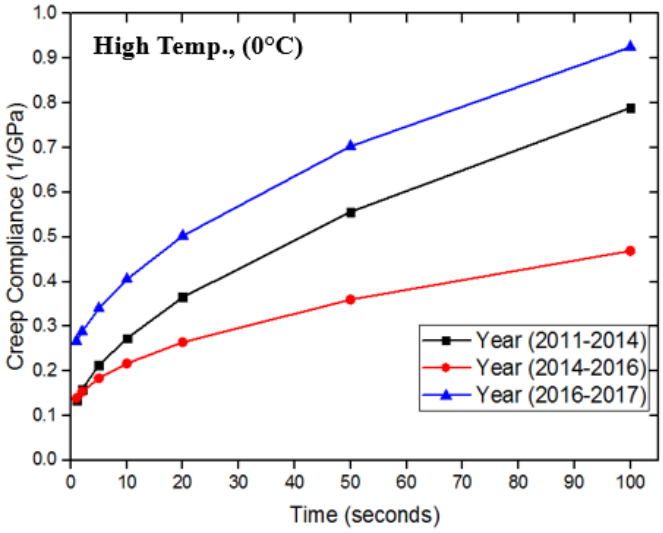

(c) Average creep compliance values (0 °C)

Figures A.6 Comparison of creep compliance values by temperature for each year

A.2.3 Resilient modulus test results

Table A.6 and Table A.7 presents the average instantaneous and total resilient modulus values obtained per contract years.

Table A.6**:** Average Instantaneous Resilient Modulus Values per contract year

Instantaneous Resilient Modulus (Mr), GPa				
Temp., °C	2010-2011	2011-2014	2014-2016	2016-2017
5	5.54	12.45	14.27	10.22
25	1.25	3.36	4.69	2.69
40	0.22	1.88	1.28	0.85

Table A.7**:** Average Total Resilient Modulus Values per contract year

Total Resilient Modulus (Mr), GPa				
Temp., °C	2010-2011	2011-2014	2014-2016	2016-2017
5	5.04	11.67	13.5	9.36
25	1.2	3.19	4.31	2.46
40	0.24	2.1	1.18	0.79

Figure A.7 (a) and (b) depicts the comparison of the average instantaneous and total resilient modulus values obtained at each test temperature per contract year respectively. As seen in Figure A.7, the instantaneous and total resilient modulus values decreases with increase in test temperature (from 5°C to 40°C). As temperature increases, asphalt binders in the mix become softer, thereby resulting in lower values of resilient modulus.

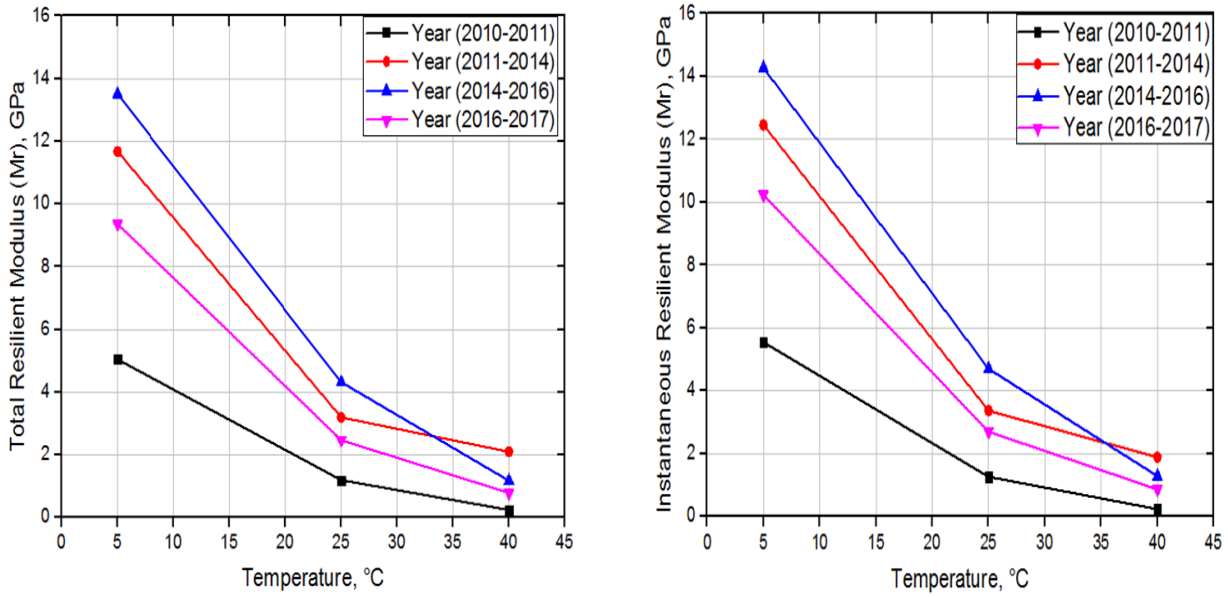

(a) Total resilient modulus (b) Instantaneous resilient modulus

Figures A.7 Comparison of creep compliance values by temperature for each year

A.2.4 IDT test results

Table A.8 presents the average IDT strength values for laboratory compacted and field core samples obtained for each year. This is further depicted in Figure A.8 (a). Figures A.8 (b) and (c) presents a breakdown of the average IDT strength values by samples type (laboratory compacted and field core) and RAP content respectively.

Table A.8**:** Average IDT Strength Values per contract year

IDT Strength , MPa			
Temp., °C	2011-2014	2014-2016	2016-2017
-10	3.15	3.76	2.72

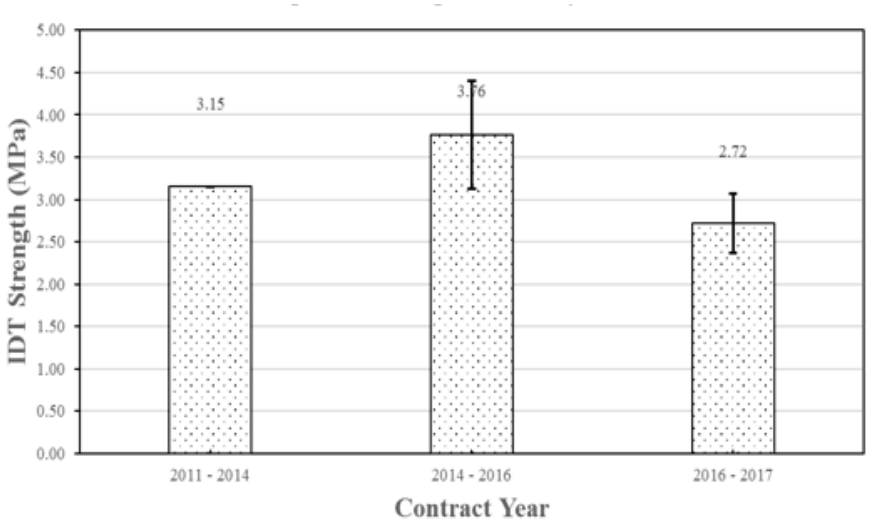

(a) Average IDT Strength Values by contract year

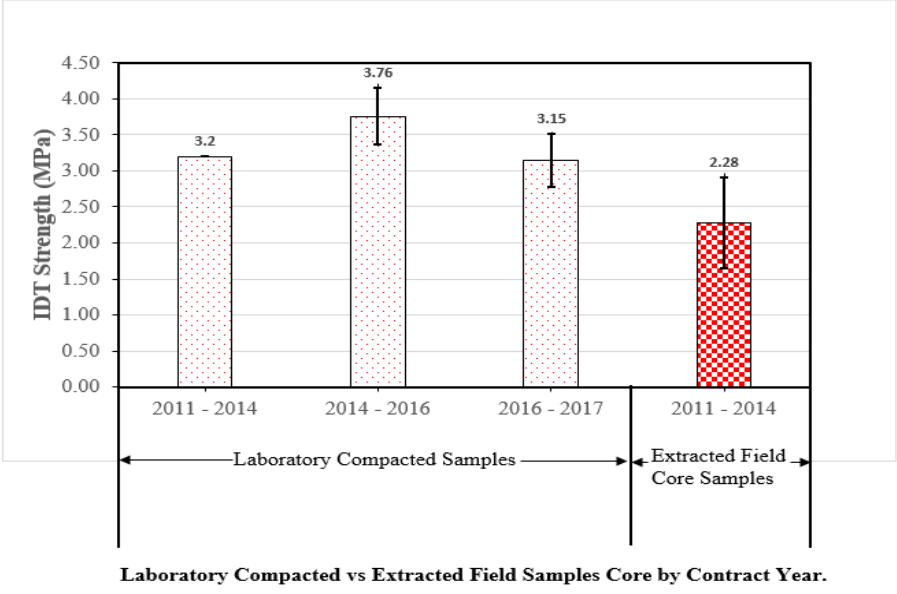

(b) Laboratory compacted and extracted field core samples by year

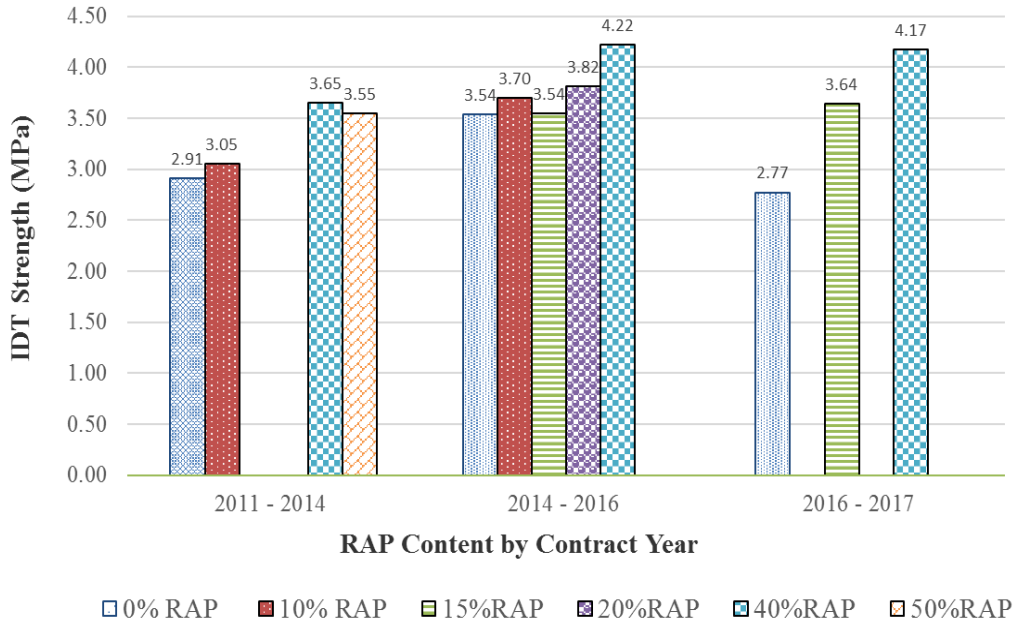

A.3 Summary of characterization test results over all contract years

Based on the advanced asphalt characterization test results on the laboratory compacted and field core samples, the following summaries were drawn:

1. Dynamic modulus test conducted for the laboratory compacted samples yielded average dynamic modulus values ranging between 0.33 GPa to 40 GPa depending on test temperature (-10°C, to 40°C) over loading freqiencies of 0.1Hz to 25 Hz.
2. Average creep compliance values obtained over all contract years ranged between 0.00400 (1/GPa) to 0.9259 (1/GPa) depending on test temperature (-20°C to 0°C)
3. The average values for Instanteneous and Total resilient resilient modulus values range from 0.22 GPa to 15 GPa depending on test temperature (5°C, 25°C and 40°C)
4. Average IDT strength values for labouratory compacted samples (3.15 to 3.76 MPa) were higher as compared to values obtained from field core samples (2.28 MPa). The lower IDT

strength in field core samples could be attributed to the larger air voids in the samples. Overall, the average IDT strength values ranged between 2.72 to 3.76 MPa over all contract years.

APPENDIX B: IDT Strength Database

Table B.1**:** Summary of IDT strength test results

Project Location	MI's Contract No.	Mix Designation (Field Samples)	Station	IDT Strength at -10 °C (MPa)	Average Values MPa (psi)[1]	Standard Deviation MPa (Psi)[1]	COV (%)
PTH 10 (PTH 1 to PTH) 25	6131	B98	111+40_15%	2.884	3.182 (461.51)	0.309 (44.82)	9.7
		B98	112+60_15%	3.501			
		B98	218+20_15%	3.161			
		B99	#1_0%	n.a	3.254 (472.10)	0 (0)	0.0
		B99	#2_0%	3.255			
		B99	#3_0%	n.a			
Foxwarren PTH 16	6133	B98	134+65_10%	3.589	3.770 (546.79)	0.217 (31.62)	5.8
		B98	226+63_10%	4.012			
		B98	248+90_10%	3.711			
		B99	129+30_0%	3.661	3.786 (549.11)	0.163 (23.64)	4.3
		B99	155+00_0%	3.728			
		B99	208+80_0%	3.971			
PTH 1 Portage la Prairie By-pass	6135	B98	285+40_40%	4.254	4.277 (620.47)	0.023 (3.34)	0.5
		B98	288+06_40%	4.301			
		B98	293+00_40%	4.277			
		B99	286+60_15%	3.939	3.817 (553.61)	0.119 (17.26)	3.1
		B99	343+00_15%	3.813			
		B99	380+20_15%	3.701			
PTH 6 Grosse Isle South	6152	B98	249+20_40%	3.413	3.903 (566.08)	0.461 (66.86)	11.8
		B98	250+00_40%	3.967			
		B98	251+60_40%	4.329			
		B99	210+00_15%	3.634	3.632 (526.78)	0.053 (7.67)	1.5
		B99	224+00_15%	3.578			
		B99	250+43_15%	3.684			
PTH 16 Gladstone (PTH 20-2.5km W of PTH 340)	6168	B98	249+20_40%	3.413	3.903 (566.08)	0.461 (66.86)	11.8
		B98	250+00_40%	3.967			
		B98	251+60_40%	4.329			
		B99	210+00_15%	3.634	3.632 (526.78)	0.053 (7.69)	1.5
		B99	224+00_15%	3.578			
		B99	250+43_15%	3.684			
PTH 16 Gladstone (PTH 20-2.5km W of PTH 340)	6168	B98	#1_20%	3.707	3.816 (553.61)	0.243 (35.24)	6.4
		B98	#2_20%	4.095			
		B98	#3_20%	3.647			
		B99	#1_10%	3.599	3.629 (526.49)	0.117 (16.96)	3.2
		B99	#2_10%	3.531			
		B99	#3_10%	3.760			

PTH 5 McCreary	6224	B98	151+70_40%	4.414	4.482 (650.20)	0.343 (49.75)	7.7
		B98	186+90_40%	4.855			
		B98	201+92_40%	4.179			
		B99	134+90_0%	3.479	3.609 (523.44)	0.184 (26.69)	5.1
		B99	209+34_0%	3.740			
		B99	218+60_0%	n.a			
PTH 1 Portage la Prairie By-pass	6045	Bit B99	238+50_15%	3.421	3.394 (492.40)	0.046 (6.67)	1.4
		Bit B99	239+30_15%	3.422			
		Bit B99	271+20_15%	3.341			
PTH 1 E. JCT. #10 To JCT. PR 340	6017	Bit B99 (Sample1)	0%	2.887	3.038 (440.77)	0.140 (20.45)	4.6
		Bit B99 (sample 9)	0%	3.165			
		Bit B99 (sample10)	0%	3.066			
PTH 8 Gimli	5895	Bit B	174+40_40%	4.142	3.646 (528.95)	0.556 (80.64)	15.3
		Bit B	158+40_40%A	3.045			
		Bit B	158+40_40%B	3.754			
		Bit B	186+40_10%	2.899	3.050 (442.51)	0.448 (65.12)	14.7
		Bit B	168+00_10%	3.555			
		Bit B	284+80_10%	2.697			
		Bit B	192+00_50%	4.142	3.566 (517.20)	0.633 (91.8)	17.8
		Bit B	125+20_50%A	3.668			
		Bit B	125+20_50%B	2.888			
		Bit B	197+80_0% A	2.899	2.907 (421.77)	0.012 (1.74)	0.4
		Bit B	197+80_0% B	2.917			
PTH 21 Deloraine	6341	B99	#1_0%	2.906	3.090 (448.17)	0.181 (26.39)	5.9
		B99	#9_0%	3.095			
		B99	#10_0%	3.269			
		B98	#3_0%	2.802	2.802 (406.40)	0.268 (39.02)	9.6
		B98	#5_0%	2.534			
		B98	#7_0%	3.071			
PTH 1 West Portage	6298	B99	99+75_15%	3.359	3.635 (527.21)	0.401 (58.31)	11.1
		B99	127+25_15%	4.096			
		B99	112+60_15%	3.450			
		B98	91+00_40%	4.411	4.168 (604.52)	0.211 (30.6)	5.1
		B98	138+70_40%	4.069			
		B98	112+60_40%	4.025			

Note: [1]IDT strength values in psi; MI = Manitoba Infrastructure; cov = coefficient of variance

APPENDIX C: Vehicle class distribution, axle load distribution, and monthly distribution for PTH 1 and PTH 23

Table C.1: Typical Manitoba Axle per Truck for PTH 1 and PTH 23

FHWA Truck Class	Single	Tandem	Tridem	Quad	Total
4 	1.00	1.09	0.00	0.00	2.09
5 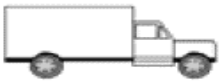	2.00	0.00	0.00	0.00	2.00
6 	1.00	1.00	0.00	0.00	2.00
7 	0.20	1.60	0.20	0.00	2.00
8 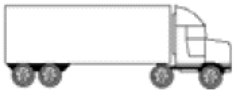	2.17	0.84	0.00	0.00	3.01
9 	1.01	1.99	0.00	0.00	3.00
10 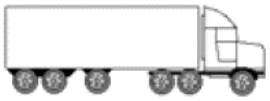	1.00	1.00	1.00	0.00	3.00
11 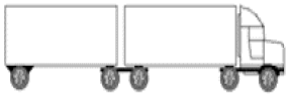	4.18	0.15	0.17	0.00	4.50
12 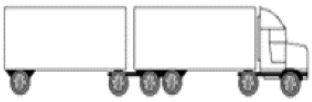	3.94	1.02	0.00	0.00	4.96
13 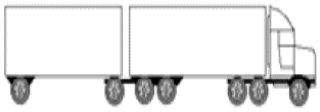	1.12	3.33	0.29	0.00	4.74

Table C.2: Vehicle Monthly Adjustment Factors for PTH 1 (Region 2): PTH 34 to PR 350

Site	Month	Class 4	Class 5	Class 6	Class 7	Class 8	Class 9	Class 10	Class 11	Class 12	Class 13
Station 65	1	1.13	0.82	0.77	0.46	0.54	0.92	0.89	0.45	0.86	0.91
Station 65	2	1.05	0.90	0.79	0.77	0.58	0.98	0.92	0.61	0.97	0.97
Station 65	3	1.17	0.94	0.99	1.39	0.74	1.03	1.02	0.51	1.01	1.03
Station 65	4	1.13	1.01	1.22	0.78	0.81	1.00	1.03	0.41	0.98	1.05
Station 65	5	0.99	1.09	1.09	1.79	0.94	1.03	1.04	0.57	1.02	1.04
Station 65	6	1.09	1.21	1.05	1.37	1.31	1.04	0.98	0.81	0.94	0.99
Station 65	7	1.00	1.10	1.04	1.07	1.47	1.00	1.01	0.96	0.90	1.04
Station 65	8	0.90	1.11	1.10	1.36	1.47	1.01	1.03	0.87	0.95	1.00
Station 65	9	0.92	1.05	1.10	0.72	1.06	1.01	1.15	0.63	1.09	1.07
Station 65	10	0.83	1.05	1.07	0.93	0.79	1.04	1.10	0.64	0.97	1.06
Station 65	11	1.07	0.92	0.97	0.82	1.75	1.01	0.96	4.83	1.41	0.97
Station 65	12	0.72	0.80	0.81	0.54	0.54	0.93	0.87	0.71	0.90	0.87

Table C.3: Vehicle Monthly Adjustment Factors for PTH 23 (Region 3): E Jct. PTH 18 to PTH 5

Site	Month	Class 4	Class 5	Class 6	Class 7	Class 8	Class 9	Class 10	Class 11	Class 12	Class 13
TTPG3	1	0.83	0.79	0.70	0.52	0.55	0.81	0.60	0.37	0.47	0.82
TTPG3	2	1.34	0.94	0.77	0.62	0.60	0.90	0.83	0.46	0.92	0.88
TTPG3	3	1.00	0.83	0.79	0.63	0.67	0.97	0.91	0.52	0.67	0.91
TTPG3	4	0.78	0.94	0.94	0.86	0.73	1.02	1.03	0.65	0.73	0.87
TTPG3	5	0.97	1.19	1.24	1.07	1.02	1.18	1.16	0.88	1.28	1.35
TTPG3	6	0.99	1.32	1.25	1.45	1.46	1.06	1.07	1.70	0.96	0.95
TTPG3	7	0.92	1.02	1.07	1.42	1.58	1.01	0.98	2.00	1.26	0.92
TTPG3	8	0.96	0.96	1.06	1.39	1.58	1.02	0.98	1.92	1.34	0.95
TTPG3	9	1.10	1.12	1.21	1.30	1.34	1.08	1.09	1.41	1.13	1.10
TTPG3	10	1.16	1.11	1.28	1.22	1.11	1.12	1.12	1.05	1.62	1.25
TTPG3	11	1.07	0.99	0.98	0.90	0.81	1.05	1.15	0.63	1.03	1.16
TTPG3	12	0.88	0.79	0.71	0.62	0.55	0.78	0.82	0.41	0.59	0.84

APPENDIX D: Pavement ME analysis output for Case 1: 150 mm HMA/300 mm base calibrated material procedure

PTH1_Case1_Calibrated_Runs_150_300

File Name: C:\Users\Administrator\Desktop\My ME Design\ASCE Paper Analysis_Re-Run\CASE 1\Calibrated\PTH1_Case1_Calibrated_Runs_150_300.dgpx

Design Inputs

Design Life: 20 years
Design Type: FLEXIBLE

Base construction: July, 2017
Pavement construction: September, 2017
Traffic opening: September, 2017

Climate Data Sources (Lat/Lon): 49.917, -99.95

Design Structure

Layer type	Material Type	Thickness(mm)
Flexible	Default asphalt concrete	150.0
NonStabilized	Crushed stone	300.0
Subgrade	A-7-5	Semi-infinite

Volumetric at Construction:	
Effective binder content (%)	9.9
Air voids (%)	3.8

Traffic

Age (year)	Heavy Trucks (cumulative)
2017 (initial)	2,420
2027 (10 years)	4,237,750
2037 (20 years)	9,107,590

Design Outputs

Distress Prediction Summary

Distress Type	Distress @ Specified Reliability		Reliability (%)		Criterion
	Target	Predicted	Target	Achieved	Satisfied?
Terminal IRI (m/km)	2.50	2.64	90.00	84.38	Fail
Permanent deformation - total pavement (mm)	19.00	12.31	90.00	100.00	Pass
AC bottom-up fatigue cracking (percent)	15.00	1.53	90.00	100.00	Pass
AC thermal cracking (m/km)	200.00	491.04	90.00	0.24	Fail
AC top-down fatigue cracking (m/km)	500.00	59.86	90.00	100.00	Pass
Permanent deformation - AC only (mm)	12.00	1.24	90.00	100.00	Pass

Distress Charts

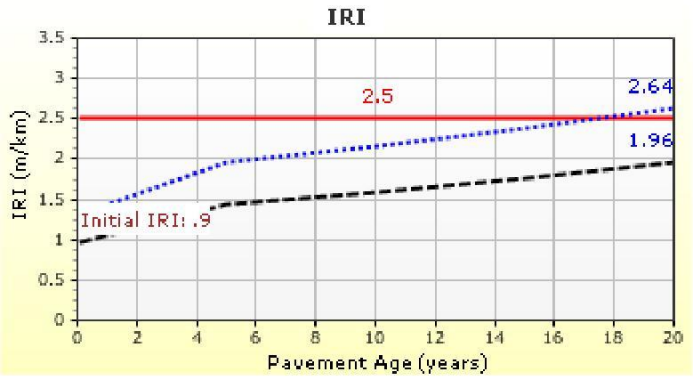

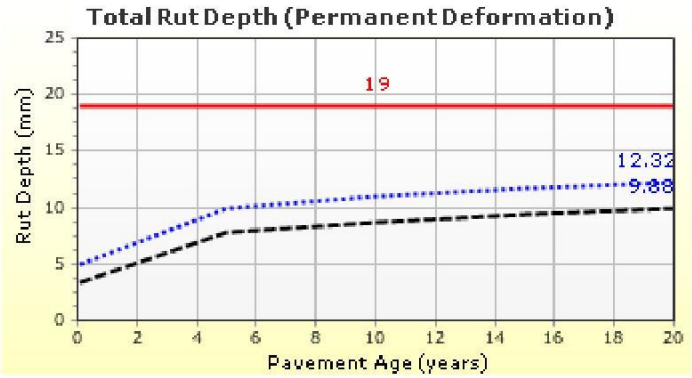

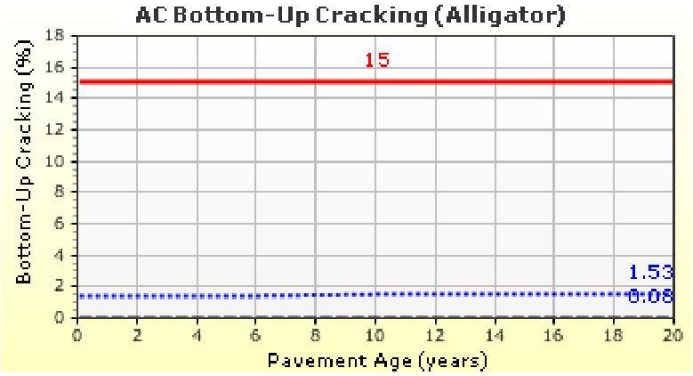

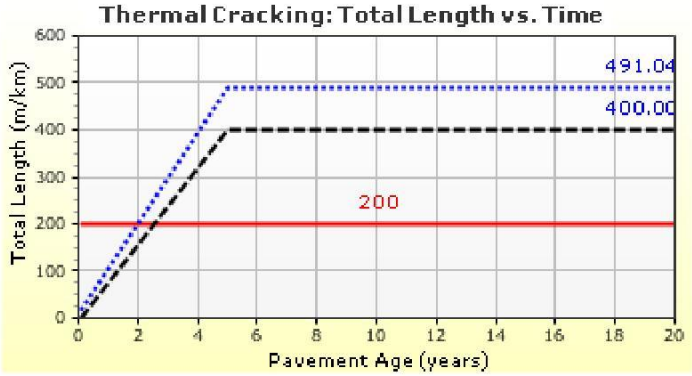

PTH1_Case1_Calibrated_Runs_150_300

File Name: C:\Users\Administrator\Desktop\My ME Design\ASCE Paper Analysis_Re-Run\CASE 1\Calibrated\PTH1_Case1_Calibrated_Runs_150_300.dgpx

Traffic Inputs

Graphical Representation of Traffic Inputs

Initial two-way AADTT:	2,420	Percent of trucks in design direction (%):	50.0
Number of lanes in design direction:	2	Percent of trucks in design lane (%):	90.0
		Operational speed (kph)	100.0

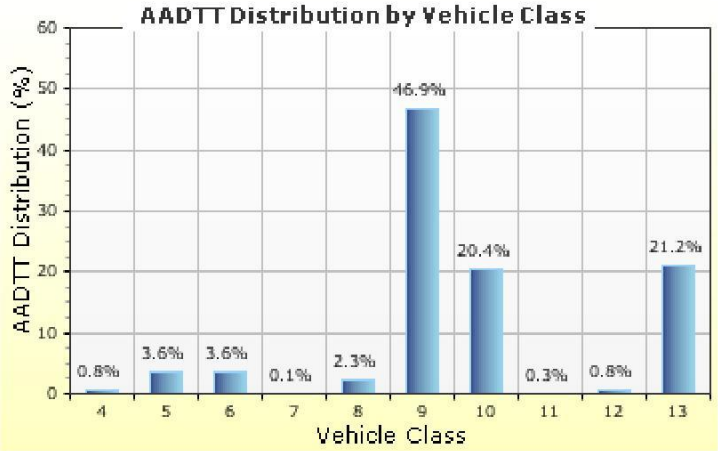

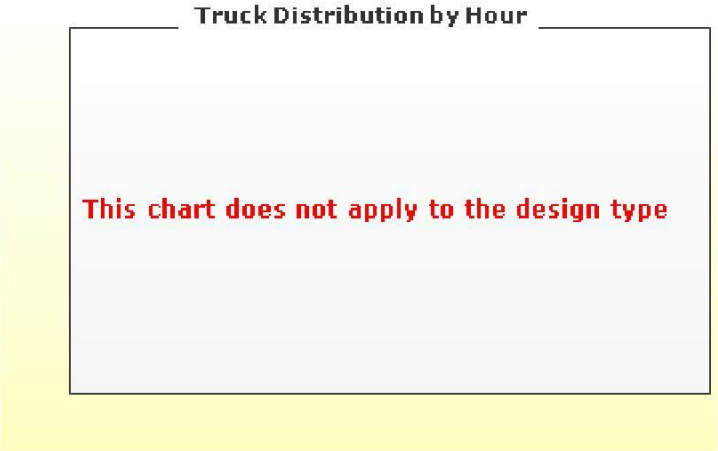

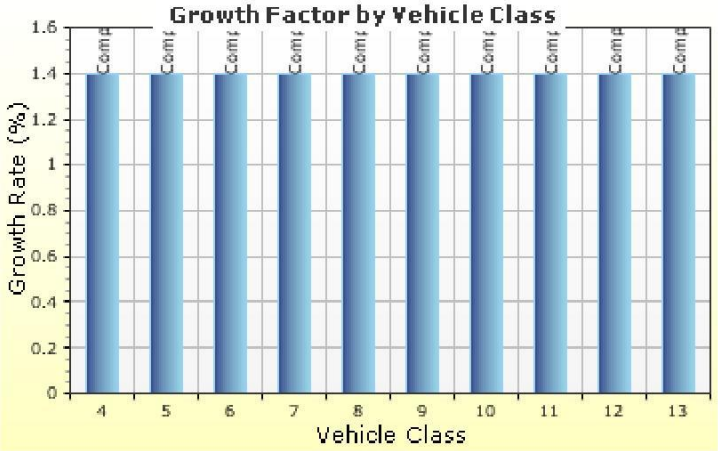

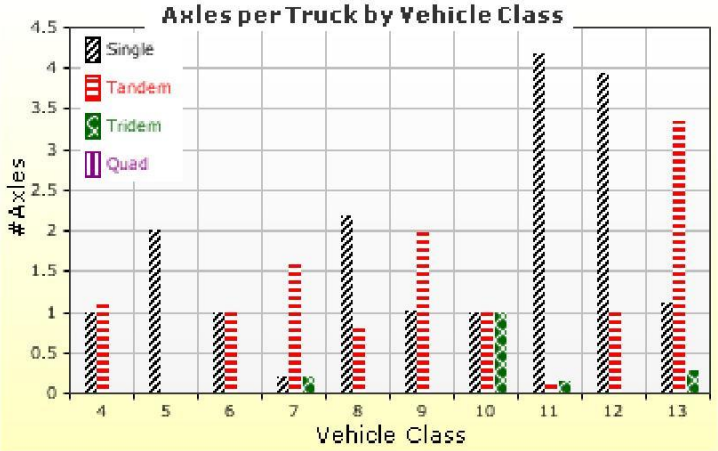

Traffic Volume Monthly Adjustment Factors

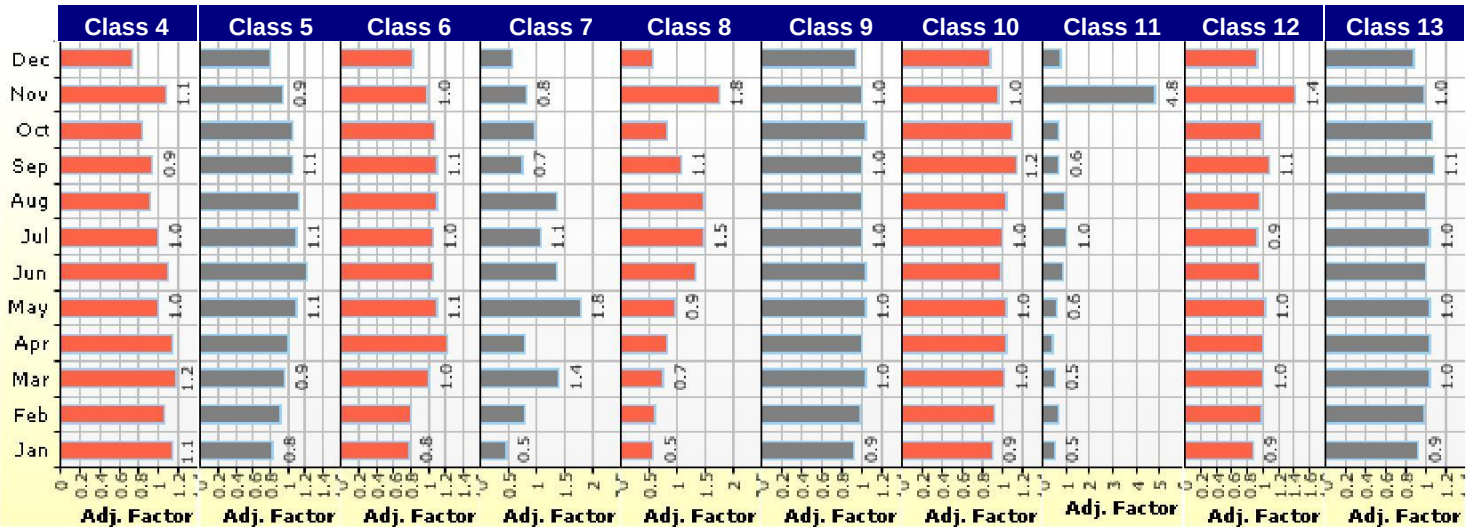

Tabular Representation of Traffic Inputs

Volume Monthly Adjustment Factors

Level 3: Default MAF

Month	Vehicle Class									
	4	5	6	7	8	9	10	11	12	13
January	1.1	0.8	0.8	0.5	0.5	0.9	0.9	0.5	0.9	0.9
February	1.1	0.9	0.8	0.8	0.6	1.0	0.9	0.6	1.0	1.0
March	1.2	0.9	1.0	1.4	0.7	1.0	1.0	0.5	1.0	1.0
April	1.1	1.0	1.2	0.8	0.8	1.0	1.0	0.4	1.0	1.1
May	1.0	1.1	1.1	1.8	0.9	1.0	1.0	0.6	1.0	1.0
June	1.1	1.2	1.1	1.4	1.3	1.0	1.0	0.8	0.9	1.0
July	1.0	1.1	1.0	1.1	1.5	1.0	1.0	1.0	0.9	1.0
August	0.9	1.1	1.1	1.4	1.5	1.0	1.0	0.9	1.0	1.0
September	0.9	1.1	1.1	0.7	1.1	1.0	1.2	0.6	1.1	1.1
October	0.8	1.1	1.1	0.9	0.8	1.0	1.1	0.6	1.0	1.1
November	1.1	0.9	1.0	0.8	1.8	1.0	1.0	4.8	1.4	1.0
December	0.7	0.8	0.8	0.5	0.5	0.9	0.9	0.7	0.9	0.9

Distributions by Vehicle Class

Vehicle Class	AADTT Distribution (%) (Level 3)	Growth Factor	
		Rate (%)	Function
Class 4	0.8%	1.4%	Compound
Class 5	3.6%	1.4%	Compound
Class 6	3.6%	1.4%	Compound
Class 7	0.1%	1.4%	Compound
Class 8	2.3%	1.4%	Compound
Class 9	46.9%	1.4%	Compound
Class 10	20.4%	1.4%	Compound
Class 11	0.3%	1.4%	Compound
Class 12	0.8%	1.4%	Compound
Class 13	21.2%	1.4%	Compound

Truck Distribution by Hour does not apply

Axle Configuration

Traffic Wander	
Mean wheel location (mm)	460.0
Traffic wander standard deviation (mm)	254.0
Design lane width (m)	3.7

Axle Configuration	
Average axle width (m)	2.6
Dual tire spacing (mm)	305.0
Tire pressure (kPa)	827.4

Average Axle Spacing	
Tandem axle spacing (m)	1.3
Tridem axle spacing (m)	1.3
Quad axle spacing (m)	1.3

Wheelbase does not apply

Number of Axles per Truck

Vehicle Class	Single Axle	Tandem Axle	Tridem Axle	Quad Axle
Class 4	1	1.09	0	0
Class 5	2	0	0	0
Class 6	1	1	0	0
Class 7	0.2	1.6	0.2	0
Class 8	2.17	0.84	0	0
Class 9	1.01	1.99	0	0
Class 10	1	1	1	0
Class 11	4.18	0.15	0.17	0
Class 12	3.94	1.02	0	0
Class 13	1.12	3.33	0.29	0

AADTT (Average Annual Daily Truck Traffic) Growth

*** Traffic cap is not enforced**

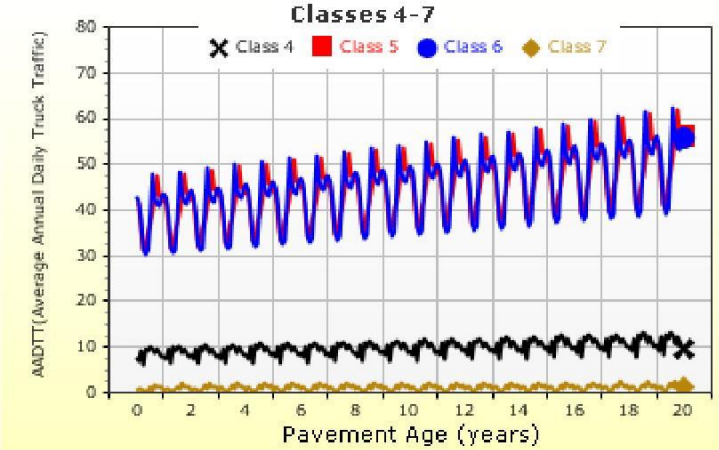

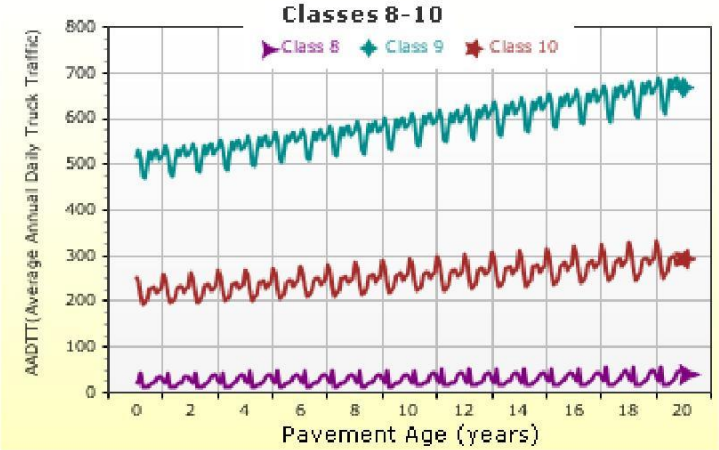

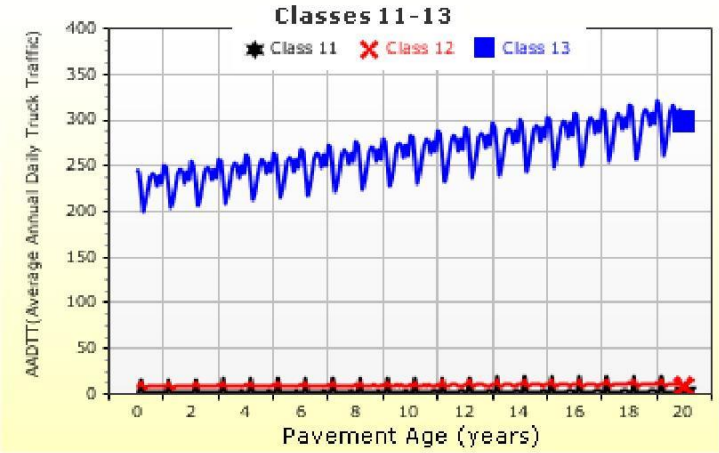

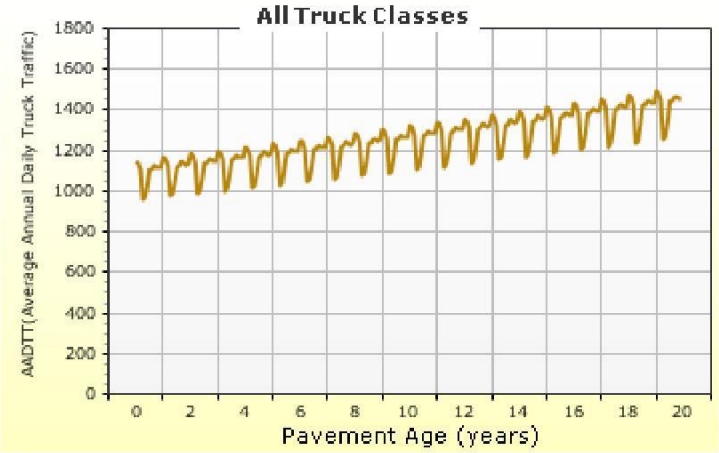

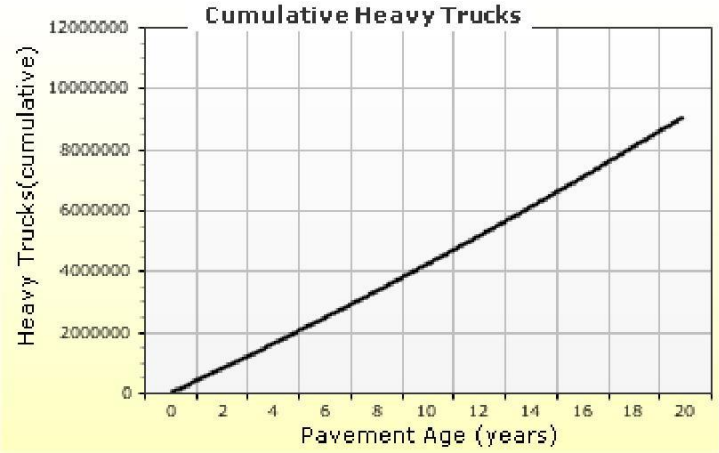

PTH1_Case1_Calibrated_Runs_150_300

File Name: C:\Users\Administrator\Desktop\My ME Design\ASCE Paper Analysis_Re-Run\CASE 1\Calibrated\PTH1_Case1_Calibrated_Runs_150_300.dgpx

Climate Inputs

Climate Data Sources:

Climate Station Cities:	Location (lat lon elevation(m))
BRANDON, MB	49.91700 -99.95000 409

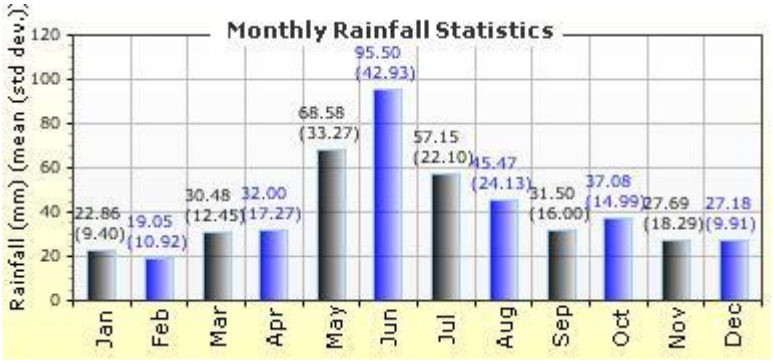

Annual Statistics:

Mean annual air temperature (ºC)	3.80
Mean annual precipitation (mm)	495.30
Freezing index (ºC - days)	1667.31
Average annual number of freeze/thaw cycles:	35.00

Water table depth (m)	10.00

Monthly Climate Summary:

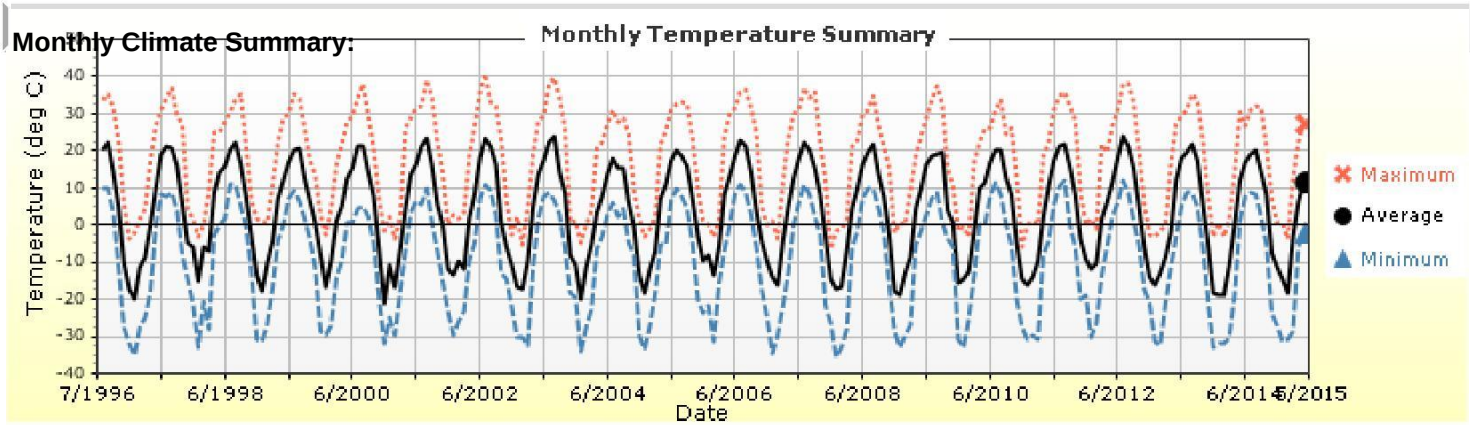

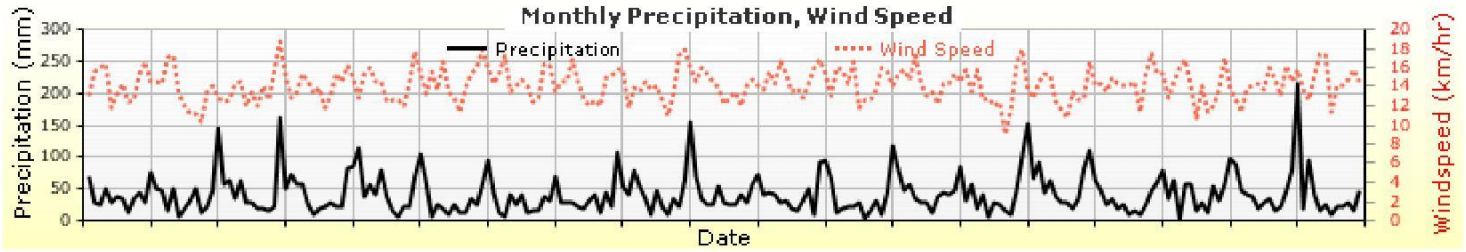

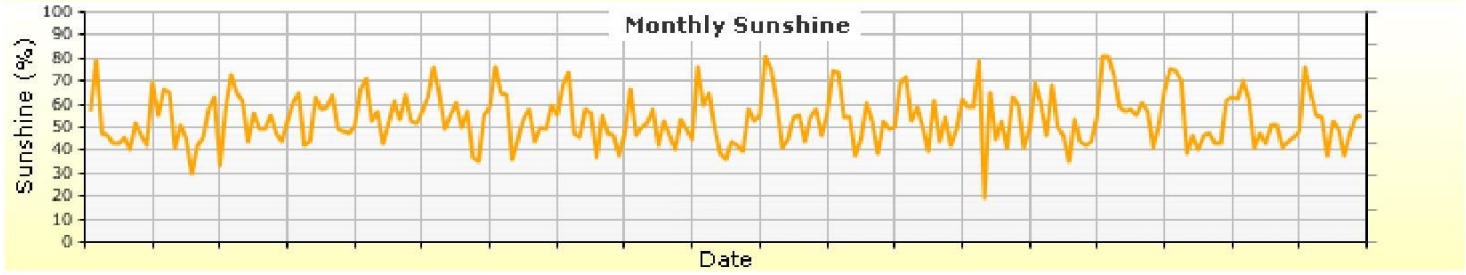

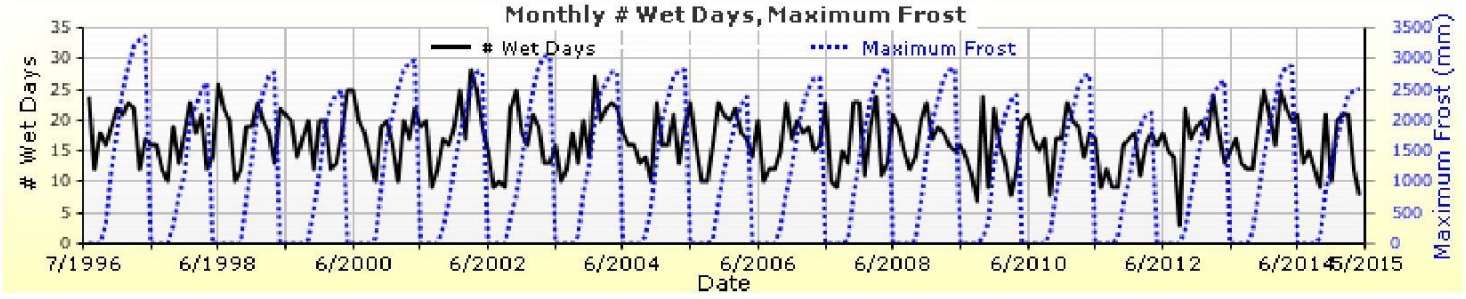

PTH1_Case1_Calibrated_Runs_150_300

File Name: C:\Users\Administrator\Desktop\My ME Design\ASCE Paper Analysis_Re-Run\CASE 1\Calibrated\PTH1_Case1_Calibrated_Runs_150_300.dgpx

Hourly Air Temperature Distribution by Month:

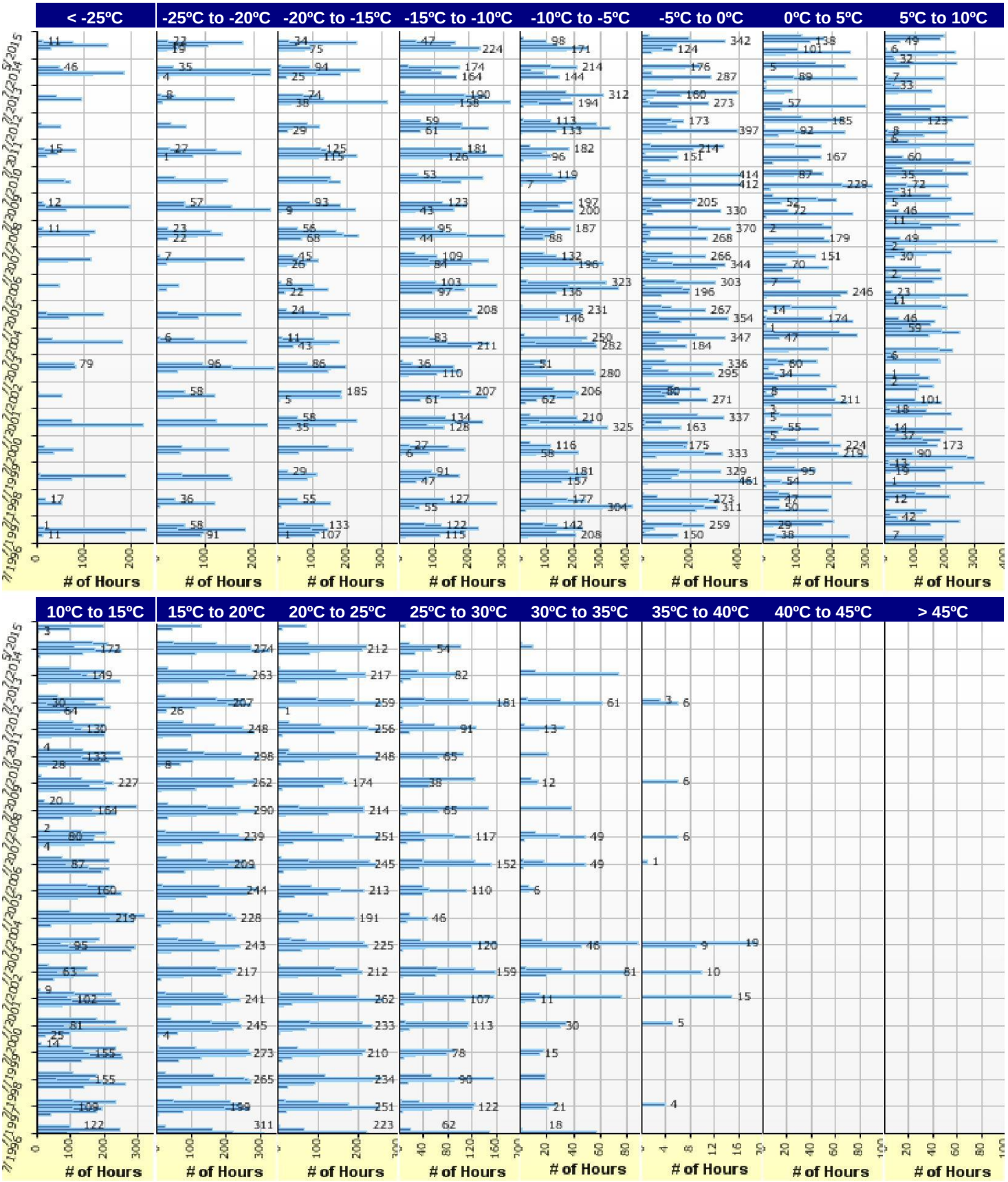

Design Properties

HMA Design Properties

Use Multilayer Rutting Model	False
Using G* based model (not nationally calibrated)	True
Is NCHRP 1-37A HMA Rutting Model Coefficients	True
Endurance Limit	-
Use Reflective Cracking	True

Layer Name	**Layer Type**	**Interface Friction**
Layer 1 Flexible : Default asphalt concrete	Flexible (1)	1.00
Layer 2 Non-stabilized Base : Crushed stone	Non-stabilized Base (4)	1.00
Layer 3 Subgrade : A-7-5	Subgrade (5)	-

Structure - ICM Properties	
AC surface shortwave absorptivity	0.85

Thermal Cracking (Input Level: 1)

Indirect tensile strength at -10 ºC (MPa)	3.49

Thermal Contraction	
Is thermal contraction calculated?	True
Mix coefficient of thermal contraction (mm/mm/ºC)	-
Aggregate coefficient of thermal contraction (mm/mm/ºC)	9.0e-006
Voids in Mineral Aggregate (%)	13.7

	Creep Compliance (1/GPa)		
Loading time (sec)	-20 ºC	-10 ºC	0 ºC
1	4.79e-002	7.56e-002	1.46e-001
2	4.94e-002	8.02e-002	1.64e-001
5	5.21e-002	8.89e-002	2.01e-001
10	5.52e-002	9.78e-002	2.43e-001
20	5.98e-002	1.09e-001	3.02e-001
50	6.84e-002	1.31e-001	4.24e-001
100	7.78e-002	1.54e-001	5.65e-001

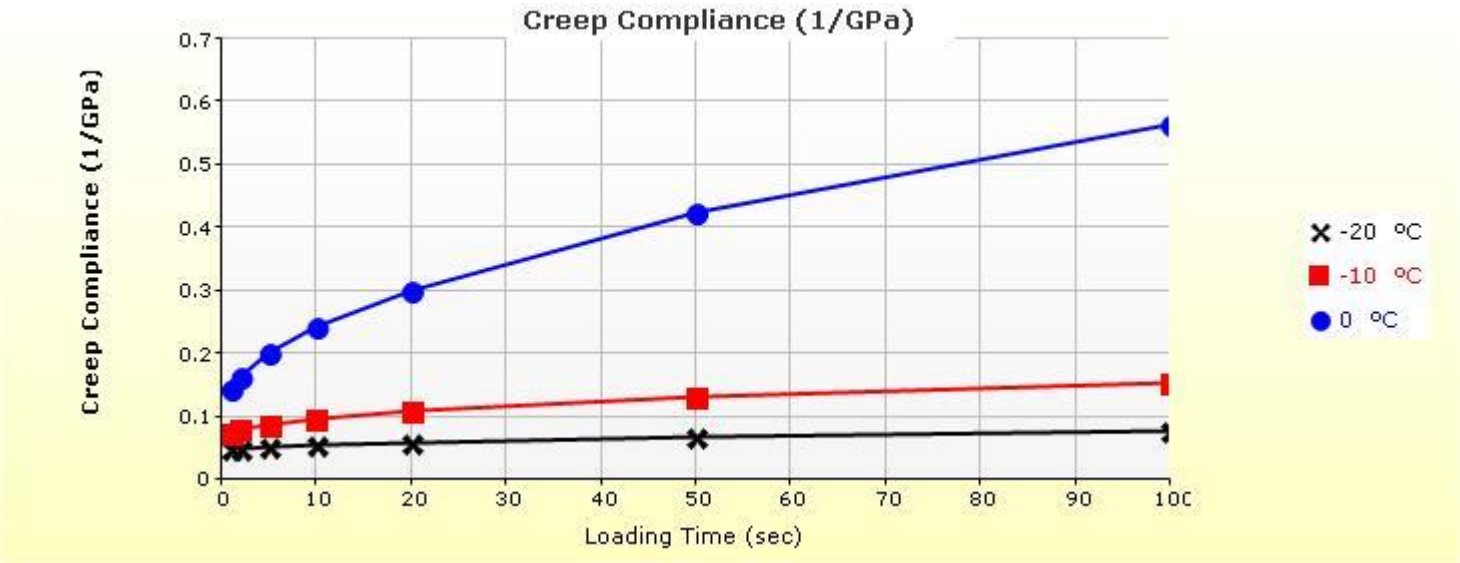

PTH1_Case1_Calibrated_Runs_150_300

File Name: C:\Users\Administrator\Desktop\My ME Design\ASCE Paper Analysis_Re-Run\CASE 1\Calibrated\PTH1_Case1_Calibrated_Runs_150_300.dgpx

HMA Layer 1: Layer 1 Flexible : Default asphalt concrete

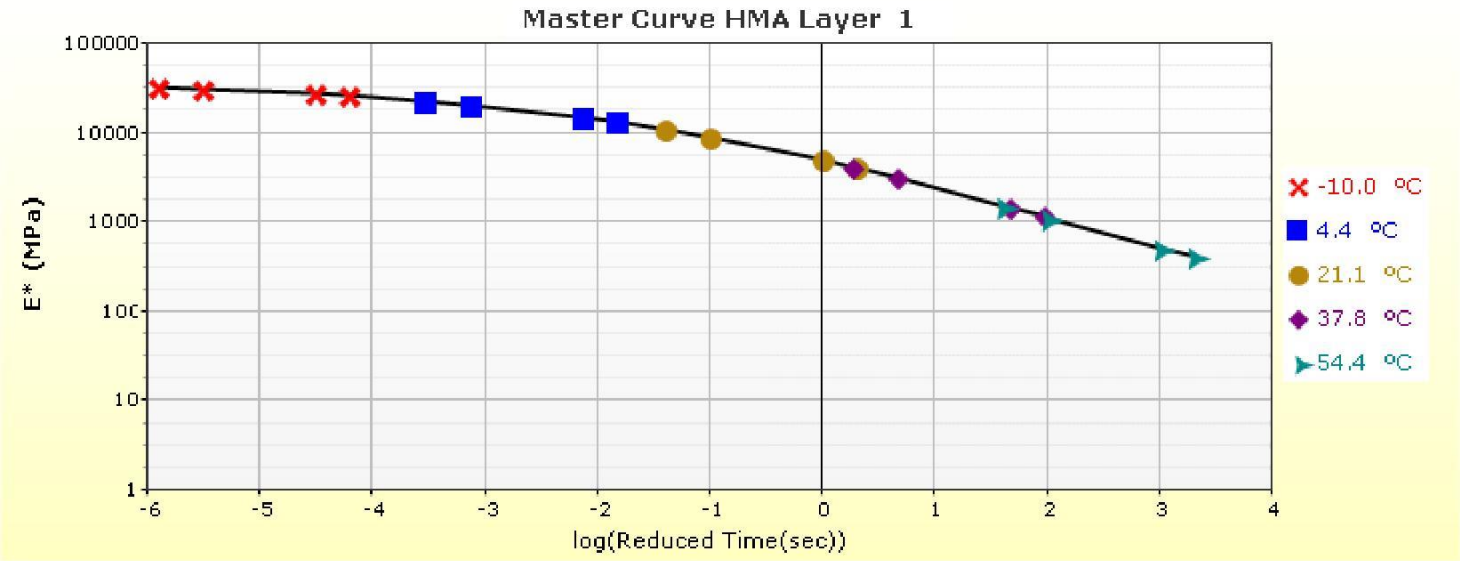

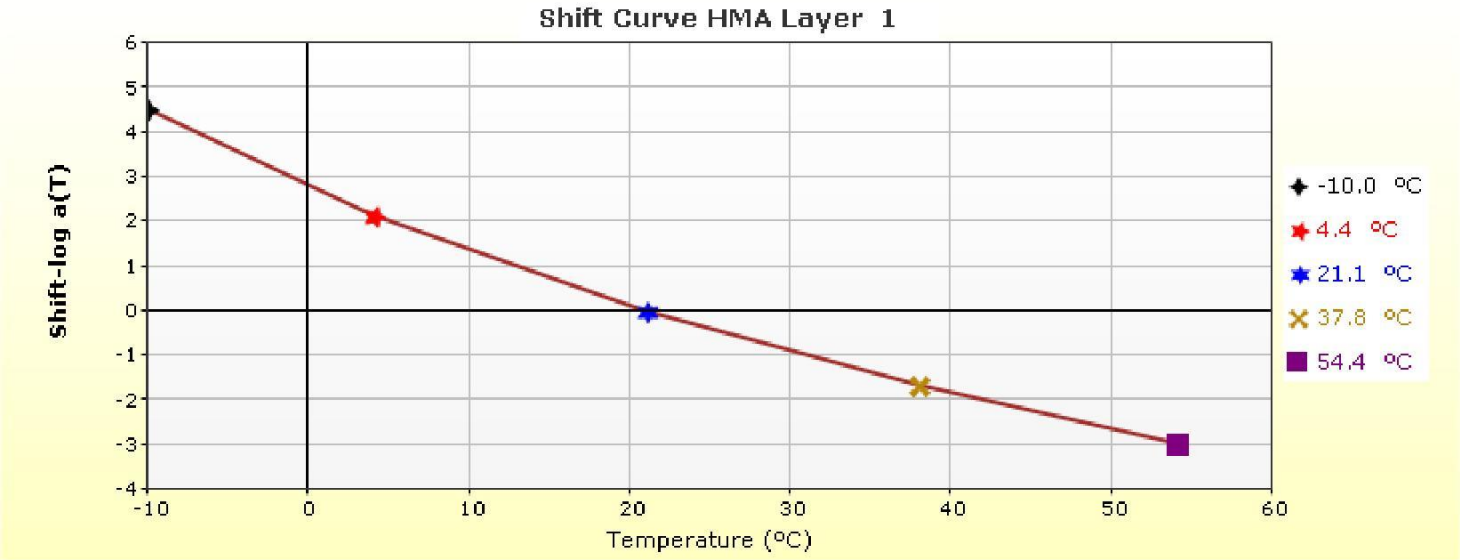

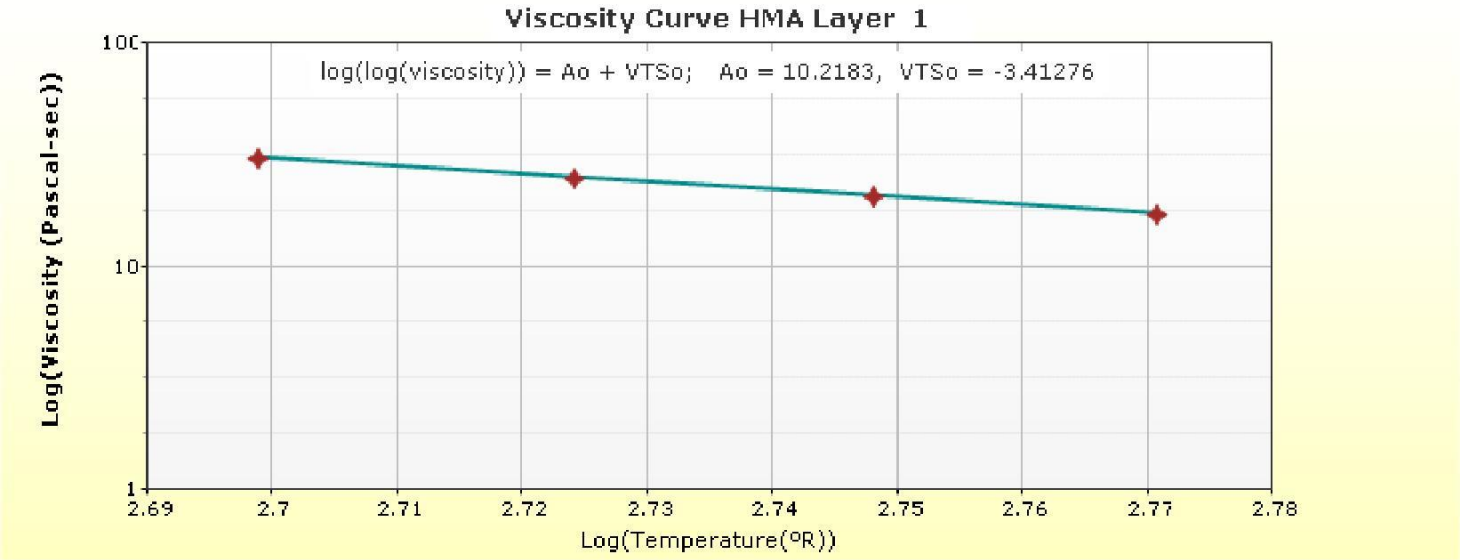

Analysis Output Charts

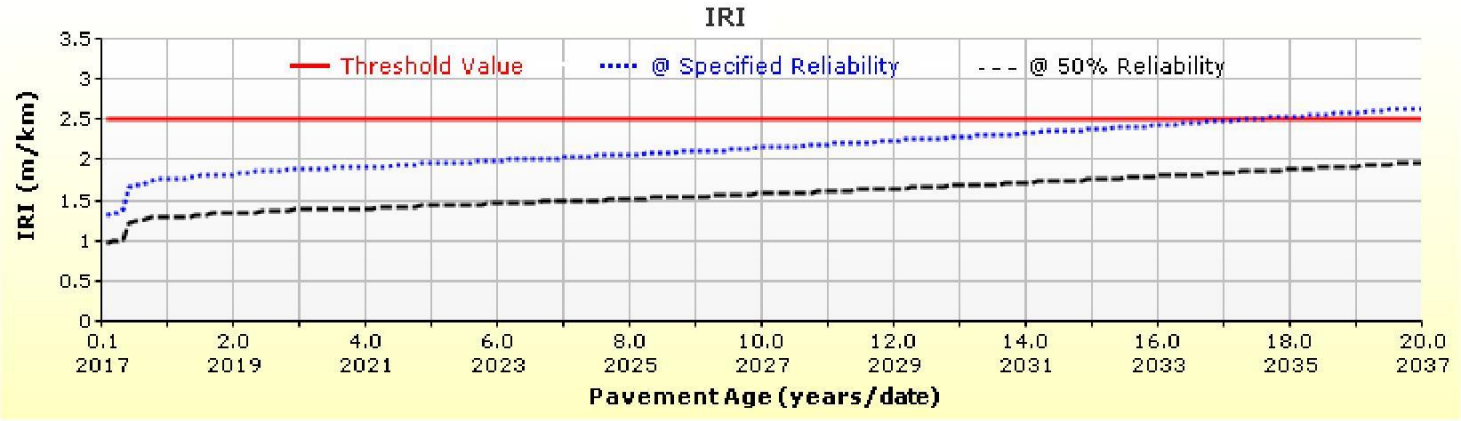

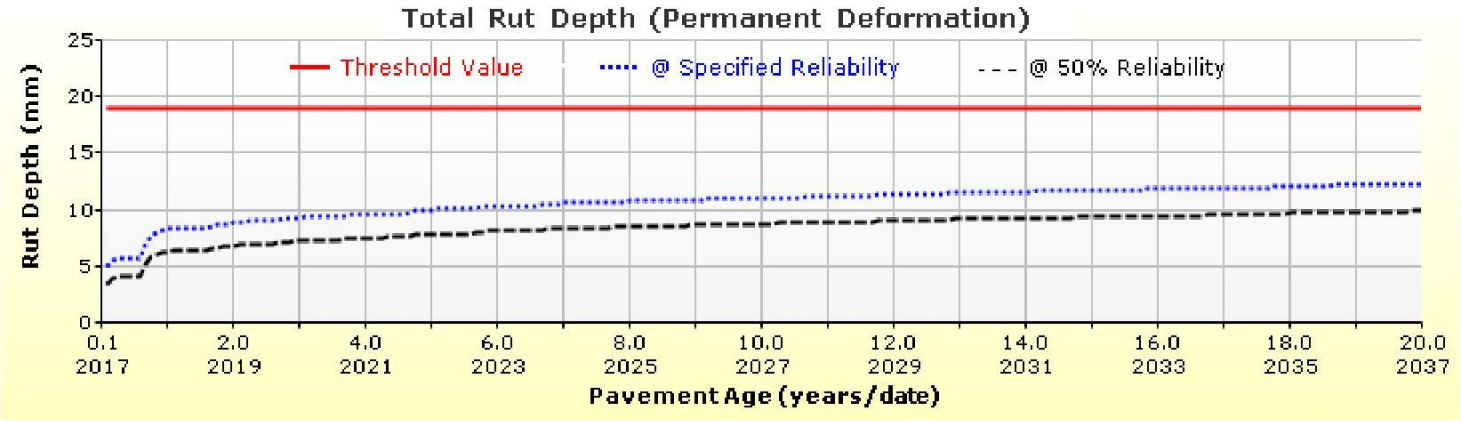

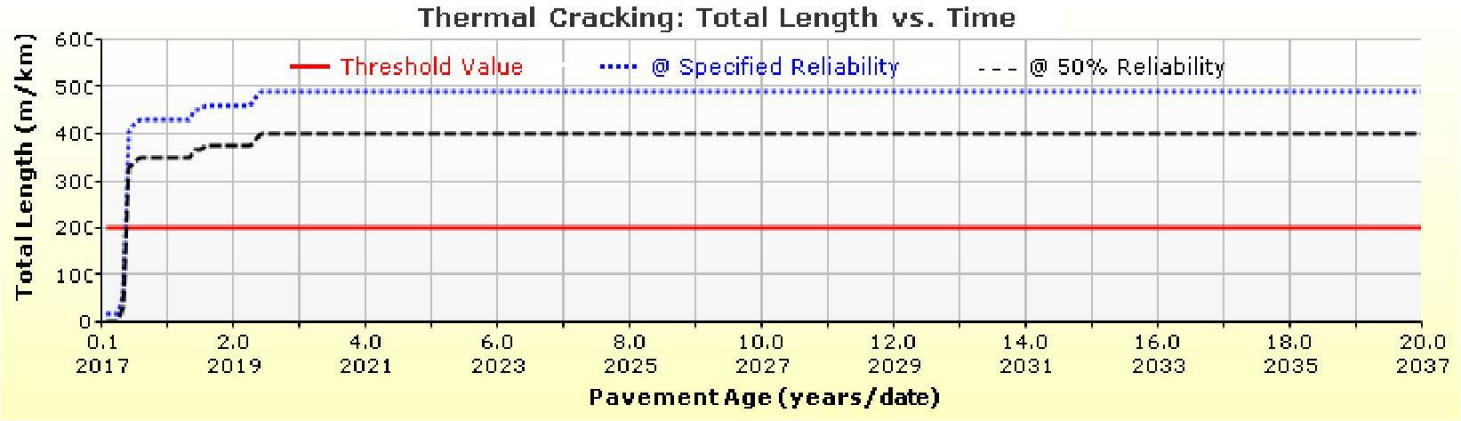

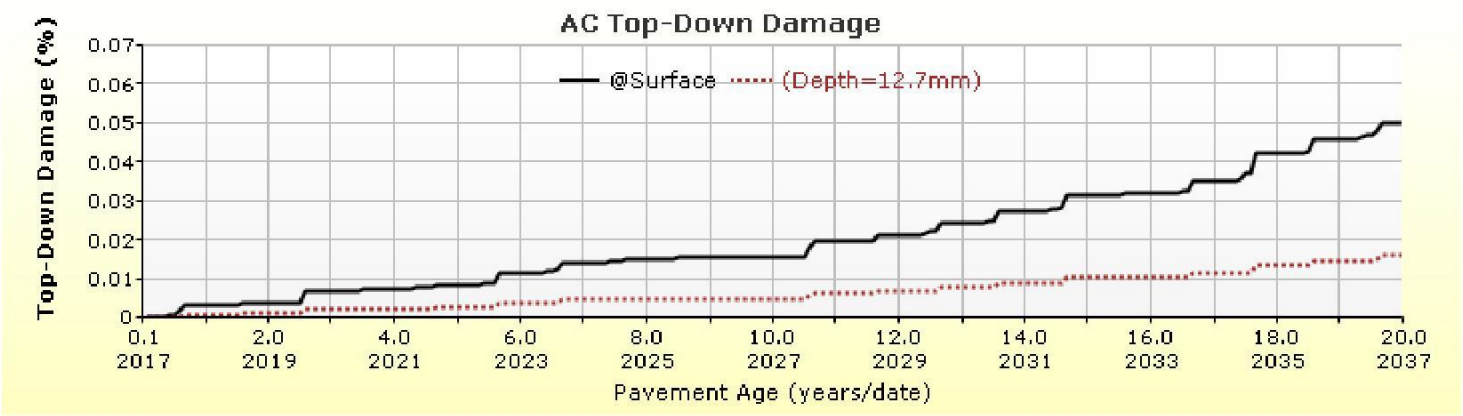
AC Top-Down Damage
Top-Down Damage (%)
@Surface
(Depth=12.7mm)
0.07
0.06
0.05
0.04
0.03
0.02
0.01
0
0.1 2017
2.0 2019
4.0 2021
6.0 2023
8.0 2025
10.0 2027
12.0 2029
14.0 2031
16.0 2033
18.0 2035
20.0 2037
Pavement Age (years/date)

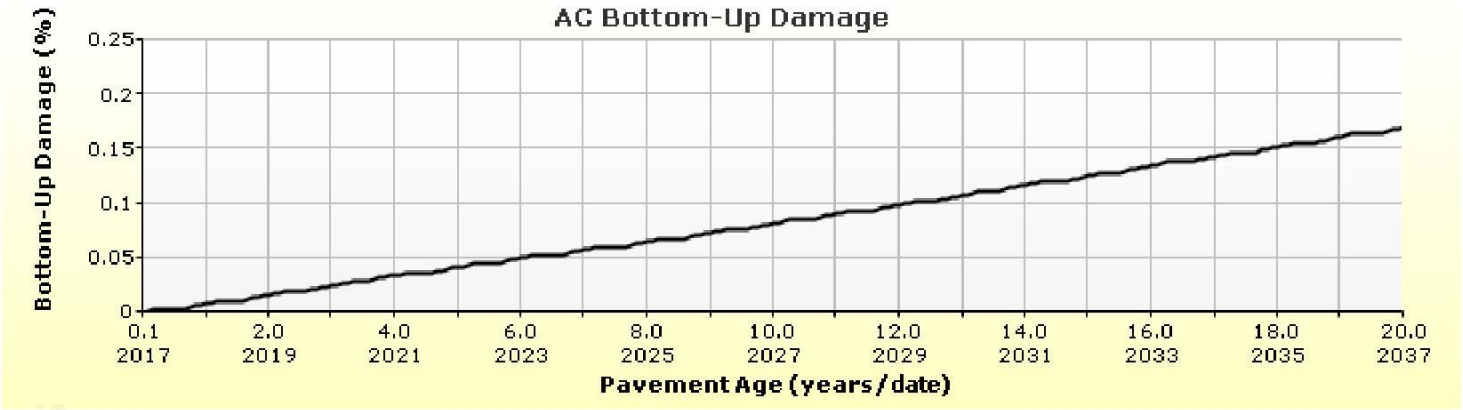
AC Bottom-Up Damage
Bottom-Up Damage (%)
0.25
0.2
0.15
0.1
0.05
0
0.1 2017
2.0 2019
4.0 2021
6.0 2023
8.0 2025
10.0 2027
12.0 2029
14.0 2031
16.0 2033
18.0 2035
20.0 2037
Pavement Age (years/date)

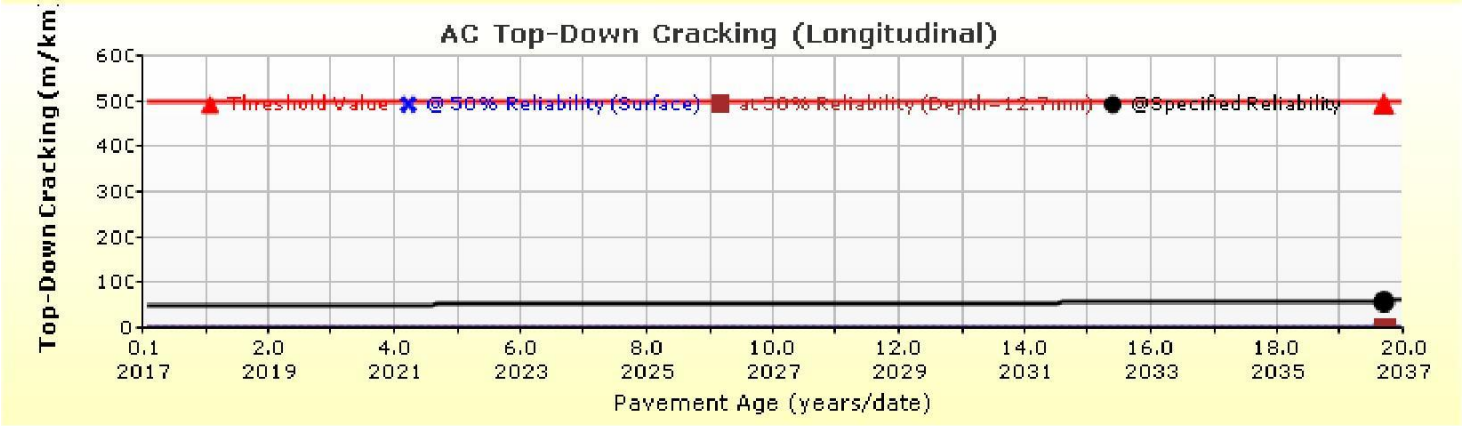
AC Top-Down Cracking (Longitudinal)
Top-Down Cracking (m/km)
Threshold Value
@ 50% Reliability (Surface)
@ 50% Reliability (Depth=12.7mm)
@Specified Reliability
600
500
400
300
200
100
0
0.1 2017
2.0 2019
4.0 2021
6.0 2023
8.0 2025
10.0 2027
12.0 2029
14.0 2031
16.0 2033
18.0 2035
20.0 2037
Pavement Age (years/date)

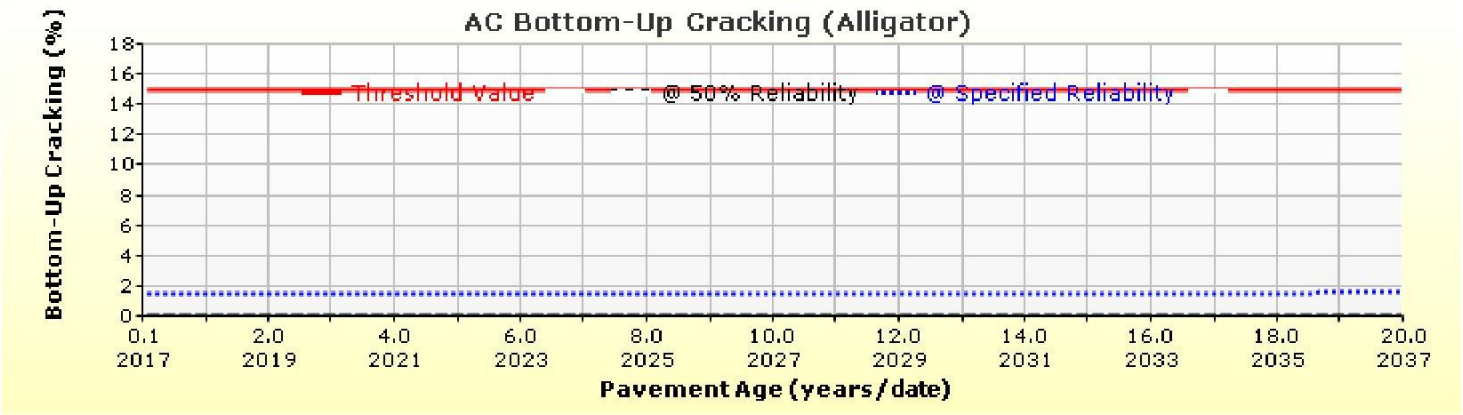
AC Bottom-Up Cracking (Alligator)
Bottom-Up Cracking (%)
Threshold Value
@ 50% Reliability
@ Specified Reliability
18
16
14
12
10
8
6
4
2
0
0.1 2017
2.0 2019
4.0 2021
6.0 2023
8.0 2025
10.0 2027
12.0 2029
14.0 2031
16.0 2033
18.0 2035
20.0 2037
Pavement Age (years/date)

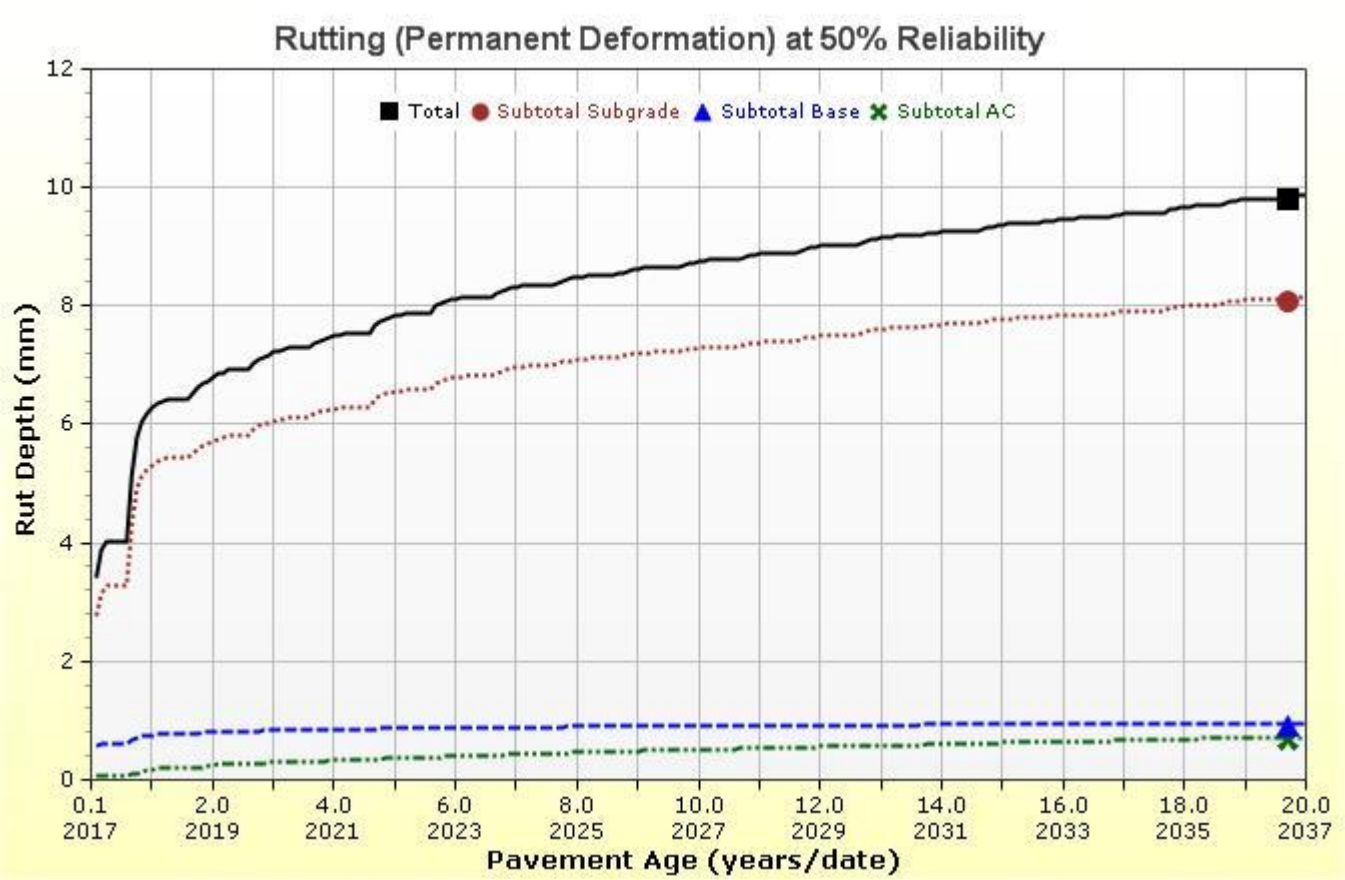
Rutting (Permanent Deformation) at 50% Reliability
Total
Subtotal Subgrade
Subtotal Base
Subtotal AC
Rut Depth (mm)
0
2
4
6
8
10
12
0.1
2017
2.0
2019
4.0
2021
6.0
2023
8.0
2025
10.0
2027
12.0
2029
14.0
2031
16.0
2033
18.0
2035
20.0
2037
Pavement Age (years/date)

PTH1_Case1_Calibrated_Runs_150_300

File Name: C:\Users\Administrator\Desktop\My ME Design\ASCE Paper Analysis_Re-Run\CASE 1\Calibrated\PTH1_Case1_Calibrated_Runs_150_300.dgpx

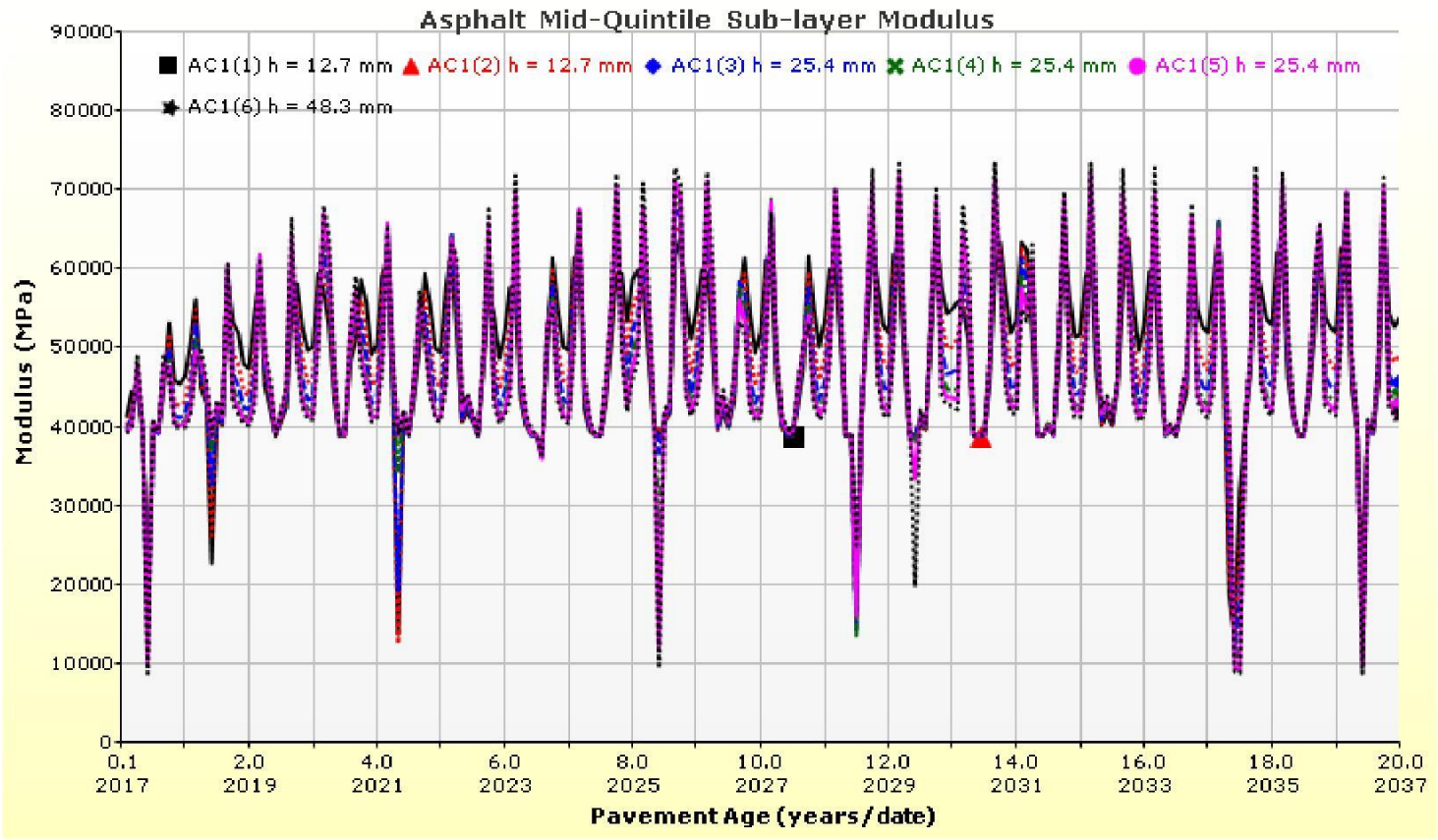

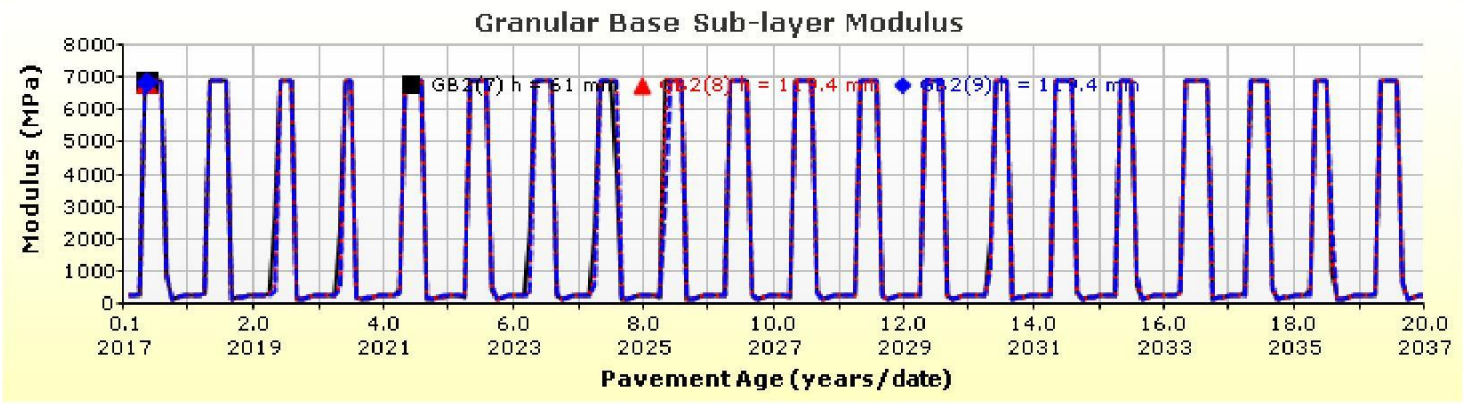

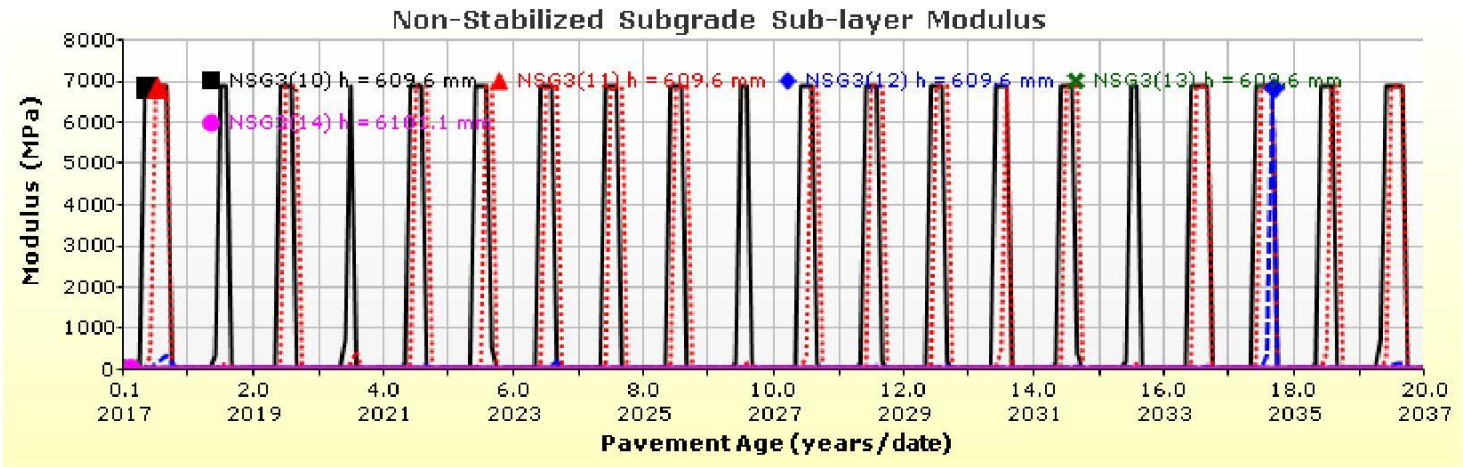

Layer Information

Layer 1 Flexible : Default asphalt concrete

Asphalt		
Thickness (mm)	150.0	
Unit weight (kgf/m^3)	2290.0	
Poisson's ratio	Is Calculated?	False
	Ratio	0.35
	Parameter A	-
	Parameter B	-

Asphalt Dynamic Modulus (Input Level: 1)

T (ºC)	0.1 Hz	0.5 Hz	1 Hz	5 Hz	10 Hz	25 Hz
-10	22672	25960	27228	29807	30762	31890
5	9270	12831	14470	18339	19976	22065
25	1746	2969	3687	5866	7030	8748
40	575	990	1255	2166	2718	3629

Asphalt Binder

Temperature (ºC)	Binder Gstar (Pa)	Phase angle (deg)
15	3640000	58
35	130000	71
58	3570	83
64	1680	85

General Info

Name	Value
Reference temperature (ºC)	21.1
Effective binder content (%)	9.9
Air voids (%)	3.8
Thermal conductivity (watt/meter-kelvin)	1.16
Heat capacity (joule/kg-kelvin)	963

Identifiers

Field	Value
Display name/identifier	Default asphalt concrete
Description of object	
Author	
Date Created	16/09/2010 12:00:00 AM
Approver	
Date approved	16/09/2010 12:00:00 AM
State	
District	
County	
Highway	
Direction of Travel	
From station (km)	
To station (km)	
Province	
User defined field 1	
User defined field 2	
User defined field 3	
Revision Number	0

Layer 2 Non-stabilized Base : Crushed stone

Unbound	
Layer thickness (mm)	300.0
Poisson's ratio	0.4
Coefficient of lateral earth pressure (k0)	0.5

Modulus (Input Level: 2)

Analysis Type:	Modify input values by temperature/moisture
Method:	Resilient Modulus (MPa)

Resilient Modulus (MPa)
181.0

Use Correction factor for NDT modulus?	-
NDT Correction Factor:	-

Identifiers

Field	Value
Display name/identifier	Crushed stone
Description of object	Default material
Author	AASHTO
Date Created	01/01/2011 12:00:00 AM
Approver	
Date approved	01/01/2011 12:00:00 AM
State	
District	
County	
Highway	
Direction of Travel	
From station (km)	
To station (km)	
Province	
User defined field 1	
User defined field 2	
User defined field 3	
Revision Number	0

Sieve

Liquid Limit	6.0
Plasticity Index	1.0
Is layer compacted?	False

	Is User Defined?	Value
Maximum dry unit weight (kgf/m^3)	False	2038.2
Saturated hydraulic conductivity (m/hr)	False	1.54e-02
Specific gravity of solids	False	2.7
Water Content (%)	False	7.4

User-defined Soil Water Characteristic Curve (SWCC)	
Is User Defined?	False
af	7.2555
bf	1.3328
cf	0.8242
hr	117.4000

Sieve Size	% Passing
0.001mm	
0.002mm	
0.020mm	
0.075mm	8.7
0.150mm	
0.180mm	12.9
0.250mm	
0.300mm	
0.425mm	20.0
0.600mm	
0.850mm	
1.18mm	
2.0mm	33.8
2.36mm	
4.75mm	44.7
9.5mm	57.2
12.5mm	63.1
19.0mm	72.7
25.0mm	78.8
37.5mm	85.8
50.0mm	91.6
63.0mm	
75.0mm	
90.0mm	97.6

Layer 3 Subgrade : A-7-5

Unbound	
Layer thickness (mm)	Semi-infinite
Poisson's ratio	0.4
Coefficient of lateral earth pressure (k0)	0.5

Modulus (Input Level: 2)

Analysis Type:	Modify input values by temperature/moisture
Method:	Resilient Modulus (MPa)

Resilient Modulus (MPa)
59.0

Use Correction factor for NDT modulus?	-
NDT Correction Factor:	-

Identifiers

Field	Value
Display name/identifier	A-7-5
Description of object	Default material
Author	AASHTO
Date Created	01/01/2011 12:00:00 AM
Approver	
Date approved	01/01/2011 12:00:00 AM
State	
District	
County	
Highway	
Direction of Travel	
From station (km)	
To station (km)	
Province	
User defined field 1	
User defined field 2	
User defined field 3	
Revision Number	0

Sieve

Liquid Limit	57.0
Plasticity Index	24.0
Is layer compacted?	False

	Is User Defined?	Value
Maximum dry unit weight (kgf/m^3)	False	1634.2
Saturated hydraulic conductivity (m/hr)	False	1.305e-06
Specific gravity of solids	False	2.7
Water Content (%)	False	20

User-defined Soil Water Characteristic Curve (SWCC)	
Is User Defined?	False
af	125.3117
bf	0.5772
cf	0.1052
hr	500.0000

Sieve Size	% Passing
0.001mm	
0.002mm	
0.020mm	
0.075mm	70.5
0.150mm	
0.180mm	77.7
0.250mm	
0.300mm	
0.425mm	83.3
0.600mm	
0.850mm	
1.18mm	
2.0mm	90.8
2.36mm	
4.75mm	94.0
9.5mm	95.7
12.5mm	96.3
19.0mm	97.3
25.0mm	97.9
37.5mm	98.4
50.0mm	98.8
63.0mm	
75.0mm	
90.0mm	99.3

Calibration Coefficients

AC Fatigue

$$N_f = 0.00432 * C * \beta_{f1} k_1 \left(\frac{1}{\varepsilon_1}\right)^{k_2 \beta_{f2}} \left(\frac{1}{E}\right)^{k_3 \beta_{f3}}$$

$$C = 10^M$$

$$M = 4.84\left(\frac{V_b}{V_a + V_b} - 0.69\right)$$

k1: 0.007566	
k2: 3.9492	
k3: 1.281	
Bf1: 1	
Bf2: 1	
Bf3: 1	

AC Rutting

$$\frac{\varepsilon_p}{\varepsilon_r} = k_z \beta_{r1} 10^{k_1} T^{k_2 \beta_{r2}} N^{k_3 \beta_{r3}}$$

$$k_z = (C_1 + C_2 * depth) * 0.328196^{depth}$$

$$C_1 = -0.1039 * H_\alpha^2 + 2.4868 * H_\alpha - 17.342$$

$$C_2 = 0.0172 * H_\alpha^2 - 1.7331 * H_\alpha + 27.428$$

Where:

$$H_{ac} = total\ AC\ thickness(in)$$

$\varepsilon_p = plastic\ strain\left(^{in}/_{in}\right)$
$\varepsilon_r = resilient\ strain\left(^{in}/_{in}\right)$
$T = layer\ temperature\left(^{\circ}F\right)$
$N = number\ of\ load\ repetitions$

AC Rutting Standard Deviation	0.24 * Pow(RUT,0.8026) + 0.001	
AC Layer	K1:-3.35412 K2:1.5606 K3:0.4791	Br1:1 Br2:1 Br3:1

Thermal Fracture

$$C_f = 400 * N\left(\frac{\log C / h_{ac}}{\sigma}\right)$$

$$\Delta C = (k * \beta t)^{n+1} * A * \Delta K^n$$

$$A = 10^{(4.389 - 2.52 * \log(E * \sigma_m * n))}$$

$C_f = observed\ amount\ of\ thermal\ cracking(ft/500ft)$
$k = refression\ coefficient\ determined\ through\ field\ calibration$
$N() = standard\ normal\ distribution\ evaluated\ at()$
$\sigma = standard\ deviation\ of\ the \log\ of\ the\ depth\ of\ cracks\ in\ the\ pavments$
$C = crack\ depth(in)$
$h_{ac} = thickness\ of\ asphalt\ layer(in)$
$\Delta C = Change\ in\ the\ crack\ depth\ due\ to\ a\ cooling\ cycle$
$\Delta K = Change\ in\ the\ stress\ intensity\ factor\ due\ to\ a\ cooling\ cycle$
$A, n = Fracture\ parameters\ for\ the\ asphalt\ mixture$
$E = mixture\ stiffness$
$\sigma_M = Undamaged\ mixture\ tensile\ strength$
$\beta_t = Calibration\ parameter$

Level 1 K: 1.5	Level 1 Standard Deviation: 0.1468 * THERMAL + 65.027
Level 2 K: 0.5	Level 2 Standard Deviation: 0.2841 * THERMAL + 55.462
Level 3 K: 1.5	Level 3 Standard Deviation: 0.3972 * THERMAL + 20.422

CSM Fatigue

$$N_f = 10^{\left(\frac{k_1 \beta_{c1} \left(\frac{\sigma_s}{M_r}\right)}{k_2 \beta_{c2}}\right)}$$

$N_f = number\ of\ repetitions\ to\ fatigue\ cracking$
$\sigma_s = Tensile\ stress(psi)$
$M_r = modulus\ of\ rupture(psi)$

k1: 1	k2: 1	Bc1: 0.75	Bc2:1.1

Subgrade Rutting

$$\delta_a(N) = \beta_{s_1} k_1 \varepsilon_v h \left(\frac{\varepsilon_0}{\varepsilon_r}\right) \left| e^{-\left(\frac{\rho}{N}\right)^{\beta}} \right|$$

$\delta_a = permanent\ deformation\ for\ the\ layer$
$N = number\ of\ repetitions$
$\varepsilon_v = average\ veritcal\ strain(in/in)$
$\varepsilon_0, \beta, \rho = material\ properties$
$\varepsilon_r = resilient\ strain(in/in)$

Granular		Fine	
k1: 2.03	Bs1: 1	k1: 1.35	Bs1: 1
Standard Deviation (BASERUT) 0.1477 * Pow(BASERUT,0.6711) + 0.001		Standard Deviation (BASERUT) 0.1235 * Pow(SUBRUT,0.5012) + 0.001	

AC Cracking

AC Top Down Cracking

$$FC_{top} = \left(\frac{C_4}{1 + e^{(C_1 - C_2 * log_{10}(Damage))}}\right) * 10.56$$

c1: 7	c2: 3.5	c3: 0	c4: 1000

AC Cracking Top Standard Deviation

200 + 2300/(1+exp(1.072-2.1654*LOG10 (TOP+0.0001)))

AC Bottom Up Cracking

$$FC = \left(\frac{6000}{1 + e^{(C_1 * C_1' + C_2 * C_2' log_{10}(D * 100))}}\right) * \left(\frac{1}{60}\right)$$

$$C_2' = -2.40874 - 39.748 * (1 + h_{ac})^{-2.856}$$

$$C_1' = -2 * C_2'$$

c1: 1	c2: 1	c3: 6000

AC Cracking Bottom Standard Deviation

1.13 + 13/(1+exp(7.57-15.5*LOG10 (BOTTOM+0.0001)))

CSM Cracking

$$FC_{ctb} = C_1 + \frac{C_2}{1 + e^{C_3 - C_4(Damage)}}$$

C1: 0	C2: 75	C3: 5	C4: 3

CSM Standard Deviation

CTB*1

IRI Flexible Pavements

C1 - Rutting
C2 - Fatigue Crack
C3 - Transverse Crack
C4 - Site Factors

C1: 40	C2: 0.4	C3: 0.008	C4: 0.015